DOE/MC/23005--2990

DE91 002071

Nozzle Development

Final Report

F.T. Dodge
L.G. Dodge
J.E. Johnson

Work Performed Under Contract No.: DE-AC21-86MC23005

For
U.S. Department of Energy
Office of Fossil Energy
Morgantown Energy Technology Center
P.O. Box 880
Morgantown, West Virginia 26507-0880

By
Southwest Research Institute
P.O. Drawer 28510
San Antonio, Texas 78228-0510

June 1989

ABSTRACT

The objective of this program has been the development of experimental techniques and data processing procedures to allow for the characterization of multi-phase fuel nozzles using laboratory tests. Test results were to be used to produce a single value coefficient-of-performance that would predict the performance of the fuel nozzles independent of system application. It is recognized that fuel nozzles or injectors must meet a number of criteria for proper system performance, and rather than define a single coefficient-of-performance, this report shows that it is more realistic to define the critical characteristics and recommend standard methods for the measurement of those characteristics.

Several different types of fuel nozzles capable of handling multi-phase fuels have been characterized for: (a) fuel flow rate versus delivery pressure, (b) fuel-air ratio throughout the fuel spray or plume and the effective cone angle of the injector, and (c) fuel drop- or particle-size distribution as a function of fluid properties. Fuel nozzles which have been characterized on both single-phase liquids and multi-phase liquid-solid slurries include a variable-film-thickness nozzle, a commercial coal-water slurry (CWS) nozzle, and four diesel injectors of different geometries (tested on single-phase fluids only). Multi-phase mixtures included CWS with various coal loadings, surfactant concentrations, and stabilizer concentrations, as well as glass-bead water slurries with stabilizing additives. Single-phase fluids included glycerol-water mixtures to vary the viscosity over a range of 1 to 1500 cP, and alcohol-water mixtures to vary the surface tension from about 22 to 73 dyne/cm. In addition, tests were performed to characterize straight-tube gas-solid nozzles using two different size distributions of glass beads in air. The experimental results have been correlated in such a form that they may be used to predict the performance of nozzles of other sizes and at other conditions that those tested here.

As a part of this program standardized procedures have been developed for processing measurements of spray drop-size characteristics and the overall cross-section average drop or particle sizes. These procedures result in average drop sizes that are more representative of the overall spray than measurements at a single location, and they allow comparison of measurements made by different instruments that sample the spray in different ways (e.g., line-of-sight integral value or point measurement). The procedures are currently being incorporated by the American Society for Testing and Materials (ASTM) as part of the basis for a standardized spray test for laser-diffraction measurements of spray characteristics. In addition, spray measurements of diesel

hole-type nozzles with a laser-diffraction particle sizer have shown the limitation of using standard laser beam diameters for these types of sprays. The improvement in spatial resolution associated with using a smaller (than standard) laser beam diameter has been demonstrated.

The improvements in experimental techniques and data processing algorithms and the experimental results for specific nozzle types and multi-phase fluids are believed to be of considerable significance to the Fossil Energy Program at Morgantown Energy Technology Center.

PREFACE

This document is the final report for U.S. Department of Energy, Morgantown Energy Technology Center (METC) Contract No. DE-AC21-86MC23005, Southwest Research Institute Project 04-1345, and covers a period of October, 1986 through April, 1989.

ACKNOWLEDGEMENTS

We would like to acknowledge the support of the Department of Energy, Morgantown Energy Technology Center for sponsoring this work. The individuals at METC responsible for the conduct of this program include Mr. Michael H. McMillian, Mr. R. Greg Cutlip, and Mr. William C. Smith as Contracting Officer's Technical Representatives, and Ms. R. Diane Manilla as Contract Specialist. Their interest and support have made this program possible. Slurry nozzle atomization tests were performed by Mr. R. C. Haufler and Mr. Michael G. Ryan. Diesel injectors were characterized by Mr. Milan J. Maymar. Rheological measurements were performed by Mr. Pierre J. Gutierrez and Mr. Ramsey J. Railsback under the direction of Dr. Richard J. Mannheimer. Dr. Mannheimer also provided valuable information concerning interpretation of the rheological data. The concept development and detailed design for the gas-solids experimental facility was accomplished by Mr. E. C. Schroeder, and the instrumentation, conduct of the experiment, and data reduction were accomplished by Mr. C. M. Wood and Mr. Steve Green. We thank Mr. M. E. LePara and Mr. F. W. Schaekel for permission to conduct some of these experiments at the Belvoir Fuels and Lubricants Research Facility (SwRI). Also, we thank Ms. Diana Bundrant for preparing this manuscript and all reports throughout the entire program.

TABLE OF CONTENTS

LIST OF TABLES

LIST OF FIGURES

1.0 EXECUTIVE SUMMARY

The reliable specification of fuel nozzles for combustion systems has been complicated by the fact that there have been no standards for measuring important spray characteristics such as drop size distribution, fuel-air ratio distribution, or cone angle. Fuel injector performance has been documented for some types of nozzles using some types of fuels, but these results have been difficult to duplicate or use because the results have been dependent on the instrumentation and procedures employed. This is especially true for fuel nozzle performance for multi-phase fuels such as coal-water slurries (CWS) where fuel properties are difficult to define and may vary with time and past history. For example, the shear viscosity of CWS usually varies with shear rate, yield values may be nonzero, and surface tension is not easily defined.

The **OBJECTIVE** of this program has been to address the shortcomings mentioned above by developing experimental techniques and data processing procedures to allow for the characterization of multi-phase fuel nozzles using well-defined techniques reproducible in different laboratories that use different instrumentation setups. A further objective was to characterize multi-phase nozzles in terms of a performance measure such as a coefficient-of-performance.

The **APPROACH** used to obtain the objective has been to improve experimental techniques used for spray diagnostics and define standard procedures for acquiring and processing these results. These techniques were then used in the study of four different types of nozzles: (1) a planar slot nozzle using air-assisted atomization, with a capability of varying the slot width of both the fuel and air passages, (2) a commercial CWS nozzle used in boiler and gas turbine applications, (3) several hole-type diesel nozzles, (4) and two simple tubes of different diameters for studying the injection of particle-laden air streams. The first type of nozzle (variable film thickness) was tested with single-phase fluids of varying viscosity and surface tension as well as with slurries of micronized coal in water and glass beads in water. The single-phase fluids spanned a viscosity range of 1 to 1500 cP and a surface tension range of 22 to 73 dynes/cm. The micronized CWS spanned a coal loading range of 40 to 60 wt. %, and also addressed the effects of additives on atomization. The glass bead slurries spanned a range of volume concentrations similar to the CWS. The second type of atomizer (commercial CWS nozzle for boilers and gas turbines) was tested with CWS with a coal loading range of 40 to 60 wt. %. The atomizers of the third type (diesel hole-type) were tested with single-phase hydrocarbon fuels with a viscosity range of 2 to 100 cSt. The fourth type of fuel injectors (gas-solid) were tested with two different sizes and various loading ratios of monosized glass beads ($40\mu m$ and $80\mu m$ diameter) dispersed in air.

It has been determined that COEFFICIENTS-OF PERFORMANCE necessary to specify fuel nozzle operation should include specifications for: (1) fuel flow rate as a function of pressure, (2) drop (or particle) size distribution as a function of fuel properties and nozzle operating conditions, and (3) fuel-air ratio distribution through the spray. The relative importance of each of these three specifications depends upon the combustion system. Some significant results important for specifying nozzle performance are discussed below.

A **SUMMARY OF SIGNIFICANT RESULTS** is as follows, with details provided in the body of the report. Sprays from the fuel nozzles for slurries (first 3 above) were characterized using a laser-diffraction particle sizer, which is the most widely used instrument for characterizing slurry sprays. This instrument is not adversely affected by the opacity or non-sphericity of individual slurry drops, as is the case for some other spray diagnostic instrumentation. Traditionally, measurements with laser-diffraction instruments have been made through the centerline of the spray cone only, resulting in a line-of-sight integral measurement over the entire length of the intersection of the laser beam and the spray. It has been shown in this program that this measurement is neither representative of the overall cross-section of the spray, nor directly comparable with measurements by other instruments. Two alternative measurement techniques with laser-diffraction instruments have been demonstrated in this program to give spray measurements which are both representative of the overall spray and comparable with other measurement techniques. These results have been published, and are presented in Appendix A. An ASTM standard for spray measurements is being developed which incorporates these techniques, thus satisfying one of the major sub-objectives of this program, to standardize procedures for specifying fuel nozzles. In addition to the procedures described in Appendix A, some of the special requirements for making spray measurements with laser-diffraction instruments in sprays from diesel hole-type injectors have been investigated. In particular, the requirement for a smaller than standard laser beam diameter has been demonstrated, coupled with other previously developed techniques from this laboratory to provide new insight into diesel sprays.

The application of the enhanced experimental techniques to the three types of slurry-fuel nozzles produced results of importance to the Fossil Energy Program at Morgantown Energy Technology Center. Results are discussed in detail in the report, but some may be summarized as follows. The degraded atomization of slurries when compared with single-phase fluids cannot be explained solely on the basis of the high viscosity of slurries, even if the slurry viscosity is measured at very high shear rates. Likewise, the degraded atomization of slurries is not, in general, due to an abnormally high extensional viscosity, as shown in a related SwRI-funded program (Mannheimer,

1989). Rather, the degraded atomization is apparently due to the higher energies required to separate particles which are "glued" together by the liquid component of the slurry. Higher particle loadings lead to more closely spaced particles and higher energies required for atomization. Effective atomization of slurries can be achieved at high relative velocities between air and slurry drops. Sonic air velocities used in the commercial boiler and gas turbine CWS nozzle were effective in atomizing the CWS.

Variations in viscosity can lead to variations in liquid film thickness on the atomizing lip of some atomizer designs, with a resulting effect on the atomization quality. However, in atomizer designs where fuel film thickness is determined by a fuel annulus or hole which is completely filled with fuel, the effect of viscosity on atomization is usually less significant than for "prefilming" designs. Therefore, for minimum sensitivity to viscosity, atomizers for CWS should force the fuel through slots or holes which are completely filled with the CWS as opposed to prefilming designs which would be adversely affected by high slurry viscosities. If possible, the slurry velocities should be low to avoid abrasive wear of the atomizer, with the high relative velocities required for atomization supplied by atomizing air. Viscosity may also have a minor effect on mass flow rate and exit velocity at a constant differential pressure. The exit velocity is not very significant to atomization for air-assist nozzles, but is significant for pressure atomizers.

The performance of the **variable film thickness nozzle** operating with single-phase fluids in terms of average drop size can be summarized in terms of operating conditions as follows:

$$D_{32} \sim w^{0.13}\, \dot{m}_l^{0.2}\, V_g^{-1.5}\, \sigma_l^{0.6}\, \mu_l^{x} \tag{1.1}$$

where D_{32} is the volume/surface mean diameter (Sauter mean diameter), w is the liquid gap width, $\dot{m}_l$ is the liquid mass flow rate, V_g is the atomizing air velocity, σ_l is the surface tension of the liquid, μ_l is the absolute viscosity of the liquid, and $x \approx 0$ for $\mu_l < 100$cP and x = variable for $\mu_l > 100$ cP.

The same data for the variable film thickness nozzle spraying single-phase fluids may be expressed in non-dimensional form by the following expression:

$$\frac{D_{32}}{w} = 5.8(Re)^{-0.025}\,(We)^{-0.612}\,(V_r)^{0.276} \tag{1.2}$$

where D_{32} is the volume/surface mean diameter, w is the liquid gap width, Re is the Reynolds number ($\rho_g w V_g/\mu_l$), We is the Weber number ($\rho_g w(V_g - V_l)^2$), and V_r is the velocity ratio of the liquid to the gas.

Slurry atomization data for the variable film thickness nozzle do not, however, correlate with the equations developed from the single-phase data given above. Even if the shear viscosity is extrapolated to very high shear rates (ca. 50000 sec) the atomization of slurries is much worse than predicted from the correlations above. The dependence of average drop size on air velocity is not constant for the different slurries, but rather shows a decreased dependence as the particle loading increases. The slurry data correlated best with an equation of the form,

$$\frac{D_{32}}{w} \sim (Re)^{-a} (We)^{-b} (V_r)^{c} \tag{1.3}$$

where the exponents b and c varied with the loading ratio of coal to water. The exponent a, conversely, was constant and about equal to the 0.025 value found for the single-phase fluids. As the loading ratio increased, b decreased from 0.61, its pure liquid value, to near zero, roughly in accordance with the relation,

$$b = 0.61 - 0.35\ (LR) \tag{1.4}$$

where LR is the loading ratio. The exponent c increased with loading ratio from roughly 0.15 to 0.25.

The **commercial CWS nozzle for boilers and gas turbines** produced a spray when spraying single-phase fluids that was too dense to characterize. It also would operate over only a narrow range of air velocities, with the spray shape jumping into a much broader cone angle when the air velocity was reduced from its nominal value by about 20 percent. Therefore, the atomization studies were limited to micronized CWS with coal loading ratios of 40, 50 and 60 wt. % at full design fuel flow rate (340 kg/hr) and half that value (170 kg/hr) with an atomizing air flow of 90.7 kg/hr. This design resulted in effective atomization of the CWS using 620 kPa (90 psig) atomizing air pressure to produce sonic air velocities (ca. 330 m/s) at the nozzle tip. Cross-section average volume/surface mean (Sauter mean) diameters were below 50 micrometers for all the micronized CWS. The CWS data could be correlated with the coal wt. % (WF) and the slurry mass flow rate in kg/hr ($\dot{m}_l$),

$$D_{32} = 1.32(WF)^{0.30} (\dot{m}_l)^{0.40} \quad (1.5)$$

or with the shear viscosity measured at 20000 sec^{-1},

$$D_{32} = 3.38(\mu_l)^{0.049} (\dot{m}_l)^{0.40} \quad (1.6)$$

where the absolute viscosity μ_l is in cP and the liquid mass flow rate is in kg/hr.

The fuel-air ratio was determined as a function of radial distance for the commercial air-assist, CWS nozzle by deconvoluting the line-of-sight integral laser-diffraction measurements. These results are reported in the text.

Four diesel hole-type atomizers of varying diameter and length-diameter ratio were tested at pressure differentials of 3.45 to 34.5 MPa (500 to 5000 psid), and single-phase fluid viscosities of 3 to 100 cSt. Volume/surface mean (Sauter mean) diameters decreased with the pressure raised to the -0.77 power, but both average size and cone angle were independent of liquid viscosity at constant differential pressure. At constant pressure, the fuel flow rate decreased about 18 percent with an increase in viscosity from 3.3 to 100 cSt. Drop size increased slightly with hole diameter, and spray width varied inversely with length/diameter. The spray shape could be described by a jet-type model.

Tests with gas-solid suspensions were conducted with two different sizes of monodispersed glass beads in air in two tube-type nozzles of similar geometry but different sizes. The resulting particle-laden gas flows corresponded closely with predictions based on jet theory, although it was necessary to account for non-equilibrium between the gas and particle velocities at the exit of the nozzles. The peak particle flux weighted by the annular area occurred at a radial location of,

$$r = 0.0354 (x + 10D) \quad (1.7)$$

where x is the axial distance, and D is the nozzle i.d. The particle mass flow was related to the pressure differential, the Reynolds number, and the Stokes number as described in the text.

2.0 INTRODUCTION

Fuel nozzles in combustion systems introduce fuel in such a manner so as to accomplish two general objectives:

(1) The fuel must have enough surface area in contact with the air to react in the residence time available in the combustion system. For liquid fueled systems, this means that the liquid must be subdivided into small enough drops to evaporate and burn in the time available. Likewise, for solid fueled systems, the agglomerated solid fuel must be broken up sufficiently to allow air to reach the surface and react in the time available.

(2) The fuel must penetrate the air and mix to an appropriate mixture ratio throughout the combustion system. This second objective usually depends upon the proper integration of the fuel nozzle with the combustion system.

These two objectives are subject to the additional requirements:

(3) Good performance must be obtained over a range of fuel flows (and atomizing air pressure drops for airblast atomizers).

(4) For many combustion systems such as gas-turbine combustors and diesel engines, the combustion must occur uniformly within the combustion chamber without hot streaks that could lead to damage to components such as turbine blades, or cool streaks which signify inefficient use of air. Uniform combustion requires uniformity in the fuel injection process, where nonuniformity could be due to non-symmetry in a single spray nozzle or non-uniform injection rates through multiple nozzles or multiple holes in a single nozzle.

(5) For continuous combustion systems, the fuel flow rate into the combustion system must be constant, independent of combustion generated pressure oscillations in the combustion chamber. If pressure variations are allowed to affect fuel flow rate, a coupling can occur that can increase the magnitude of pressure oscillations and lead to destruction of the combustion system or flame blowout.

(6) A further requirement of fuel injection equipment in intermittent combustion systems (e.g., diesels and spark-ignition engines) is the injection of fuel at the proper time and rate relative to piston position.

The best fuel nozzle is not necessarily the one which provides the smallest drops or particles, maximizing the surface area of the fuel to the air, or which provides the most uniform mixing of fuel and air in the combustion zone. For example, the stratification of fuel in a diesel is a key to its efficient idle performance at very lean overall fuel-air ratios, well beyond the lean limit for combustion for perfectly mixed gases. Also, drops which are too small will not penetrate the combustion zone, resulting in poor fuel-air mixing. Thus, a fuel nozzle must be matched with a combustion chamber and the overall combustion process for optimum performance.

The problem of specifying fuel nozzle performance may be summarized with the following **PROBLEM STATEMENT**:

> Although fuel nozzles are generally specified in terms flow rate and spray shape (e.g., solid cone spray with a 60 degree cone angle), other important criteria such as the drop size and fuel-air mixing are usually unspecified. In those cases where some measure of drop size or fuel-air mixing is specified, the procedure used to obtain these values is not defined in any standard way, so that the reported values can generally not be compared with results for another nozzle. Thus, procedures are not available to adequately specify or compare nozzle performance.

The above problem statement applies to any fuel nozzle spraying liquid fuels or multi-phase fuel mixtures. However, in the case of multi-phase fuels such as slurries, additional problems are encountered in characterizing and correlating spray behavior. The atomization performance of nozzles spraying single-component fuels is usually correlated in terms of fuel viscosity and surface tension. Slurry fuels such as coal-water mixtures are generally non-Newtonian with viscosity varying with shear rate, as shown in this report. Further, slurries often have non-zero yield values, and are sometimes reported to have abnormally high extensional viscosities compared with their shear viscosities (Rakitsky et al, 1986). Further, surface tension is neither easily measured nor even defined for slurries. Surface tension of the continuous phase (water in the case of CWS) is well known, but may not be the appropriate correlating parameter for slurry atomization.

Also, the separation of particles necessary for atomization of slurries requires overcoming both inter-particle attractive forces and the breaking of thin liquid surfaces between the particles; therefore, the basic atomization process and energy required for slurry atomization appear to be different from that required for conventional single-component fuels. Hence, the properties of multicomponent fuels such as slurries that may be important to atomization are difficult to measure or specify.

3.0 PROGRAM OBJECTIVE

The **OBJECTIVE** of this program has been to address these shortcomings mentioned above by developing experimental techniques and data processing procedures to allow for the characterization of multi-phase fuel nozzles using well-defined techniques reproducible in different laboratories using different instrumentation. The results allow for the characterization of multi-phase nozzles in terms of coefficients-of-performance. The performance of several types of multi-phase fuel nozzles has been characterized using these procedures, and the results correlated in terms of coefficients-of-performance.

4.0 BACKGROUND

The requirements for fuel nozzles are discussed in a general way in the INTRODUCTION above. The requirements for specific combustion systems have been discussed in more detail in an earlier report for this program by Dodge et al (1986). In addition, requirements for gas-turbine combustor fuel nozzles have been described by McVey et al (1986), Hudson (1980), Sturgess (1980), Ballal and Lefebvre (1980), and Odgers and Kretschmer (1986). Some of the particular problems associated with coal fuels are discussed in the last reference above, and by Rosfjord (1985). The design of pressure-swirl atomizers, which dominated early gas turbine combustors, is described by Giffen and Muraszew (1953). More recent gas turbine combustors often include air-assist atomizers, with designs described by Lefebvre (1980, 1983, 1989).

In order to meet the requirements of injection into high-pressure air over a short period of time, diesel engines usually employ multi-hole nozzles for direct-injection engines, and pintle nozzles for pre-chamber (indirect-injection) engines. Both of these types of nozzles require very high liquid injection pressures, and air-assist atomization is not commercially used. The very high injection pressures require close-tolerance pumps which can be incompatible with CWS fuels. The requirements and design of fuel nozzles for diesels have been described by Obert (1973) and Lichty (1951). Some of the particular problems associated with the injection of coal slurries in diesels have been described by Rao et al (1989), Hsu (1989), Ryan et al (1982), Ryan and Dodge (1984), and Ryan et al (1987).

Industrial boilers often require injection of high-viscosity fuels at relatively high flow rates, and make use of the steam or high-pressure air available within the system. The commonly used Y-jet or T-jet air-assist atomizers used for high-viscosity liquid fuels such as No. 4 or No. 6 fuel oil can be used with minimal modifications for CWS fuels. Atomizers for industrial applications are described by Allen et al (1985), Pohl et al (1985), and Hauserman et al (1985).

The injection of dry coal into combustion systems is often accomplished by entraining the coal in an air stream. The nozzles used to inject the gas-solid mixtures can be as simple as a converging nozzle (Wilson, 1984), a converging-diverging nozzle with supersonic flow (Ishii and Umeda, 1986), or special tips can be used to shape the fuel flow for enhanced mixing (Liu and Schmidt, 1985).

The requirements for the fuel injection systems described above illustrate the need to characterize at least three aspects of fuel nozzle performance: (1) fuel flow rate, (2) drop or particle size distribution, and (3) distribution of fuel within the fuel spray. Fuel flow rate as a function of fuel pressure is usually easily determined and specified in terms of a flow number, which is equal to the mass flow rate divided by the square root of the pressure differential across the nozzle. (By Bernoulli's equation, the mass flow rate is proportional to the square root of the pressure differential.) But, the distribution of drop or solid particle sizes and fuel concentration throughout the spray is more difficult to determine.

The problems associated with determining and specifying the drop-size distributions of fuel nozzles are perhaps best exemplified by a recent round robin test of two sets of "standard" nozzles conducted by 15 different laboratories using 17 different drop-sizing instruments (Dodge, 1987). Even using well-defined test procedures and standard liquids, the spray characteristics measured with different instruments varied widely, as illustrated in Figure 4.1 for one of the round robin nozzles. Part of this difference was attributed to the different sampling volumes of the various instruments. For example, Figure 4.2 shows the general spray structure common to the two types of pressure-swirl atomizers used for these round robin tests, and the sample volumes of a laser-diffraction instrument compared with an instrument that measures at a point. It is clear that in cases where average drop sizes vary as a function of radius by a factor of almost 10, as was the case for the two types of atomizers used for these tests, the different sampling volumes of different instruments resulted in very different values for average drop sizes. It is clear from Figure 4.2 that the best representation would be to average the spray characteristics over the spray cross-section with appropriate weighting factors for the drop density and the area of each ring. Such a procedure has been developed during this project for instruments that sample along a line-of-sight (e.g., laser-diffraction in Figure 4.2) or at a point in the spray (e.g., phase/Doppler in Figure 4.2), and the details are presented in Appendix A.

The measurement of fuel drop density within a spray or solid particle density within a gas-solid stream can be measured with many types of optical particle sizing instruments, or by collection of samples within probes (patternator). Appendix A describes a technique for computing spatially resolved values of liquid drop volume fraction from line-of-sight integral measurements with a laser diffraction instrument. The use of patternators to determine the liquid volume flux within a spray has been discussed by McVey et al (1986).

Although the measurement of spray characteristics and correlation of those characteristics with fuel properties is difficult for liquid fuels, it is far more complicated for multi-phase fuels such as CWS. The atomization characteristics of CWS and single-phase simulants of CWS have been studied by Smith et al (1985), Cronin and Sojka (1986), Cronin et al (1985), and Rosfjord (1985). The correlations developed are generally limited to a fairly narrow range of slurry properties, and exponents on correlation equations tend to be variables rather than constants. It is unclear from previous work how slurry properties such as viscosity should be measured and correlated with atomization properties.

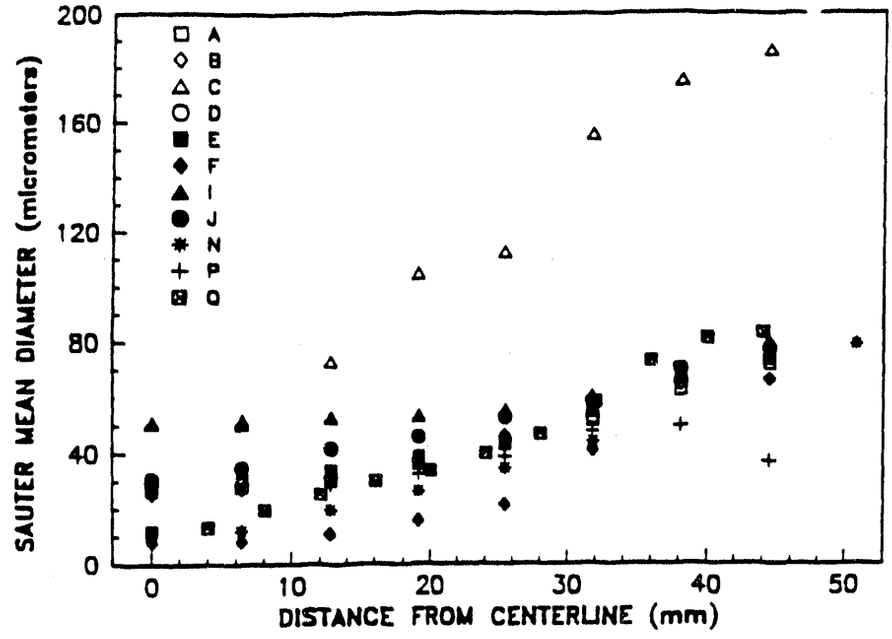

Figure 4.1. Comparison of Measured Sauter Mean Diameters (D_{32}) as a Function of Radial Location for Nominally Equivalent Sprays Using 11 Different Instruments

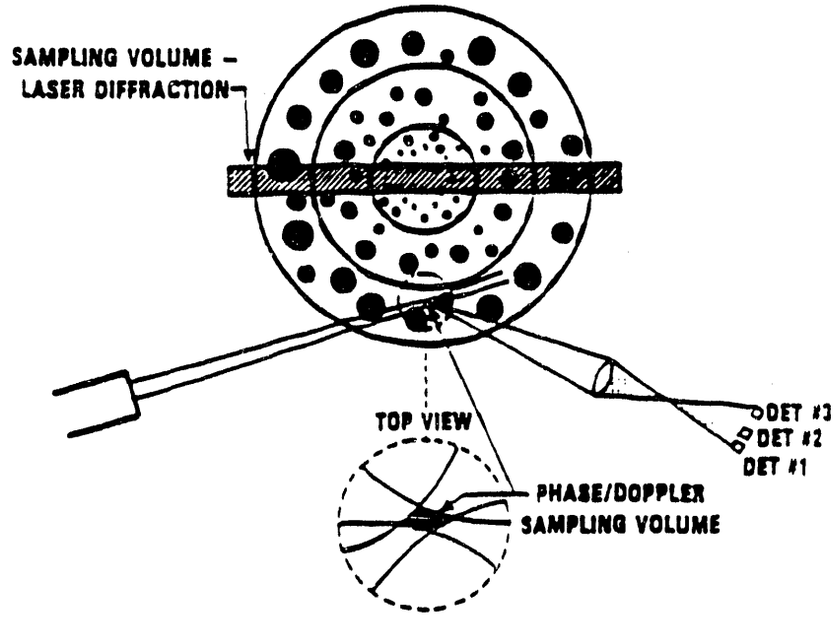

Figure 4.2. Comparison of Sample Volumes of Phase-Doppler and Laser-Diffraction Instruments

5.0 METHODOLOGY

Standardized Techniques for Characterizing Fuel Injectors

Measurements of the fuel injection characteristics of four different types of multi-phase fuel injection systems were characterized during this program, as described later. The first three types of injectors were for liquid-solid mixtures such as CWS, while the fourth type was for gas-solid mixtures such as coal entrained in air. The principal experimental diagnostic chosen for the three nozzle types used to inject liquid-solid mixtures was a laser-diffraction particle sizer that measures not only drop size, but also liquid volume fraction. This is the most common particle sizing instrument used to characterize CWS sprays. The principal experimental diagnostic for the gas-solid nozzle type was a phase-Doppler particle analyzer that measures not only particle size and volume flux, but also particle velocity. The particle velocity and volume flux were particularly important for the gas-solid nozzle, leading to the choice of the phase-Doppler instrument. It should be noted that the phase-Doppler instrument is not suitable for sizing slurry drops that are neither transparent nor perfectly smooth and round. The phase-Doppler instrument requires either transparent or smooth round drops for proper drop sizing.

Before using the laser-diffraction instrument for measurements of the CWS and single-phase liquid sprays, certain limitations of the instrument were investigated and resolved. Three problems concerning measurements with the laser-diffraction instrument were investigated and resolved during this program. The first problem was how to obtain a representative measurement of the overall spray cross-section using an instrument that samples along a line-of-sight through the spray, as shown in Figure 4.2. The second problem was how to obtain spatially resolved values of liquid volume fraction (essentially fuel/air ratio) as a function of radial location from line-of-sight measurements of volume fraction and size distribution. The third problem was specific to diesel hole-type atomizers, and pertained to the size of the laser beam relative to the spray cone diameter to measure the spatial characteristics of the spray accurately. The first two problems were resolved with techniques which have been published as a result of this program, and are described in detail in Appendix A. The third problem has been studied less extensively, but some significant results are discussed later in the section describing the diesel spray results.

In addition to the problems of obtaining a representative sample of the spray as discussed in Appendix A, it is also necessary to choose an "average" diameter to represent the fineness of the spray. Typical choices for the average drop diameter include the Sauter mean diameter (volume/surface mean diameter), D_{32}, the volume mean diameter, D_{30}, and the volume median

diameter, $D_{V0.5}$ (Allen, 1981). In words, the Sauter mean diameter is that diameter of a fictitious monodisperse spray composed of drops of uniform size and having the same drop surface to drop volume ratio as the actual spray. Since drop evaporation rates correlate closely with the surface to volume ratio, the Sauter mean diameter (volume/surface) is the most commonly used representative average diameter for combustion applications. Chin and Lefebvre (1985) have presented further reasons for the choice of Sauter mean diameter for combustion applications. Because of its widespread use in combustion applications, Sauter mean diameter (SMD or D_{32}) was chosen as the representative diameter for this program.

Experimental Apparatus

Three types of liquid-solid nozzles were tested: (1) a variable-film-thickness (VFT), air-assist, slot atomizer, (b) a commercial CWS atomizer for gas-turbine or boiler applications, and (c) diesel hole-type injectors. The gas-solid injector studies were conducted with straight tubes of two different sizes. Because the experimental arrangements were different for each of these nozzles, the discussion of the experimental apparatus for each of the nozzles is described along with the experimental results in the order listed above.

6.0 VARIABLE-FILM-THICKNESS NOZZLE

In this section, the experiments are described that used the variable-film-thickness, 2-dimensional, air-assist liquid-solid nozzle. This nozzle geometry is advantageous for two reasons. First, both the liquid gap and air gap can be adjusted to study the effects of the various film thicknesses on the atomization process. Second, the flat fan spray produced by the nozzle can be sampled with a laser-diffraction drop sizer without the complications of the cylindrical geometry associated with standard coaxial atomizers.

The discussion is organized as follows. Section 6.1 describes the experimental apparatus for operating the atomizer and characterizing the particle-size distributions. Section 6.2 describes the test liquids and slurries, including a detailed discussion of the rheological measurements of the slurries. Section 6.3 describes the results obtained in the atomization tests, and Section 6.4 summarizes those results. Section 6.5 describes the flow capacity results.

6.1. DESCRIPTION OF TEST APPARATUS FOR VARIABLE-FILM-THICKNESS, SLOT NOZZLE TESTS

A schematic of the test apparatus used for the variable-film-thickness, 2-D, air-assist atomizer is shown in Figure 6.1. Because the atomizer was an air-assist type, both liquid and air were supplied.

Liquid and Air Supply

Liquid flow was supplied by applying pressurized nitrogen over the liquid reservoir. Flow rate was adjusted by a valve just upstream of the atomizer, and measured by a Micromotion Model D-6 Coriolis-Effect flowmeter. Liquid temperature was reduced, in some cases, to increase the liquid viscosity by using a cold water bath. The liquid temperature and pressure were measured at the inlet to the atomizer using a thermocouple and pressure gauge, respectively.

Atomization air was supplied by the "house-air" compressors. Air flow rate was measured with a Brooks Rotameter Model 1110-10H3B1A, Tube R10M-25-1. Air pressures at the outlet of the rotameter, which ranged from 28 to 276 kPa above atmospheric pressure (4 to 40 psig), were monitored and used to correct rotameter readings for density effects. Air pressure was also monitored at the atomizer.

Variable-Film-Thickness Atomizer

The variable-film-thickness (VFT), 2-D, air-assist atomizer is shown schematically in Figure 6.2. The liquid flows through the center slot and air flows through the slots on each side. The air flows can be set independently, although for these tests the air flows on each side were kept equal. The liquid slot width is adjusted with screws from each side which tend to pull the normally-closed gap open. Stainless steel shims are inserted at each end of the fuel slot to maintain a constant gap width. The length of the liquid slot is 32 mm (1.25 in.), but this is reduced by the shims to about 25 mm (1.0 in.). The air slots on each side of the liquid slot are 32 mm (1.25 in.) long. The width of the air slots is made variable by the use of shims at the attachment point for the air deflectors, as shown in Figure 6.2. The majority of the data reported here were for fuel slot widths of 0.381 mm (0.015 in.) or 1.27 mm (0.050 in.), and air slot widths of 1.78 mm (0.070 in.).

Spray Drop-Size Measurements

Drop-size measurements of the spray were made with a Malvern Model 2200 laser-diffraction drop sizer. Photons in the laser beam are diffracted by the drops and the diffraction angle is characteristic of the drop size (Swithenbank et al, 1977). A multi-element detector is used to measure the diffraction angle. A computer model included as part of the instrument converts the light-scattering distribution into a drop-size distribution. This instrument was calibrated using a procedure developed at this laboratory (Dodge, 1984), and showed excellent agreement when compared with a calibrated reticle (Hirleman and Dodge, 1985). All data reported here were assumed to follow a Rosin-Rammler drop-size distribution (Allen, 1981).

For the VFT nozzle, the axial distance between the nozzle exit and the centerline of the laser beam was 57 mm.

Spray Collection

The spray was collected in a 55-gallon oil drum using twisted-metal screens for mist removal. An exhaust fan was used to provide air flow through the collection device.

6.2. TEST LIQUIDS AND LIQUID-SOLID MIXTURES

Four types of test fluids were used in the VFT nozzle tests. First, glycerol-water mixtures were used to vary the viscosity over a range from about 0.8 to 1500 cP, while maintaining surface tension in the range of about 63 to 73 dynes/cm. Second, mixtures of water and alcohol (70 vol.% ethanol and 30 vol.% methanol) were used to vary the surface tension over the range of about 23 to 73 dynes/cm while maintaining a constant viscosity of about 0.9 cP. Third, coal-water mixtures composed of 40 to 60 wt.% micronized coal with various levels of surfactants and stabilizers were tested. Finally, glass-bead water mixtures were used to study the atomization of slurries using a more reproducible solid than coal, which can have a broad range of properties.

Liquid Mixtures

The two liquid mixtures allowed the viscosity and surface tension to be varied (almost) independently, to determine their separate effects on atomization. This independence is shown in Table 6.1 and Figure 6.3, which show the range of viscosities and surface tensions for the glycerol-water and alcohol-water mixtures. Properties for the liquids are specified at the temperatures where they were determined (18°C for some of the surface tensions) or at the temperatures close to those of the tests. Most of the tests were conducted at fluid temperatures of about 27.5°C (81°F), but the properties were corrected to the actual test temperatures.

Coal-Water Mixtures

The coal-water mixtures (CWM) were blended at Southwest Research Institute (SwRI) from dry-powder, micronized coal, except for one formulation which was obtained commercially. Coal dust was blended with distilled water, surfactant, stabilizer, and biocide. The details of the blend formulations, which include coal loading of 40, 50, 55, 60, and 65 wt.% are given in Table 6.2. The coal was a micronized, cleaned, low-ash, dry-powder coal obtained from the United Coal Company (UCC) of Bristol, Virginia. The coal was from the Pond Creek Seam of Pike County in Eastern Kentucky. Its chemical properties as measured at SwRI and UCC are shown in Table 6.3, along with the purchase specification.

TABLE 6.1. VISCOSITY AND SURFACE TENSION OF LIQUIDS USED IN VFT ATOMIZATION TESTS[1]

Blend		Viscosity cP	Surface Tension dyne/cm
Glycerol wt.%	Water wt.%		
0.0	100.0	0.89 @ 25C	73.1 @ 18C
64.0	36.0	10.38 @ 27.5C	68.6 @ 18C
83.0	17.0	55.10 @ 27.5C	66.4 @ 18C
88.0	12.0	104.00 @ 27.5C	65.3 @ 18C
93.0	7.0	217.70 @ 27.5C	64.3 @ 18C
98.5	1.5	567.00 @ 27.5C	63.4 @ 18C
100.0	0.0	1499.00 @ 20.0C	63.1 @ 18C
Alcohol[2] wt.%	Water wt.%		
0.0	100.0	0.840 @ 27.5C	71.5 @ 27.5C
5.0	95.0	0.842 @ 27.5C	50.6 @ 27.5C
14.0	86.0	0.842 @ 27.5C	39.2 @ 27.5C
30.0	70.0	0.852 @ 27.5C	27.2 @ 27.5C
100.0	0.0	0.860 @ 27.5C	22.2 @ 27.5C

1 Estimated from values for 100% alcohol and 100% water

2 70 vol% ethanol, 30 vol% methanol

TABLE 6.2. COAL-WATER MIXTURES

	CF56-W	CF14-W	CF15-W
Coal, wt.%	40.0	50.0	55.0
Water, wt.%	58.4	48.4	43.4
Formaldehyde, wt.%	0.3	0.3	0.3
Surfactant Type	SF2068LF	SF2068LF	SF2068LF
Surfactant Conc., wt.%	1.25	1.25	1.25
Stabilizer Type	Xanthan	Xanthan	Xanthan
Stabilizer Conc., wt.%	0.05	0.05	0.05
	CF16-W	CF17-W	AMAX
Coal, wt.%	60.0	65.0	50.0
Water, wt.%	38.4	33.4	48.3
Formaldehyde, wt.%	0.3	0.3	0.1
Surfactant Type	SF2068LF	SF2068LF	Proprietary
Stabilizer Conc., wt.%	1.25	1.25	1.50
Stabilizer Type	Xanthan	Xanthan	Proprietary
Stabilizer Conc., wt.%	0.05	0.05	0.03

TABLE 6.3. PROPERTIES OF COAL FUEL

	Specification		UCC	SwRI
Property	Minimum	Maximum	Analysis	Analysis
Proximate Analysis				
Moisture, wt.%		8.0	0.61	0.36
Ash, wt.%		1.0	0.99	1.00
Volatile Matter, wt.%	35.0		35.63	37.04
Fixed Carbon, wt.%			62.77	61.60
Total			100.00	100.00
Heat of Combustion, Gross (Btu/lb)			15,368	15,100
Heat of Combustion, Net (Btu/lb)				14,590
Ultimate Analysis				
Carbon, wt.%				85.21
Hydrogen, wt.%				5.50
Sulfur, wt.%		1.0		0.61
Nitrogen, wt.%				3.79
Oxygen (Difference), wt.%				4.89
Total				100.00

The commercially obtained CWM was a 50 wt.% micronized coal blend from Amax Engineering Research and Development. It was blended to have properties similar to formulation CF14-W in Table 6.2. The additives were proprietary to Amax, but the surfactant and stabilizer concentrations were similar to those used at SwRI, as shown in Table 6.2.

Particle size analysis of the powdered coal can be performed with two different techniques at SwRI. The first technique involves a combination of scanning electron microscopy (SEM) and computerized image analysis. First SEM photographs of the particles are made, and then Image Plus (Dapple Systems) software is used to edit the images as projected on a video screen and to automatically size the particles. This system is only suitable for sizing the dry particles. The second particle sizing system is the laser-diffraction particle sizer. Both of these systems have been used in this program. The size distribution of the coal powder used for blending CWM at SwRI were sized with the SEM and image analysis system, with results as shown for the "as-received" coal in Figures 6.4. The top particle size (95 percent wt. or vol. fraction below size) can be seen from Figure 6.4 to be 15 micrometers. The once-ground and twice-ground coals were used in another program at SwRI. The particle-size distribution for the Amax CWM was determined by diluting the CWM with water, and then analyzing the sizes with the Malvern laser-diffraction instrument. The results are shown in Figure 6.5. The top particle size (95 percent cut) was 18 micrometers. Some of the rheological properties of the CWM have been measured and are described later.

Glass-Bead and Water Mixtures

The glass-bead and water mixtures were blended with Xanthan as a stabilizer. Xanthan was blended with water at the rate of 0.45 wt.% before the addition of the glass beads. This resulted in a Xanthan concentration in the final slurry of 0.09 to 0.166 wt.%, depending on the glass-bead weight fraction. A larger amount of stabilizer was required for the glass-bead slurries than the CWM because of the higher density of glass beads (specific gravity of about 2.4 compared with 1.4 for coal). Two size distributions of glass beads were obtained from Ferro Corp. The finer distribution is designated number 4000, and has a nominal size range of 1 to 37 micrometers. The cumulative size distribution measured by the Malvern laser-diffraction instrument is shown in Figure 6.5, which shows a top particle size (95 percent cut) of 38 micrometers. The coarser glass beads are designated 2332.5 and have a nominal size range of 44 to 62 micrometers. These coarser beads were not successfully used due to problems in stabilizing the mixtures.

The glass beads were blended in water to get the same volume fraction, or packing density, as the coal-water mixtures. Because the specific gravity of the glass beads was greater than that of the coal (2.4 versus 1.4), the weight fraction of the glass-beads in the mixtures was significantly larger than that of the coal to get equivalent volume fraction. Coal-water mixtures are usually specified by weight fraction. From Table 6.4, it may be seen that a 50 wt.% CWM requires a solids wt.% of 63.2. The weight fractions of glass-bead solids are shown in Table 6.4 to achieve equivalent volume fractions for 50, 60, and 70 wt.% CWM.

TABLE 6.4. COMPARISON OF WEIGHT FRACTIONS REQUIRED FOR EQUIVALENT VOLUME FRACTIONS OF COAL-WATER AND GLASS-BEAD WATER MIXTURES

Coal-water mixtures			
% by wt. solids	50.0	60.0	70.0
% by vol. solids	41.7	51.7	62.5
Glass-bead water mixtures			
% by wt. solids	63.2	72.0	80.0
% by vol. solids	41.7	51.7	62.5

Rheological Measurements of Test Liquids and Solid-Liquid Mixtures

The viscosities of the glycerol-water and alcohol-water mixtures were determined with traditional viscometer tubes, with results as presented previously in Table 6.1 and Figure 6.3. Surface tensions were measured with a DuNouy Ring and reported in the same table and figure.

However, the characterization of the solid-liquid mixtures is considerably more involved. Surface tensions cannot be measured using any conventional device, and even defining surface tension in these complex suspensions is difficult. Slurries are also usually non-Newtonian, with viscosity varying with shear rate, and are sometimes time-dependent. Both a bob-and-cup rotational viscometer and a capillary-tube viscometer were used to characterize properties of some of the slurries. The rotational viscometer was used over the shear rate range of about 10 to 1000 sec^{-1}. Different gaps were used in the rotational viscometer and different tube diameters and length/diameter ratios in the capillary-tube viscometer to check for slip and other non-ideal effects. Generally, measurements were made with both increasing and decreasing shear rates to evaluate hysteresis effects.

Results for the Amax 50 wt.% coal-water slurry are shown in Figure 6.6 for a shear rate range of 10 to 10000 sec^{-1} and in Figure 6.7 for the range of 500 to 70000 sec^{-1}. Some hysteresis and possible plugging were observed under some conditions, but these measurements established the general rheological behavior over a very broad range of shear rates.

The 50 wt.% CWM blended at SwRI (CF14-W in Table 6.2) exhibited similar behavior to the Amax CWM over the lower range of shear rates, as shown in Figure 6.8. Also shown in Figure 6.8 are the apparent viscosities for the other CWM in Table 6.2. The high shear rate viscosity (apparent) over the shear rate range from 3,000 to 50,000 s^{-1} is shown for the 40, 50, 55, and 60 wt.% CWM in Figures 6.9 - 6.12. The non-linear increase of viscosity with coal loading is clear from Figures 6.8 - 6.12. Also the non-Newtonian behavior of these CWM is clearly demonstrated, with shear-thinning behavior at lower shear rates and shear-thickening behavior at higher shear rates. The AMAX coal slurry shear thickens more than the comparable 50 wt.% CWM blended at SwRI, but the reason for this difference in behavior is unknown.

The glass bead and water mixtures also showed non-Newtonian rheological behavior, but different from the CWM. The 63.2 wt.% glass-bead slurry, equivalent in volume fraction to the 50 wt.% CWM, had shear-thinning rheological properties over the entire shear-rate range as shown in Figure 6.13. Due in part to the high concentration of Xanthan stabilizer (0.166 wt.%), this slurry exhibited a high viscosity at low shear rates. However, at higher shear rates suggested to be important to atomization (ca. 10000 sec^{-1} or greater), the viscosity is on the order of only 20 cP, which should lead to good atomization quality.

Glass beads were also blended with a 50 cP viscosity glycerol-water mixture to evaluate the effects of viscosity of the continuous phase on the rheology and atomization of slurries. The slurry was blended with 59 wt.% glass beads to get the same volume fraction as a 50 wt.% CWM. The rheology was evaluated with both a rotational viscometer and a capillary tube viscometer with results as shown in Figure 6.14. This slurry is shear-thinning at lower shear rates, but appears to have a fairly constant viscosity at shear rates of about 1000 sec^{-1}.

6.3. ATOMIZATION RESULTS FOR VARIABLE-FILM-THICKNESS, SLOT ATOMIZER

The test apparatus described in Section 6.1 has been used to evaluate the atomization of the liquids and slurries described in Section 6.2. Both nozzle operating conditions and liquid and slurry properties have been varied to evaluate the various effects on atomization. Specifically, atomizer operating conditions have been varied in terms of air and liquid flow rates and in the liquid film thickness. Viscosity and surface tension have been varied independently by using glycerol-water and alcohol-water mixtures. Coal-water mixtures with various coal loadings, surfactant concentrations, and stabilizer concentrations have been evaluated for atomization characteristics. Glass-bead and water mixtures have also been evaluated.

Many of the experimental results reported here were obtained for at least two different liquid flow rates, five different air flow rates, and two different liquid gap heights. This allows both an evaluation of the effects of varying these parameters, and an evaluation of the repeatability of the trends observed at any single condition. Liquid flow rates were varied over a range of 0.293 kg/min (0.646 lbm/min) to 0.885 kg/min (1.95 lbm/min) through liquid gaps of 0.381 mm (0.015 in.) and 1.27 mm (0.050 in.). These mass flow rates correspond to velocities on the order of 0.5 to 1.5 m/s for the 0.381 mm gap and 0.15 to 0.46 m/s for the 1.27 mm gap. Reynolds numbers for the liquids were a maximum of about 700, with correspondingly lower Reynolds numbers for liquids and slurries of higher viscosities. For this atomizer the Reynolds number for the liquid is given by $Re = 656\dot{m}(kg/\min)/\mu(cP)$.

Air mass flow rates varied from 0.25 to 1.14 kg/min (0.55 to 2.5 lbm/min). This corresponded to air velocities of 31 to 143 m/s. For the 1.78 mm air gap, the air velocity is related to the mass flow rate by $V(m/s) = 125\dot{m}(kg/\min)$. Although data are presented in this report in terms of air mass flow rate, air velocity is probably a more appropriate correlating parameter.

A more complete listing of experimental results has been given by Dodge et al (1987), but selected results are presented here.

Effect of Liquid Flow Rate on Atomization

The effect of liquid flow rate on average drop size as represented by the Sauter mean diameter (Allen, 1981) or D_{32} is shown in Figure 6.15 for water with a viscosity of 0.8 cP. The Sauter mean diameter or D_{32} is defined as,

$$D_{32} = \frac{\sum_i N_i D_i^3}{\sum_i N_i D_i^2} \tag{6.1}$$

where N_i is the number of drops of diameter D_i.

Tests with glycerol-water mixtures with viscosities of 0.8, 48, and 206 cP showed that D_{32} increases with the liquid flow rate raised to the 0.2 power.

Effect of Air Flow Rate on Atomization

The effect of air flow rate on D_{32} may be seen in Figure 6.16 for alcohol-water mixtures of various surface tensions. As expected for an air-assist atomizer, the average drop size depends strongly on air velocity (or mass flow rate), with D_{32} being proportional to the air velocity raised to the -1.5 power.

Effect of Surface Tension on Atomization

In air-assist atomizers, the surface tension is usually a significant correlating parameter in the atomization process. This was also true with this atomizer. Figure 6.17 shows the same data as shown in Figure 6.16 except that D_{32} is presented explicitly as a function of surface tension for the alcohol-water mixtures. It can be seen that for all air flows, the average drop size depends on the surface tension of the liquid. The dependence can be summarized as D_{32} increases with surface tension raised to the 0.6 power.

Effect of Liquid Viscosity on Atomization

Liquid viscosity is often a significant correlating parameter for atomization processes. However, in some air-assist atomizers, changes in viscosity have little or no effect on average drop sizes produced. Depending on atomizer design, viscosity can be important in determining the thickness of the liquid film as it leaves the atomizer. For example, in a pressure-swirl atomizer, increases in viscosity lead to a reduction in the air core and an increase in the liquid film thickness. Increases in the film thickness lead to increases in average drop size at sheet breakup. Likewise, in prefilming air-assist atomizers, increases in viscosity may lead to increases in film thickness and drop size.

However, in the VFT atomizer the liquid film thickness at the nozzle exit is determined by the slot width and is independent of the viscosity. Downstream of the nozzle exit and prior to sheet breakup, the liquid sheet thickness may depend upon the liquid viscosity or visco-elastic effects. However, because the film thickness at the nozzle exit is independent of viscosity, it might be expected that the drop sizes produced would be relatively independent of viscosity.

For these experiments the viscosity of the single-phase fluids were varied over more than three orders of magnitude using glycerol-water blends, with results as shown in Figures 6.18 and 6.19. Between 1 and 100 cP viscosities, the Sauter mean diameter (D_{32}) is essentially independent of viscosity. For viscosities above 100 cP, D_{32} increases somewhat with viscosity, although the viscosity dependence is weak and seems to vary with the liquid flow rate and liquid slot width. This behavior is not well understood at this point, but it does establish the atomization behavior over a broad range of viscosities for single-phase fluids in the VFT atomizer.

Atomization of Coal-Water and Glass-Bead Water Mixtures

The atomization of coal-water mixtures (CWM) was investigated over the same range of atomizer conditions as used for the single-phase fluids. Limited tests were performed at the 0.381 mm (0.015 in.) liquid gap widths, but plugging was a problem under those conditions. Thus, a majority of the results are reported for the 1.27 mm (0.050 in.) gap width.

The atomization of the Amax 50 wt.% micronized CWM is compared with that of glycerol-water mixtures having a viscosity range of 0.8 to 1500 cP in Figure 6.20. From Figures 6.6 and 6.7 the viscosity of the Amax CWM varies from about 30 to 160 cP. However, Figure 6.20 shows that the atomization performance of the CWM is significantly worse than even the 1500 cP glycerol-water mixture. Could the atomization of the CWM be limited by the coal particle-size distribution? Reference to Figure 6.5 shows the top particle size (95 wt.% cut) to be 18 micrometers, much smaller than the smallest D_{32} for the CWM in Figure 6.20, indicating the drop size is not limited by the coal particle size. These results suggest that the atomization of this micronized CWM can not be predicted from the shear viscosity using single-phase fluid correlations, even using viscosities measured at shear rates as high as 70000 sec^{-1}. These results were obtained for the 0.381 mm (.015 in.) fuel gap, but similar results were found using the wider 1.27 mm (.050 in.) fuel gap as discussed below.

The atomization of the Amax 50 wt.% micronized CWM was also evaluated in the VFT nozzle at the 1.27 mm fuel gap with results as shown in Figure 6.21 for a flow rate of 0.885 kg/min. Again, the CWM with a shear viscosity of 30 to 160 cP showed much poorer atomization at the higher air flows than single-phase fluids with viscosities of 0.8, 50, or 500 cP. This supports the previous observation that viscosity alone does not explain the degraded atomization of the CWM.

Figure 6.21 also shows atomization results for the 63.2 wt.% glass-bead slurry which has the same solids volume fraction as the 50 wt.% CWM. Although the glass-bead slurry has larger base particle sizes than the CWM (from Figure 6.5), and a higher level of Xanthan stabilizer, its atomization at high air velocities is better than the CWM. Comparing the viscosity of the Amax CWM from Figures 6.6 and 6.7 with that of the glass-bead slurry in Figure 6.13, it may be seen that the viscosity of the CWM is higher only for shear rates greater than 2000 sec^{-1}. From Figure 6.21, note that the atomization characteristics of the CWM and glass-bead slurry are similar at low air flows (corresponding to lower shear rates) and diverge at higher air flows (corresponding to higher shear rates). The comparisons of the CWM and glass-bead slurry atomization give qualitative support to the argument for correlating atomization with high-shear rate viscosity.

Coal loading in CWM has a direct impact on atomization quality as shown in Figures 6.22 and 6.23. These CWM were blended at SwRI and the 40, 50, 55, and 60 wt.% coal blends correspond to CF56-W, CF14-W, CF15-W, and CF16-W in Table 6.2 respectively. The atomization quality is in the same rankings as the viscosities of the CWM shown in Figures 6.8 - 6.12, but again the atomization is much poorer than single-phase fluids of the same viscosities.

The loading of glass-bead water mixtures also has an effect on atomization as shown in Figure 6.24. Increasing loading leads to degraded atomization, similar to the trend observed for CWM. However, at lower air velocities (lower shear rates) the CWM tend to converge to similar average drop sizes, while at higher air velocities (higher shear rates) the CWM tend to separate based on coal loading. The glass-bead water mixtures are different from the CWM in that the more highly loaded slurry exhibits larger average drop sizes at all air velocities. At higher air velocities the glass-bead slurries atomize better than CWM of the same volume fraction loading (50 wt.% CWM and 63.2 wt.% glass-bead, 60 wt.% CWM and 72.0 wt.% glass-bead). It may be speculated that the relatively poorer atomization of the CWM at high air shear rates is due to their higher viscosities at high shear rates.

Effect of Additives on Atomization of Coal-Water Mixtures

Because the atomization of the CWM did not correspond to that of a Newtonian fluid of the same viscosity, and because the additives used in the preparation of CWM were suspected of having non-ideal rheological properties, the effect of additive concentration on atomization was evaluated. Both surfactant concentration and stabilizer concentration were varied to determine their impact on atomization. Neither could be reduced to zero. Some surfactant was required in order to allow wetting of the powdered coal by the water. Some stabilizer was required to keep the coal suspended long enough to obtain atomization data. The effect of reducing the surfactant concentration of the 50 wt.% CWM (CF14-W) from the standard 1.25 wt.% by a factor of two and a factor of four is shown in Figure 6.25. The reduced surfactant levels make blending the CWM more difficult and degrade the pourability of the mixture, but the atomization is not strongly affected by even a factor of four reduction in surfactant concentration.

Xanthan stabilizers are suspected of having abnormally large extensional viscosities (relative to shear viscosities), and also of being visco-elastic and exhibiting yield. Any of these properties could result in degraded atomization relative to what would be expected from the measured shear viscosity. To evaluate this possibility, Xanthan concentration in a 50 wt.% CWM (CF14-W) was increased by a factor of four above the standard level of 0.05 wt.% with results as shown in Figure 6.26. Although the viscosity at low shear rates appeared to increase significantly (from observed handling properties), the atomization was relatively unaffected. As a further evaluation of possible atomization degradation by Xanthan stabilizer, the relatively high level of 0.45 wt.% Xanthan was added to water and a 500 cP glycerol-water mixture and the atomization was compared to that for the same fluids without the stabilizer. As shown in Figure 6.27, the high concentration of stabilizer, which seemed to significantly increase the low shear rate viscosity, had little effect on the atomization. These results for the Xanthan tests suggest two important points. First, the shear viscosity at low shear rates has little effect on the atomization of single-phase fluids or CWM. Second, because of the independence of atomization on low shear rate viscosity, high levels of stabilizers might be used to increase stability of CWM without degrading atomization. The second point would have to be verified on the particular CWM being used.

Effect of Continuous-Phase Properties on Slurry Atomization

The surface tension of single-phase fluids has been shown in Figure 6.17 to be important to the atomization process. Therefore, the surface tension of the continuous phase of a 50 wt.% CWM (CF14-W) was reduced by the substitution of methanol for 20 wt.% of the water in the CWM. This reduced the surface tension of the continuous phase from about 73 to 46 dyne/cm (mN/m). The atomization of the reduced surface tension CWM and the standard CWM (50 wt.%) are compared in Figure 6.28, which shows negligible difference in atomization behavior. The same level of methanol substitution for water was made in a glass-bead water mixture and again the results were not dramatic. Thus, although surface tension is critical in the atomization of single-phase fluids, it may be that other factors dominate the atomization of slurries.

Using a similar concept, the viscosity of the continuous-phase of a glass-bead and water mixture was increased by the substitution of glycerol for some of the water. The viscosity of the continuous phase was increased from about 0.8 to 50 cP, with results as shown in Figure 6.29. In contrast with the results for the variation of surface tension, the increase in viscosity dramatically degraded the atomization. Of course, the viscosity of the continuous-phase was changed by a factor of over 60, while the surface tension was changed by only 37 percent, but previous tests with single-phase fluids indicated only minor sensitivity to viscosity. The viscosities of the two slurries, both with and without glycerol, were previously presented in Figures 6.13 and 6.14. Because more Xanthan was used to stabilize the lower continuous-phase viscosity mixture (0.17 wt.% versus 0.13 wt.%), the viscosity at very low shear rates was higher for the mixture without glycerol. However, at a shear rate of 1000 sec^{-1} the glycerol-containing mixture was about 13 times the viscosity of the water based mixture. These results for the glycerol-containing slurries suggest that the atomization of slurries depends upon the viscosity of the continuous phase.

6.4. SUMMARY OF DROP SIZE RESULTS FOR VARIABLE-FILM-THICKNESS, SLOT ATOMIZER

Atomization tests with the variable-film-thickness, 2-D, air-assist atomizer using single-phase fluids showed that the average drop sizes as represented by the Sauter mean diameter, or D_{32}, varied with the atomizer operating conditions and the liquid properties. These results may be summarized as follows.

$$D_{32} \sim \dot{m}_L^{0.2} V_A^{-1.5} \sigma_L^{0.6} \mu_L^x w^{0.13} \tag{6.2}$$

where:
- $\dot{m}_L$ = liquid mass flow rate
- V_A = atomizing air velocity
- σ_L = surface tension of liquid
- μ_L = absolute viscosity
- w = nozzle width
- x = 0, $\mu_L < 199cP$
- x = variable, $\mu_L > 100cP$

The correlation of the slurry atomization results is more difficult. The dependence of Sauter mean diameter (D_{32}) on air velocity is less for the slurries than the single-phase liquids, but the dependence varies with the coal loading. These trends correspond qualitatively to what might be expected based on the measured shear viscosity for the CWM. As the air velocity increases, the shear rate increases, and because the CWM are shear-thickening at higher shear rates, the effective viscosity increases with air velocity. However, it is clear that the atomization of CWM cannot be predicted from the shear viscosity using the same relations as developed for single-phase fluids. The atomization of micronized CWM is significantly worse than what would be predicted from the shear viscosity alone, even based on very high shear rates (ca. 50000 sec^{-1}). The presence of particles changes the basic atomization process, and introduces new cohesive forces in addition to those present in single-phase fluids This is particularly apparent at high air shear conditions where the smallest drops are produced.

Drop sizes produced with the micronized CWM at reasonable air velocities are not limited by the base particle size. The smallest drops produced with CWM were on the order of 80 micrometers, while the coal particles were below 20 micrometers in diameter. A glass-based slurry

of significantly larger base particle size than the coal slurry atomized to smaller average drop size at high air velocities. This behavior correlated with the high-shear-rate viscosities which were greater for the CWM than the glass-bead slurry.

Changes in the viscosity of the continuous-phase of a glass-bead slurry were shown to dramatically affect atomization, while changes in surface tension of the continuous-phase had little impact on atomization. This behavior was different from that of the single-phase fluids which were more sensitive to surface tension than viscosity in determining atomization quality. This observation supports the concept that atomization of slurries is dominated by particle-particle interaction, and is different from atomization of single-phase liquids.

6.5. FLOW CAPACITY RESULTS

The flow capacity as given by the flow number is not so significant for an air-assist atomizer like the VFT nozzle as for a pressure atomizer where high liquid pressures are required to produce high liquid velocities for effective atomization. However, the flow number expressed in the conventional units of lbm/hr psid (for conversion to kg/s pa, multiply by 1.52 E-6) was calculated for several of the glycerol-water mixtures for the fuel gaps of 0.381 mm (0.015") and 1.27 mm (0.050"), with the results as shown in Figure 6.30. The flow number decreases with increasing viscosity, as expected, but does not increase with increasing fuel gap as much as it is expected to. The flow number for the AMAX coal through the 0.381 mm fuel gap was about 25, in agreement with the relatively low viscosity measured for this CWS.

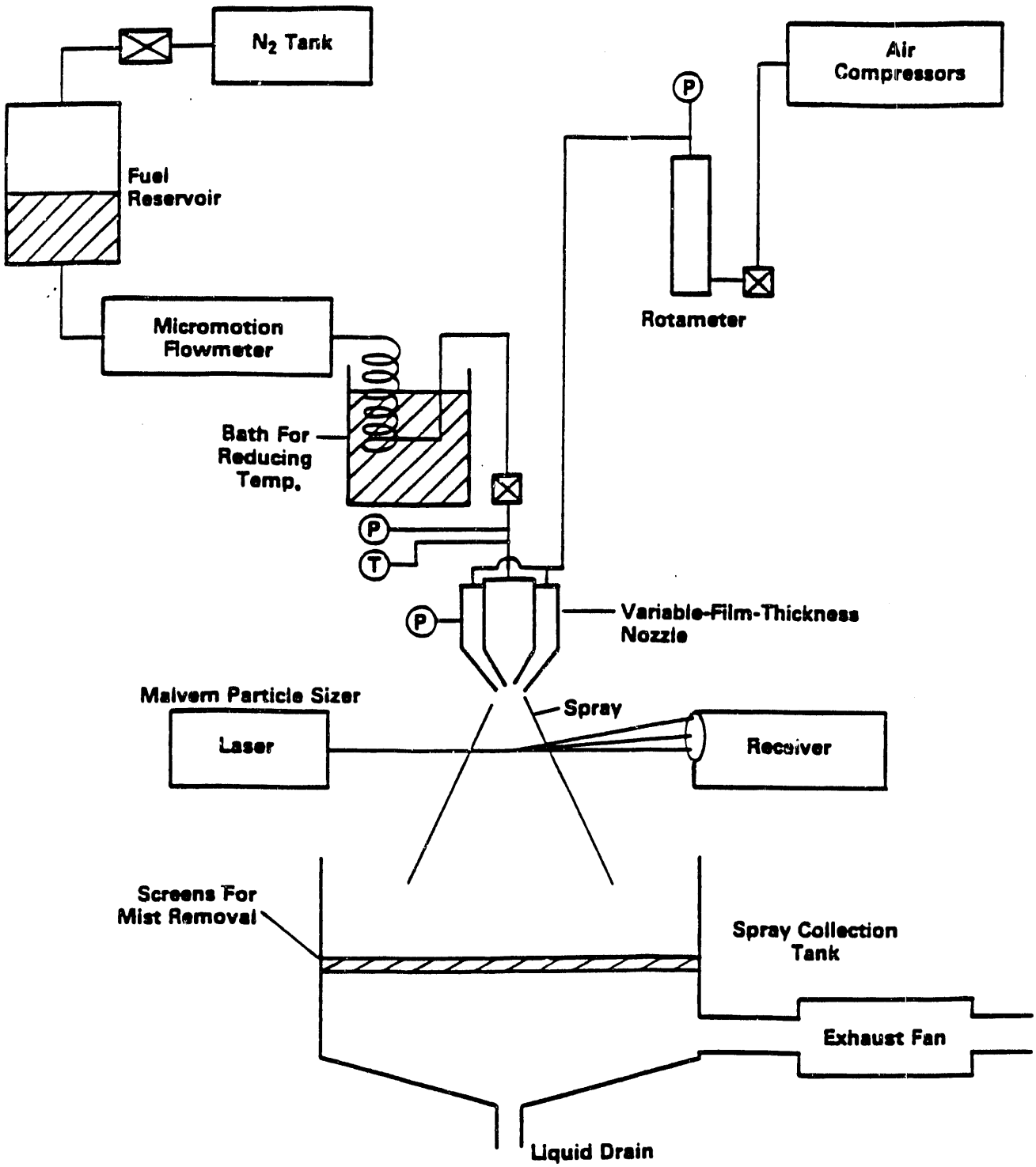

Figure 6.1. Experimental Apparatus for Variable-Film Thickness Nozzle Tests

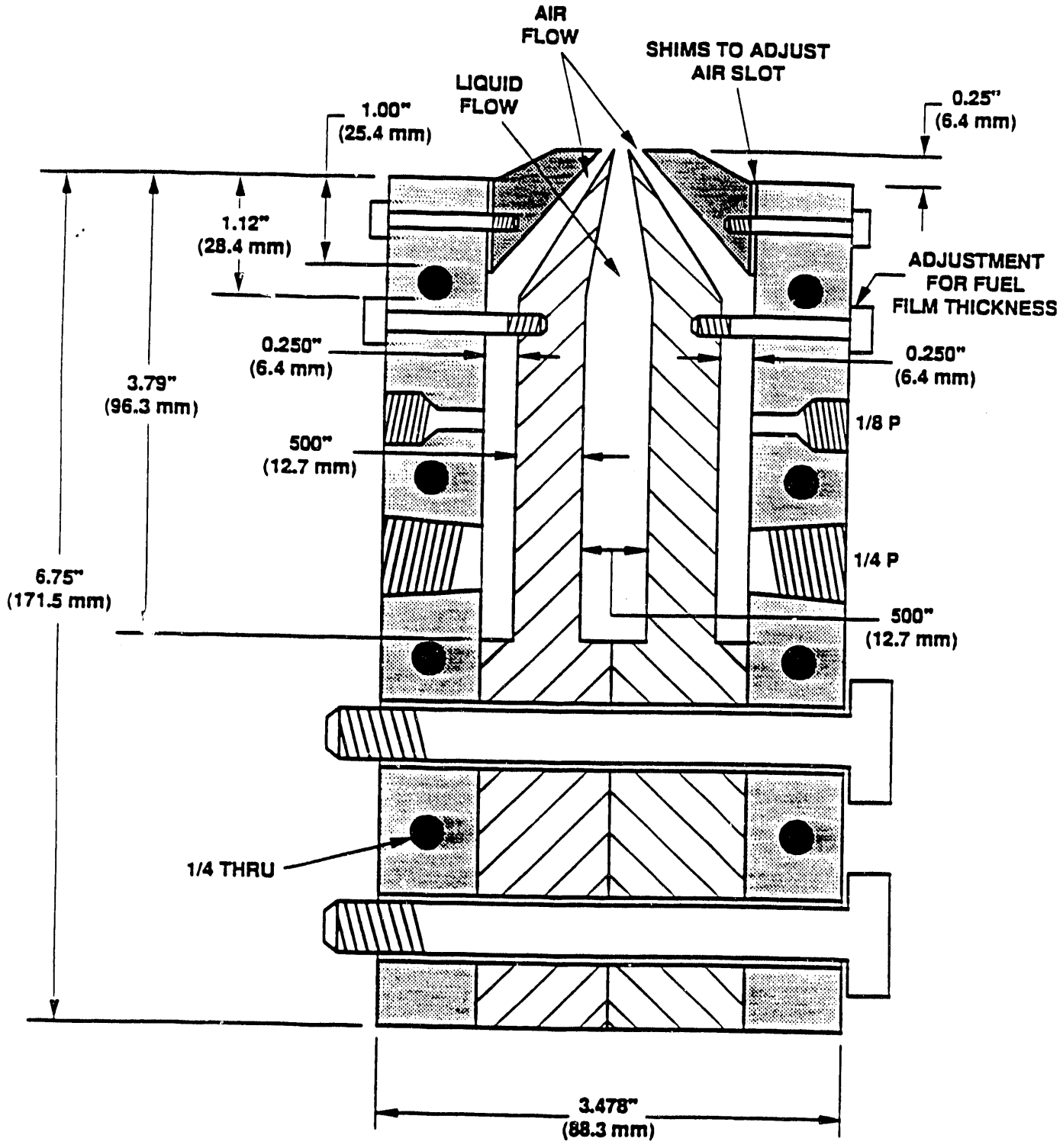

Figure 6.2. Schematic of Variable-Film-Thickness, 2-D, Air Assist Atomizer

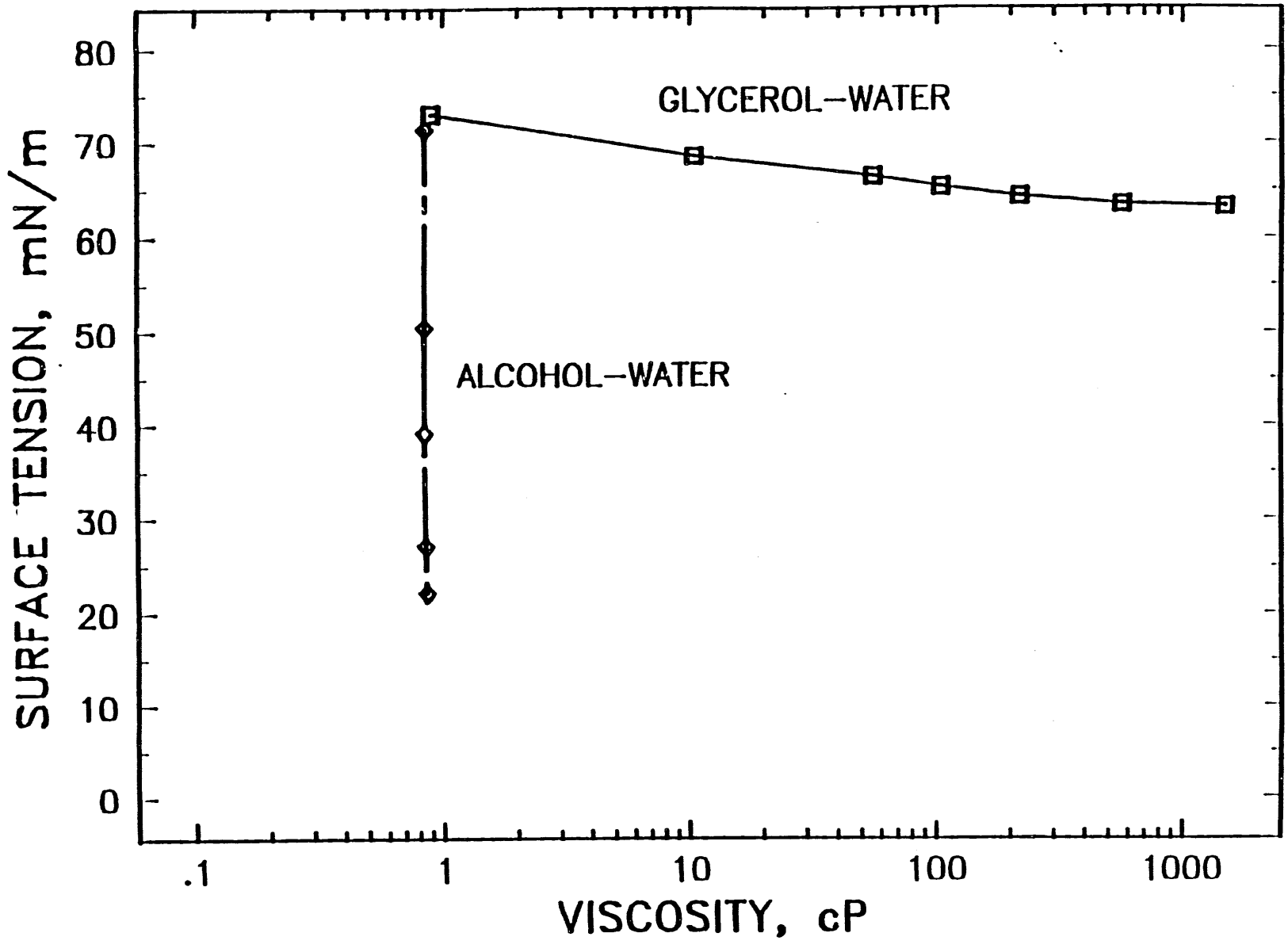

Figure 6.3. Physical Properties of Glycerol-Water and Alcohol (70 vol.% ethanol, 30 vol.% methanol) - Water Mixtures Showing Independent Variation of Surface Tension and Viscosity

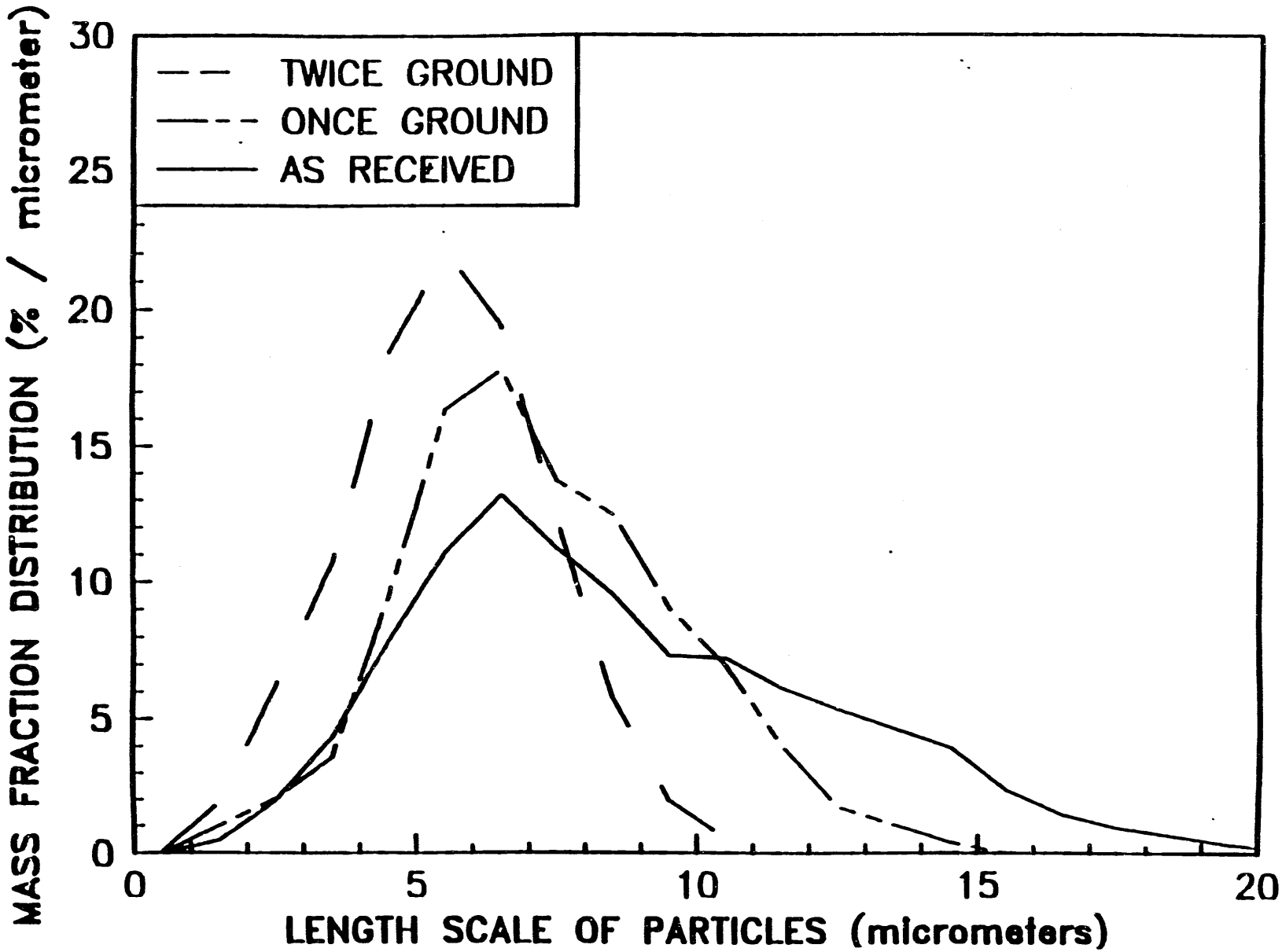

Figure 6.4. Cumulative Coal Particle-Size Distribution for Dry-Powder Coal Used in Blending Coal-Water Mixtures

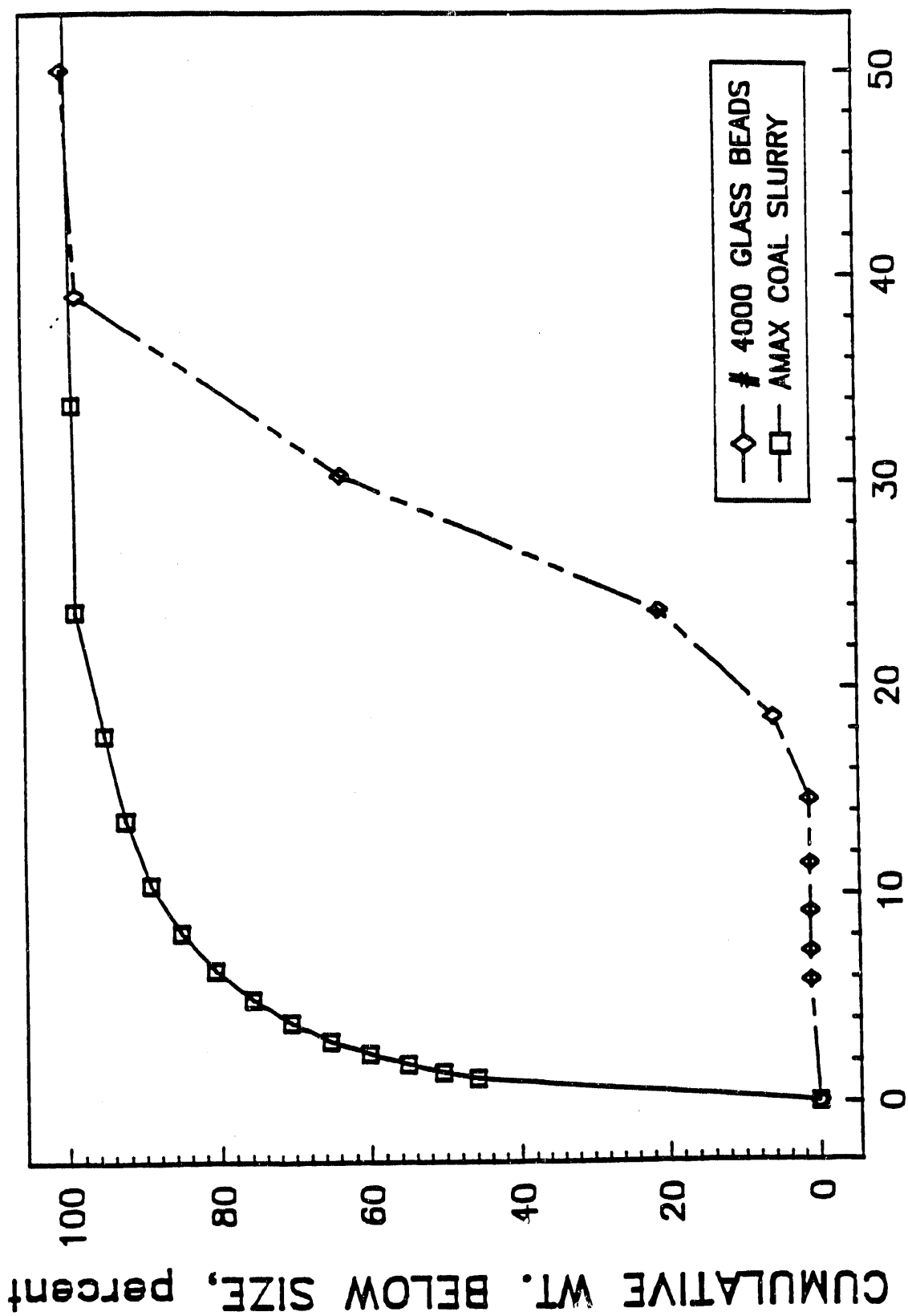

Figure 6.5. Cumulative Particle-Size Distribution for Amax Coal Slurry and Ferro #4000 Glass Beads

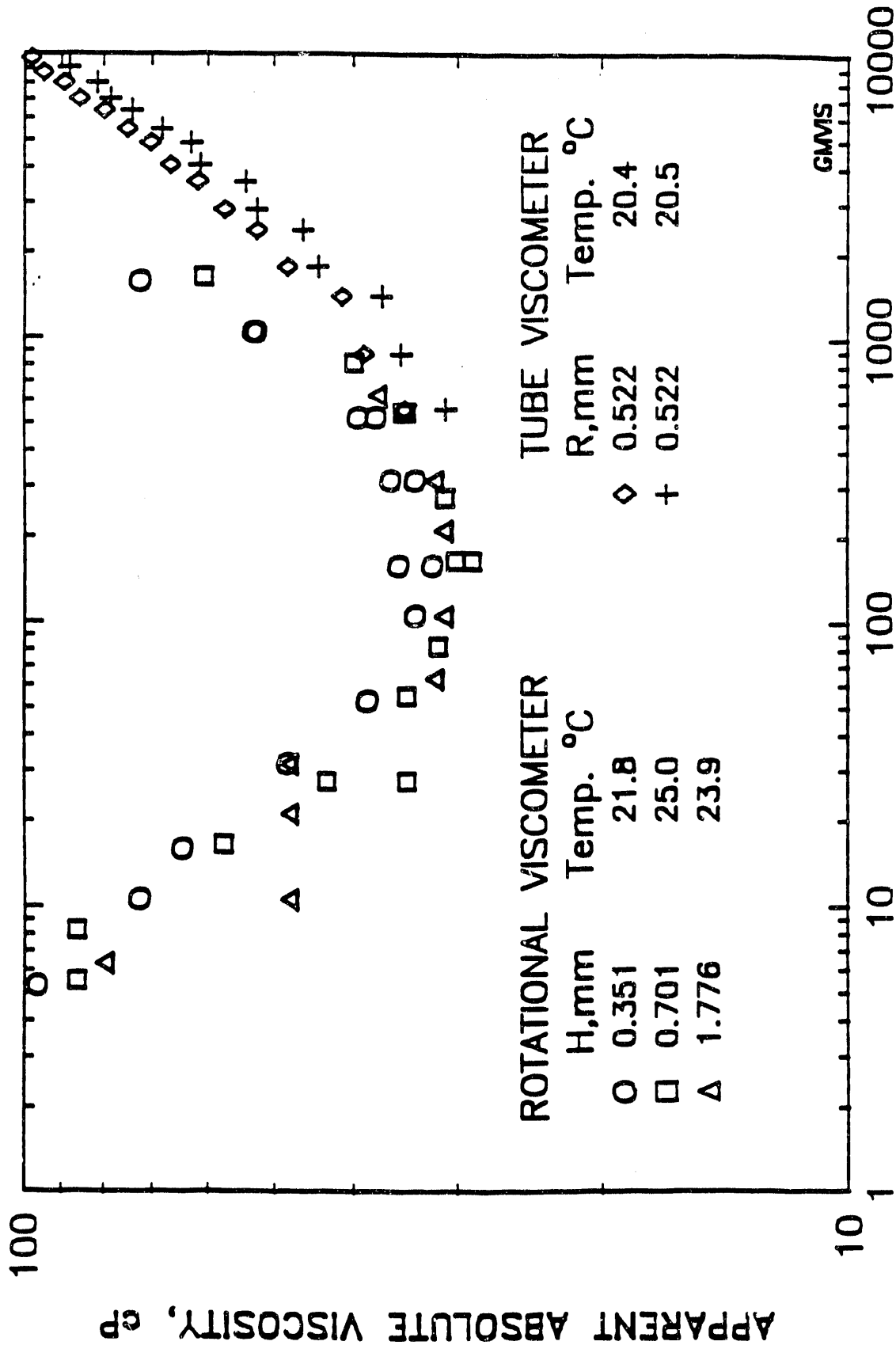

Figure 6.6. Apparent Viscosity for Amax 50 wt.% Micronized Coal-Water Mixtures for Shear Rate Range of 10 to 10000 sec^{-1}

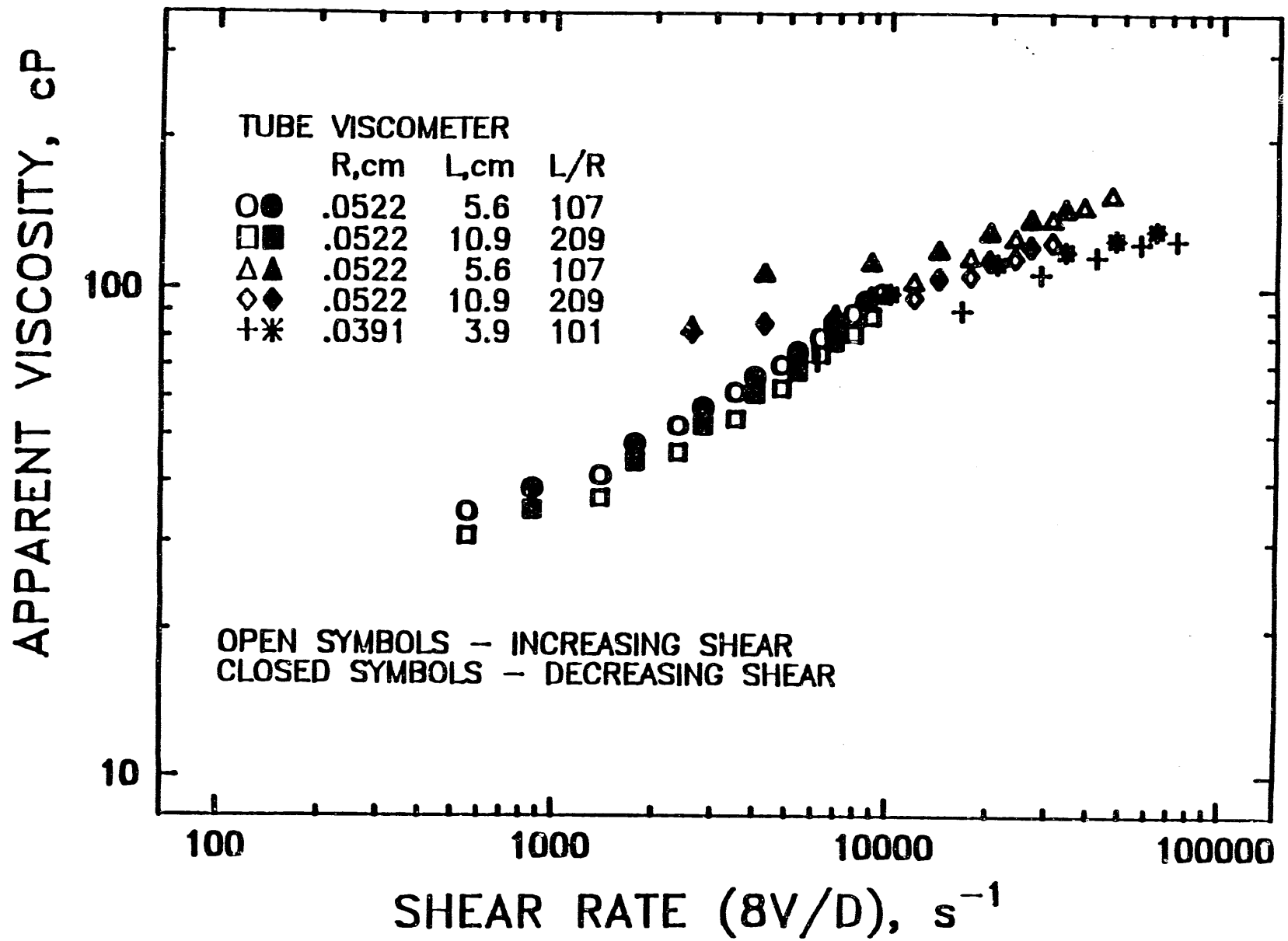

Figure 6.7. Apparent Viscosity for Amax 50 wt.% Micronized Coal-Water Mixture for Shear Rate Range of 500 to 70000 sec^{-1}

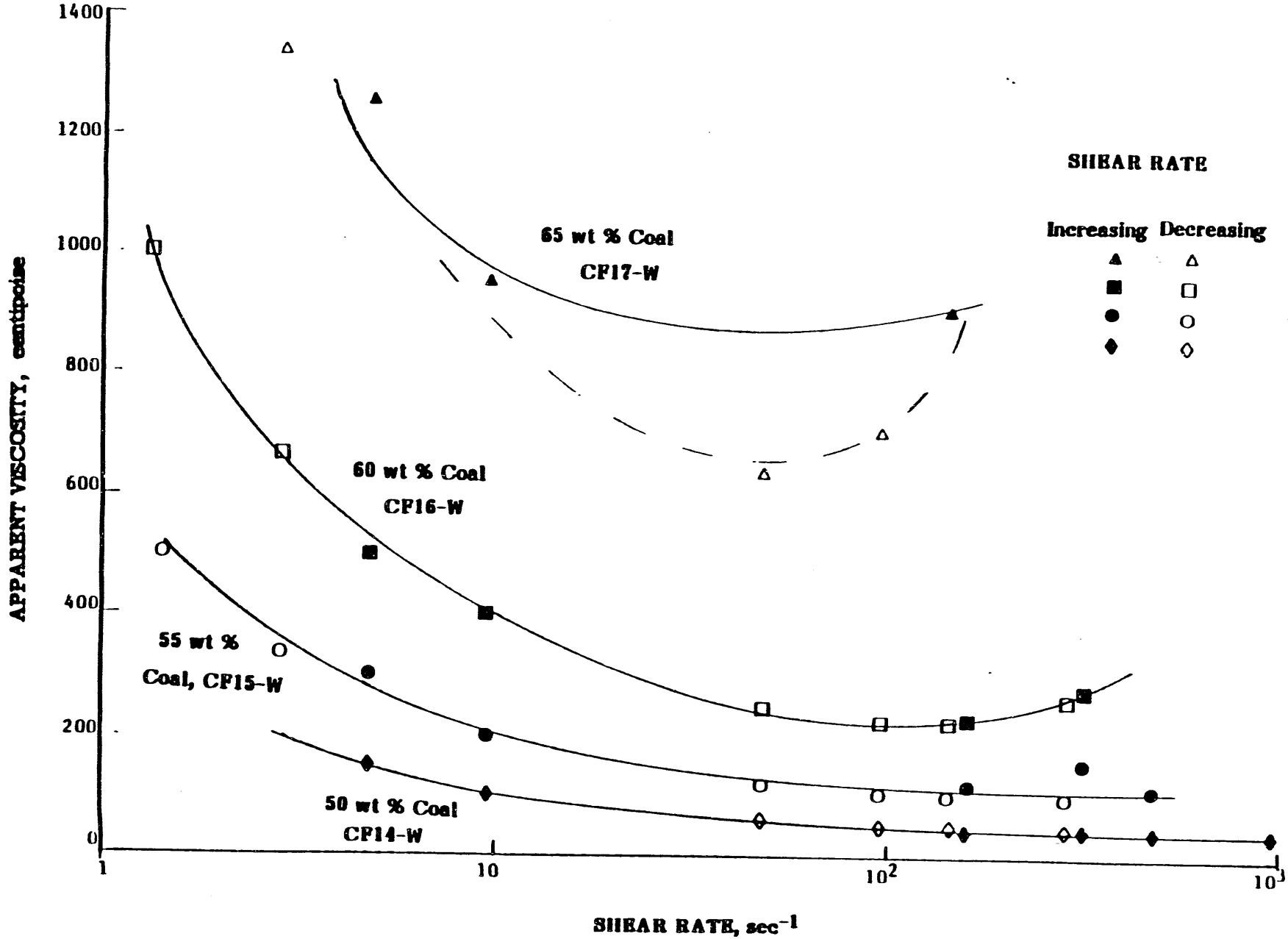

Figure 6.8. Apparent Viscosity Versus Shear Rate for 50, 55, 60, and 65 wt.% Micronized Coal-Water Mixtures Blended at SwRI

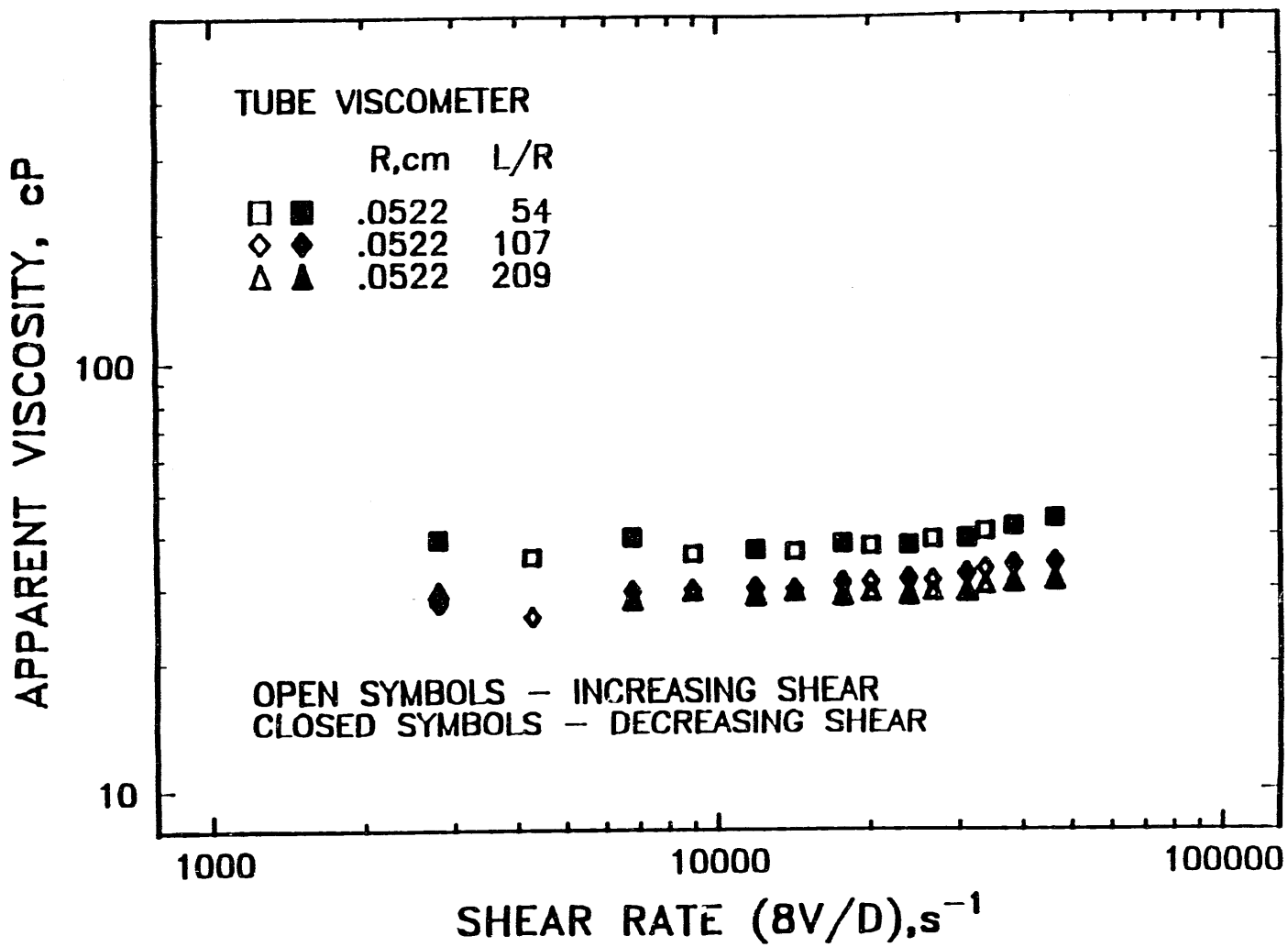

Figure 6.9. Apparent Shear Viscosity for 40 wt.% Micronized Coal-Water Mixture, CF56-W, Over Shear Rate Range of 3000 to 50,000 sec^{-1} (21.0°C)

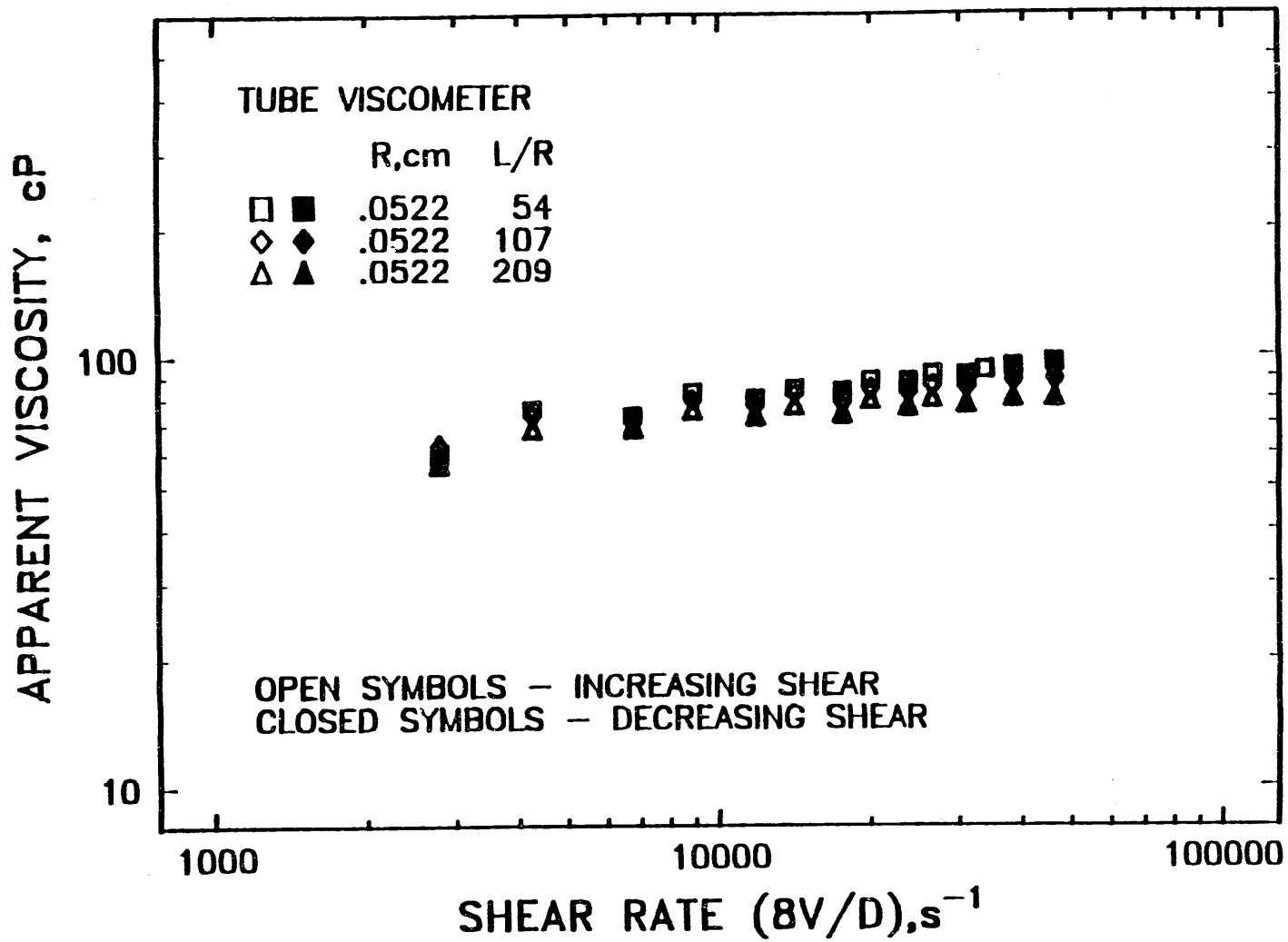

Figure 6-10. Apparent Shear Viscosity for 50 wt.% Micronized Coal-Water Mixture, CF14-W, Over Shear Rate Range of 3000 to 50,000 sec^{-1} (21.0°C)

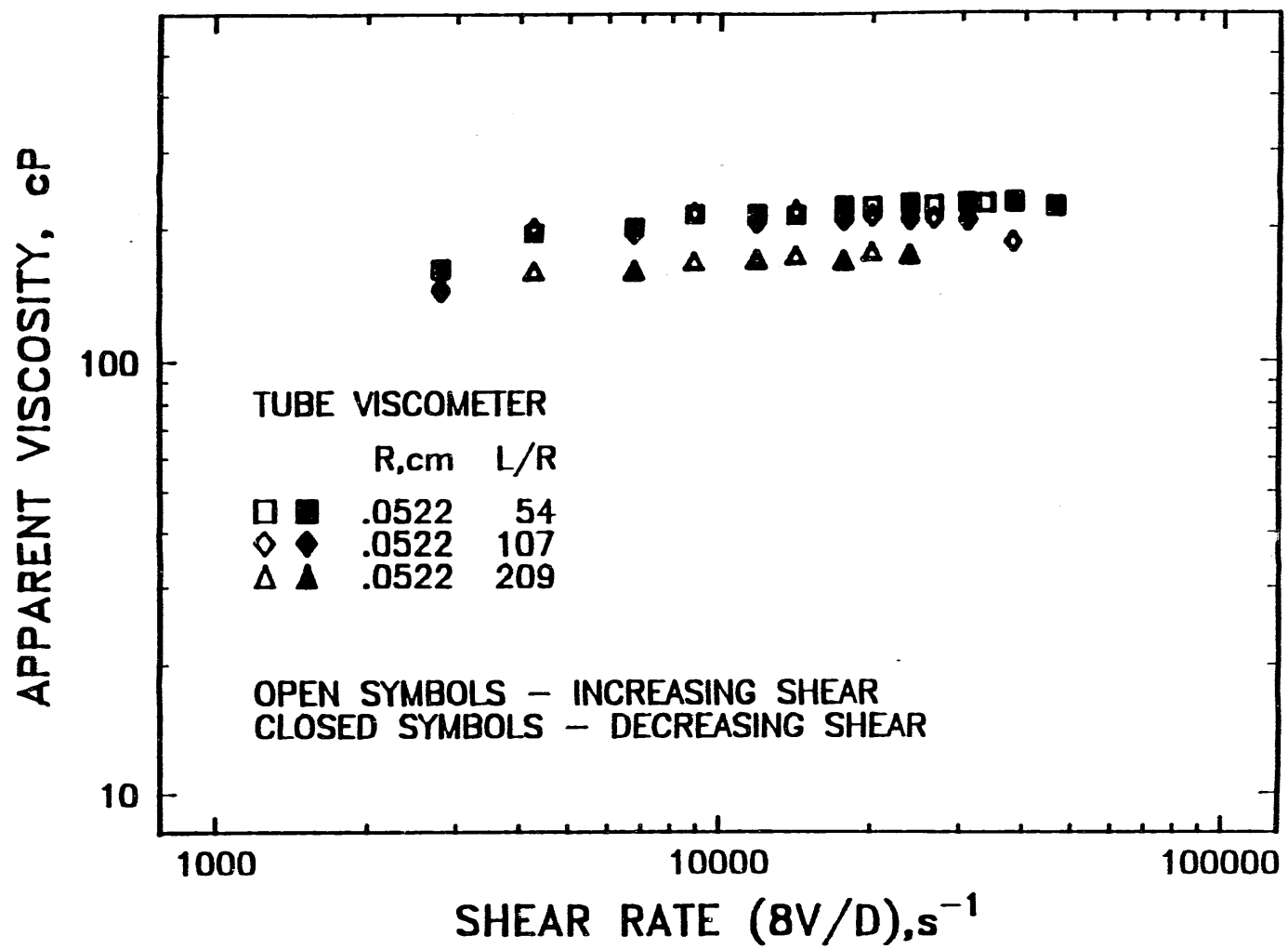

Figure 6.11. Apparent Shear Viscosity for 55 wt.% Micronized Coal-Water Mixture, CF15-W, Over Shear Rate Range of 3000 to 50,000 sec^{-1} (21.0°C)

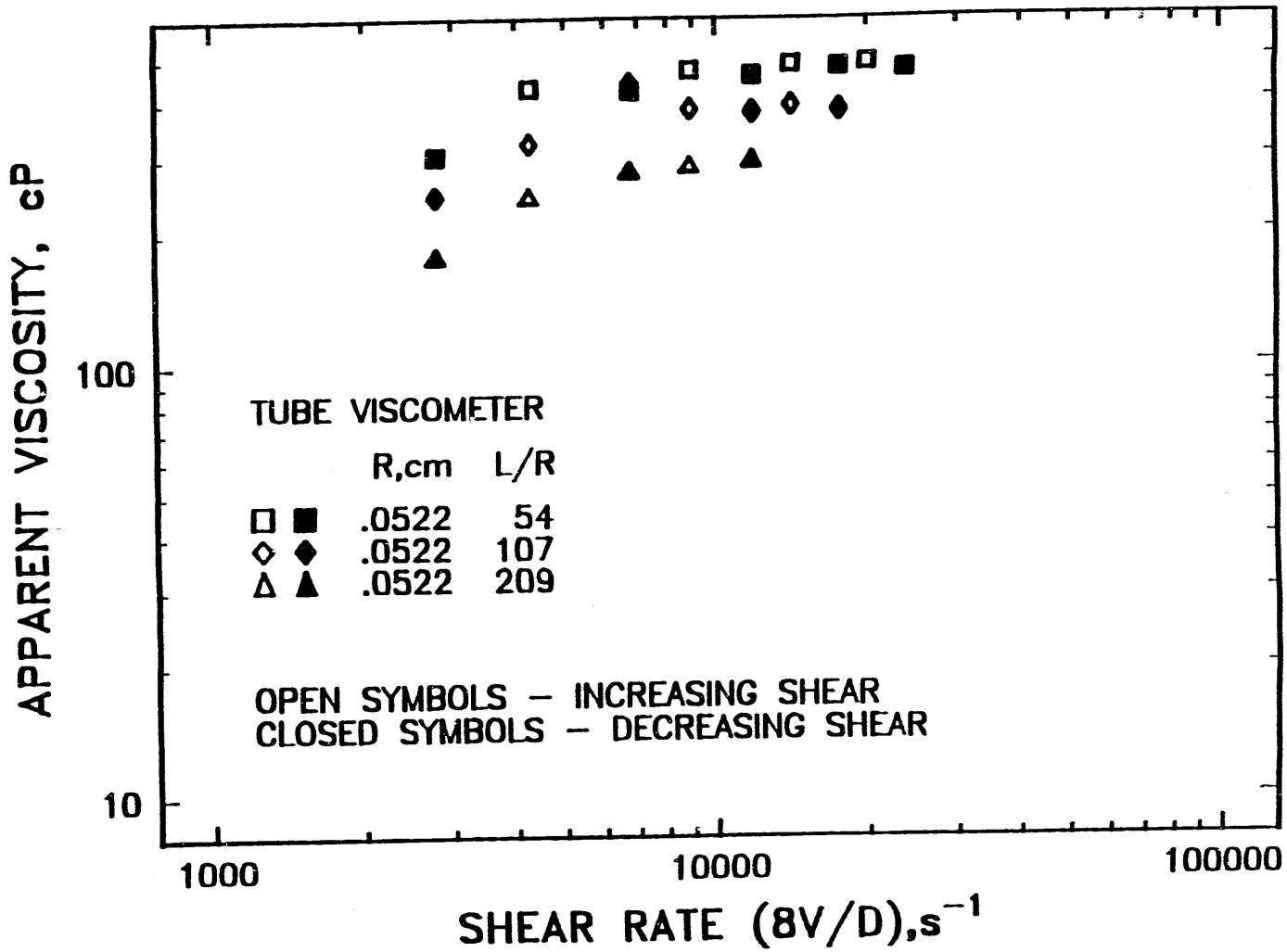

Figure 6.12. Apparent Shear Viscosity for 60 wt.% Micronized Coal-Water Mixture, CF16-W, Over Shear Rate Range of 3000 to 25,000 sec^{-1} (21.0°C)

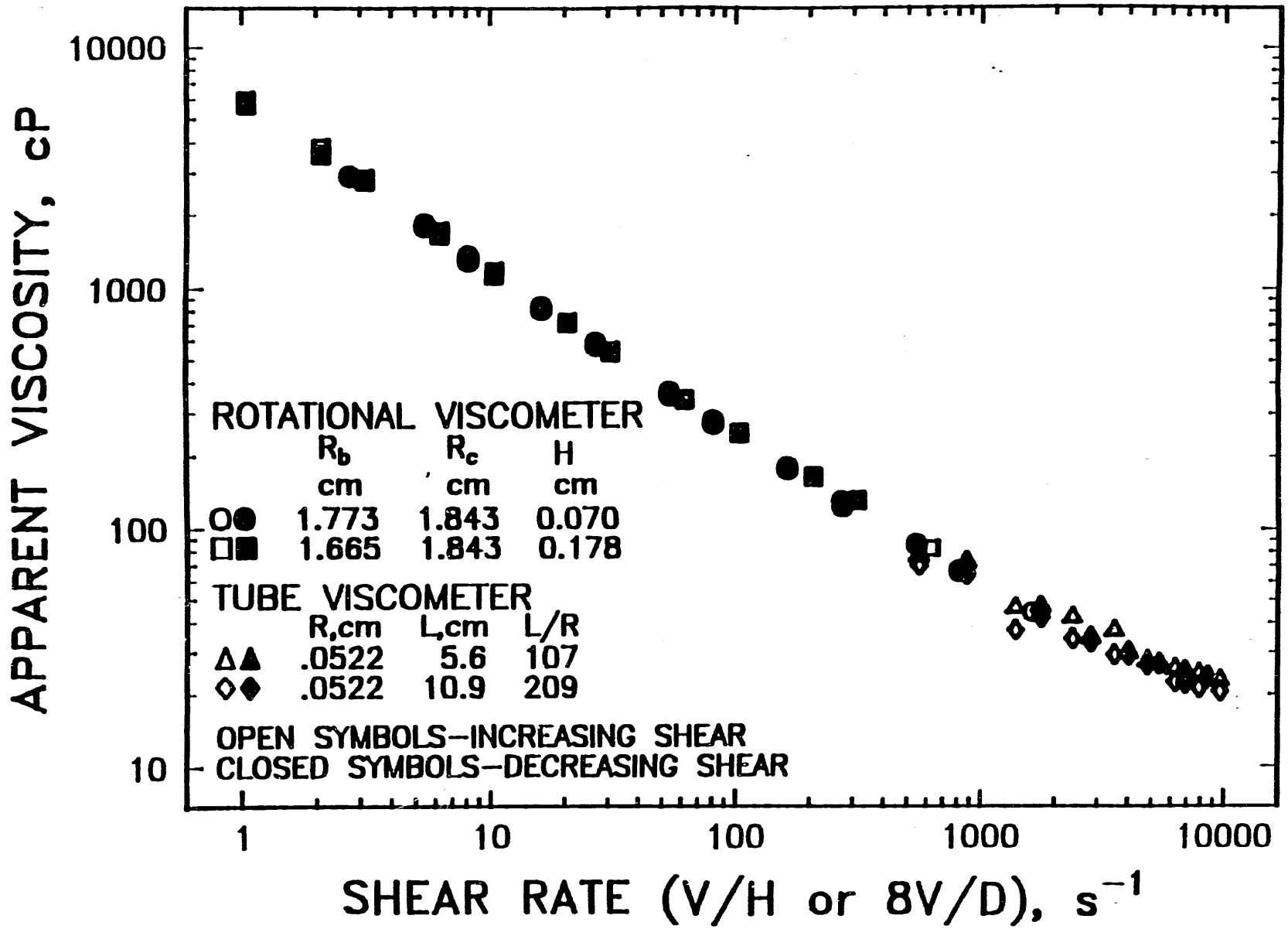

Figure 6.13. Apparent Viscosity of 63.2 wt.% #4000 Glass Bead and Water Mixture

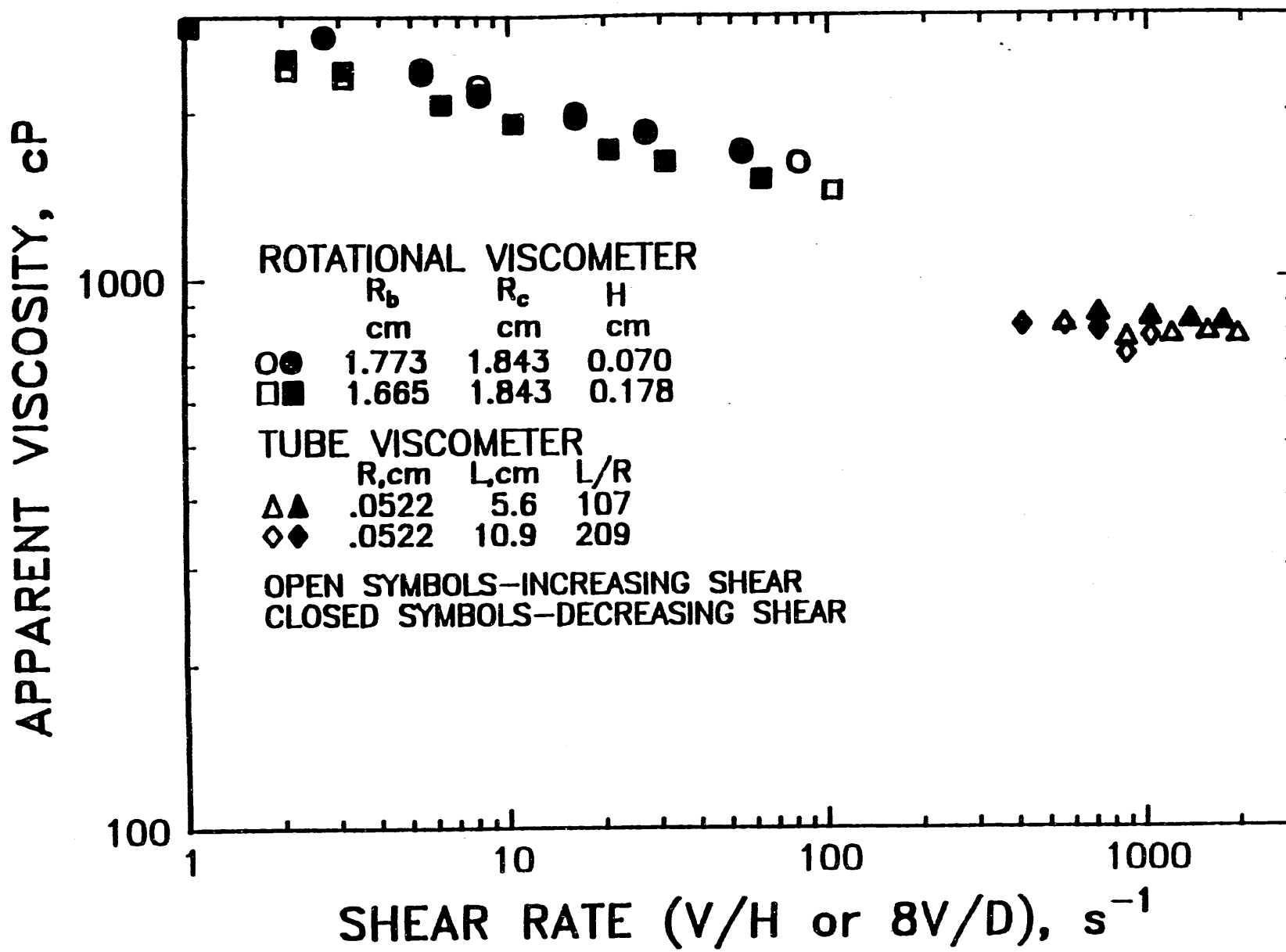

Figure 6.14. Apparent Viscosity for 59 wt.% #4000 Glass Bead and 50 cP Glycerol-Water Mixture

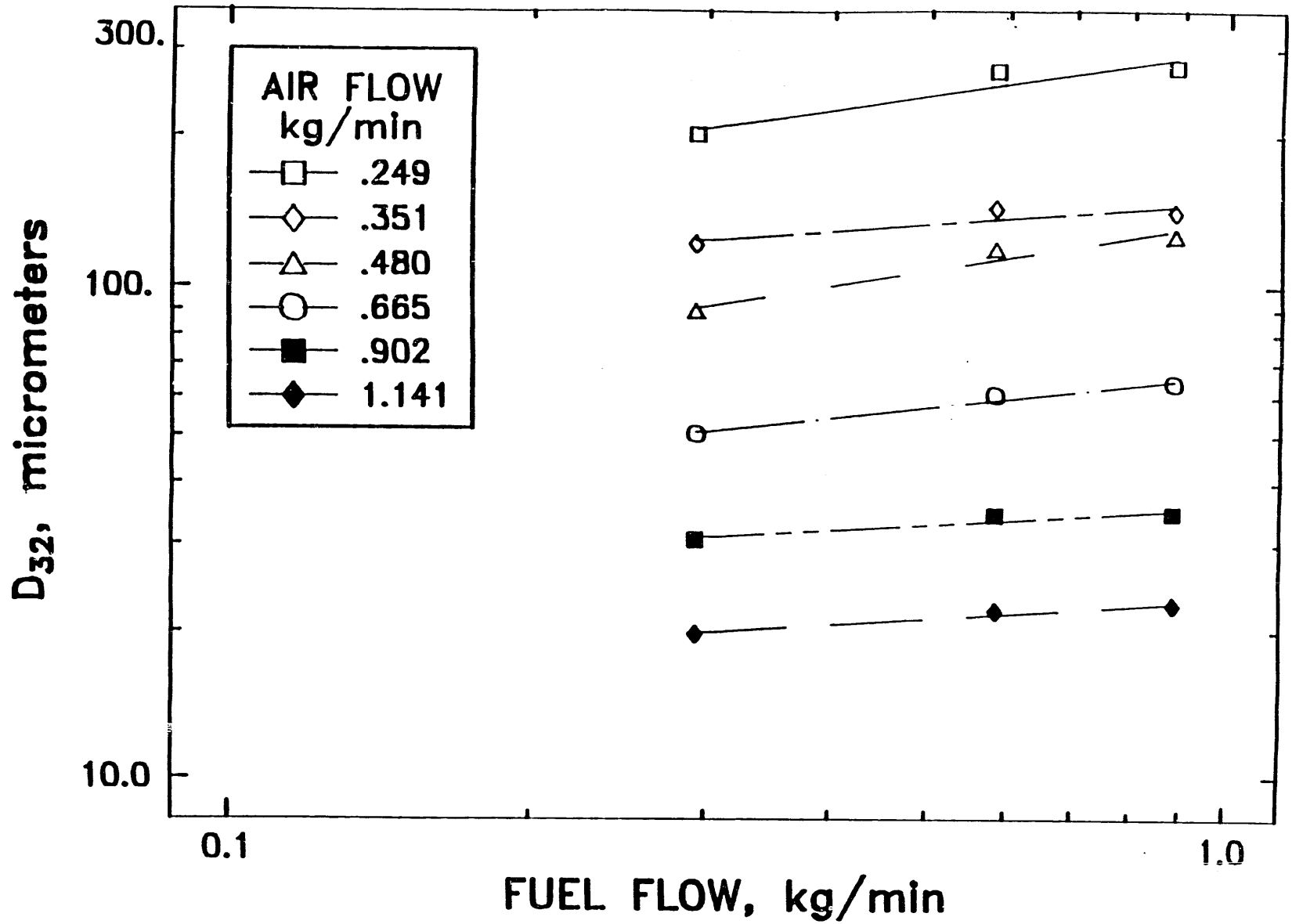

Figure 6.15. Effect of Fuel Flow on Atomization of VFT Nozzle, Water, Fuel Gap 0.381 mm, Air Gap 1.78 mm

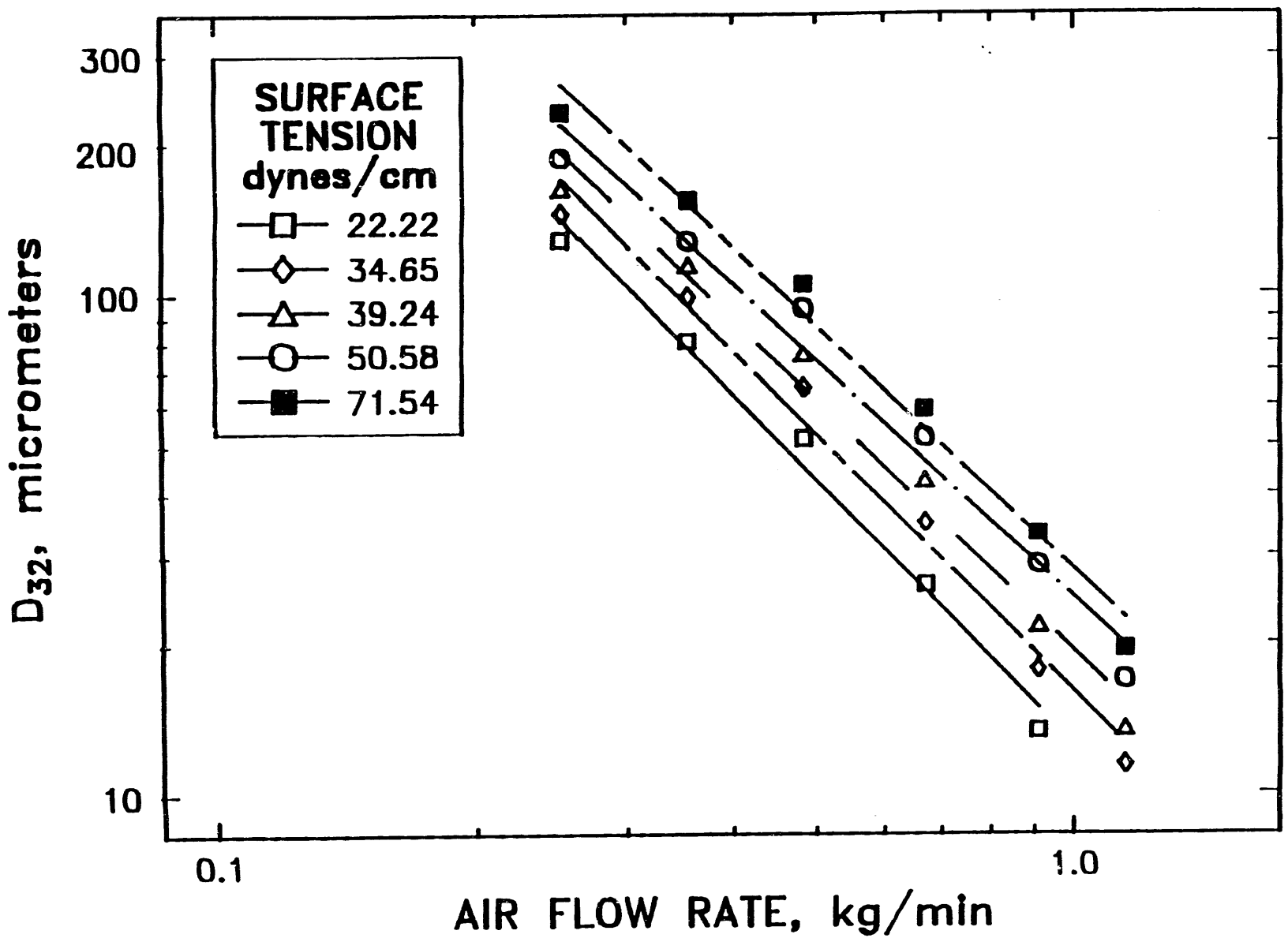

Figure 6.16. Effect of Air Flow on Atomization of VFT Nozzle, Alcohol-Water Flow Rate 0.293 kg/min, Fuel Gap 1.27 mm, Air Gap 1.78 mm

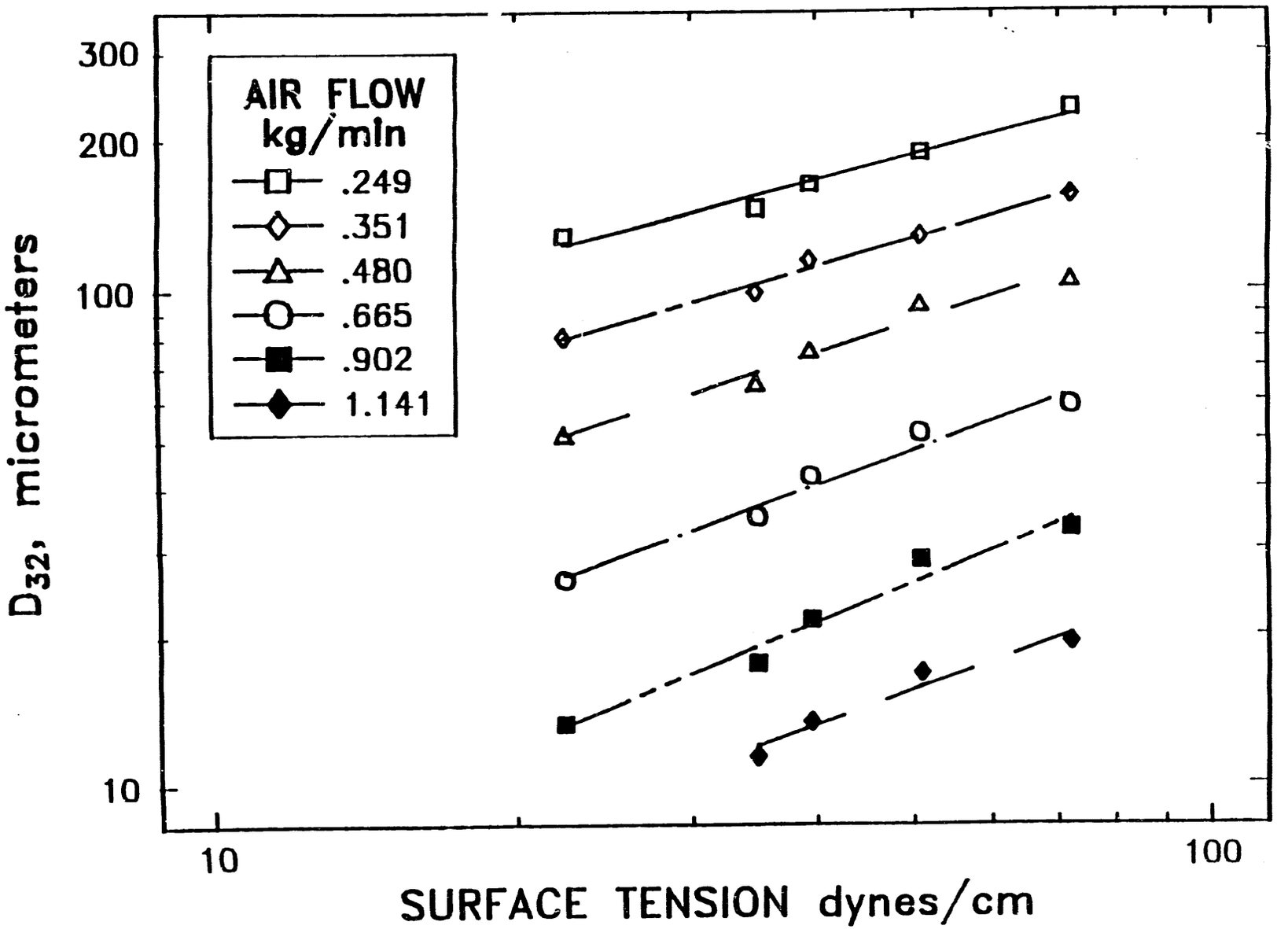

Figure 6.17. Effect of Surface Tension on Atomization of VFT Nozzle, Alcohol-Water Flow Rate 0.293 kg/min, Fuel Gap 1.27 mm, Air Gap 1.78 mm

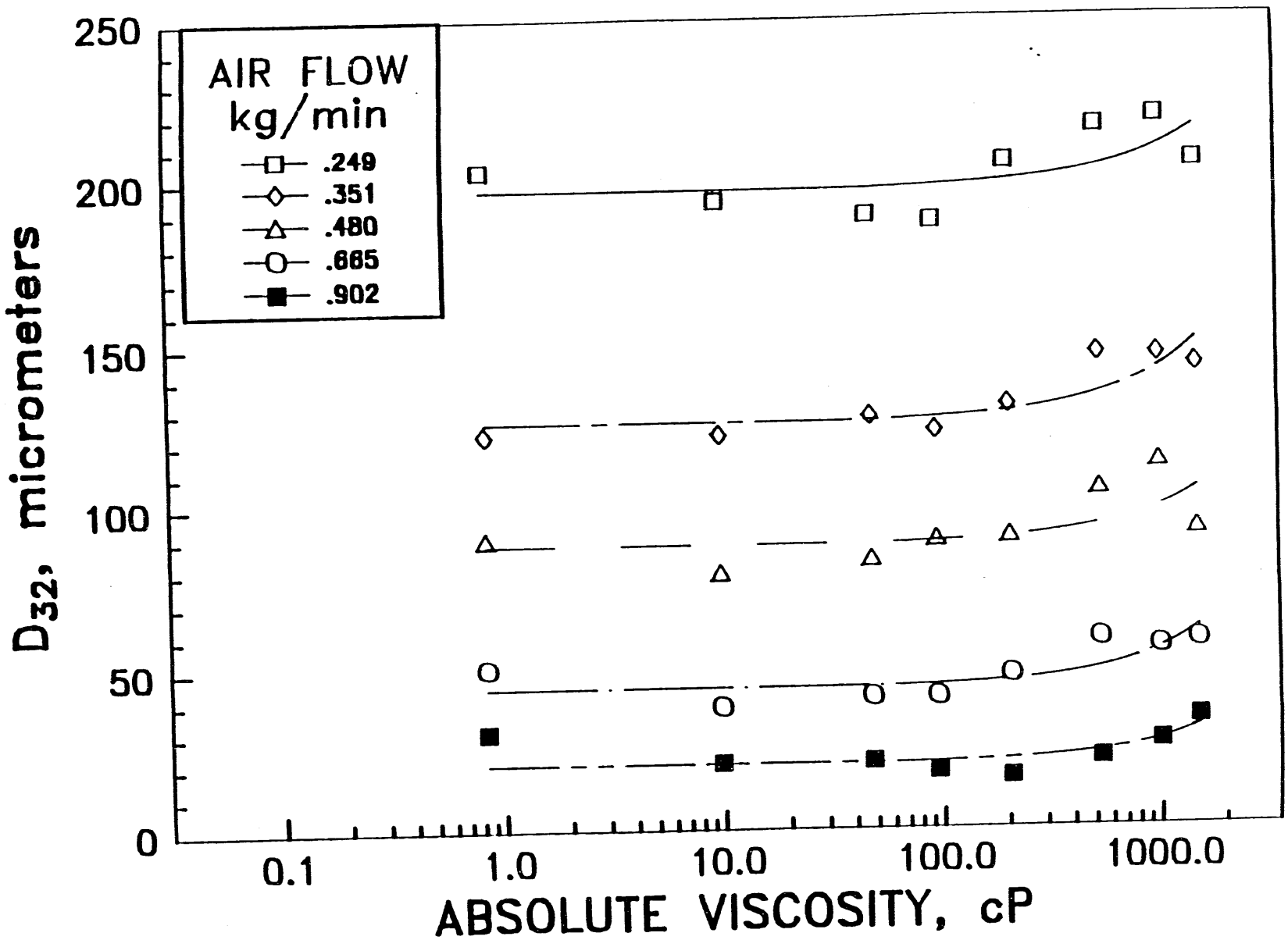

Figure 6.18. Effect of Viscosity on Atomization of VFT Nozzle, Glycerol-Water Flow Rate 0.293 kg/min, Fuel Gap 0.381 mm, Air Gap 1.78 mm

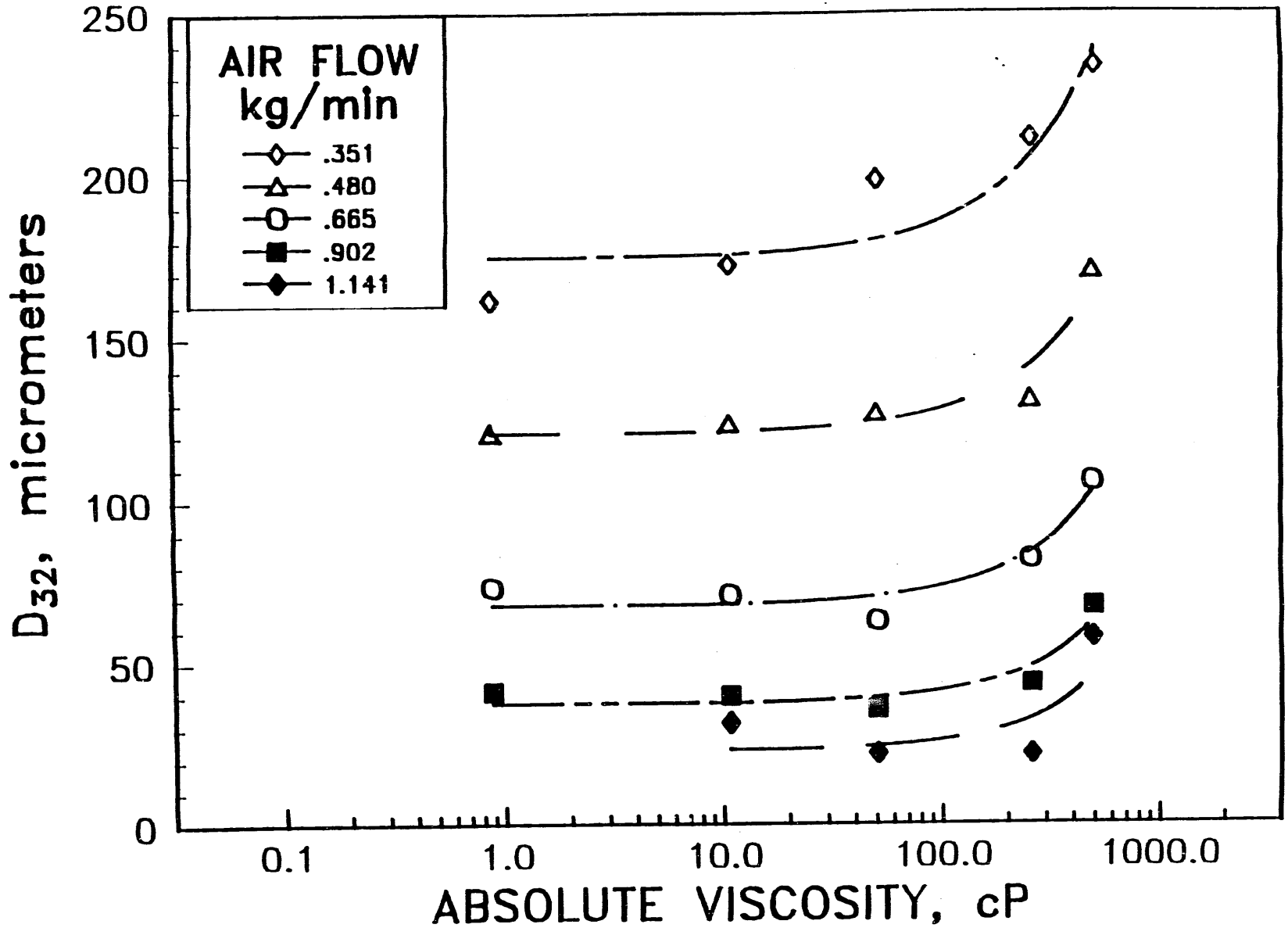

Figure 6.19. Effect of Viscosity on Atomization of VFT Nozzle, Glycerol-Water Flow Rate 0.885 kg/min, Fuel Gap 1.27 mm, Air Gap 1.78 mm

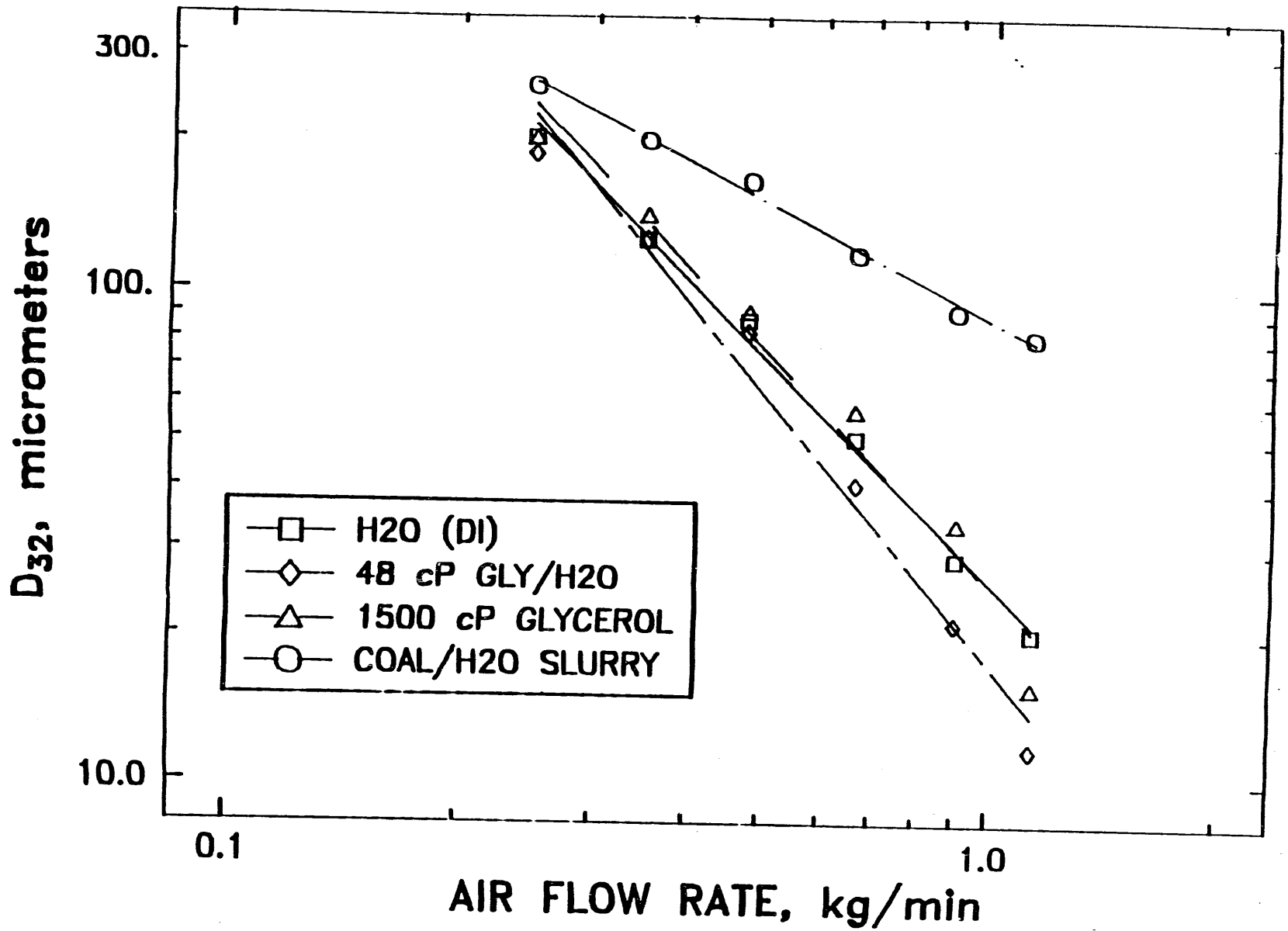

Figure 6.20. Comparison of Atomization of Amax 50 wt.% CWM and Single-Phase Fluids of Varying Viscosities in VFT Nozzle at Flow Rate 0.293 kg/min, Fuel Gap 0.381 mm, Air Gap 1.78 mm

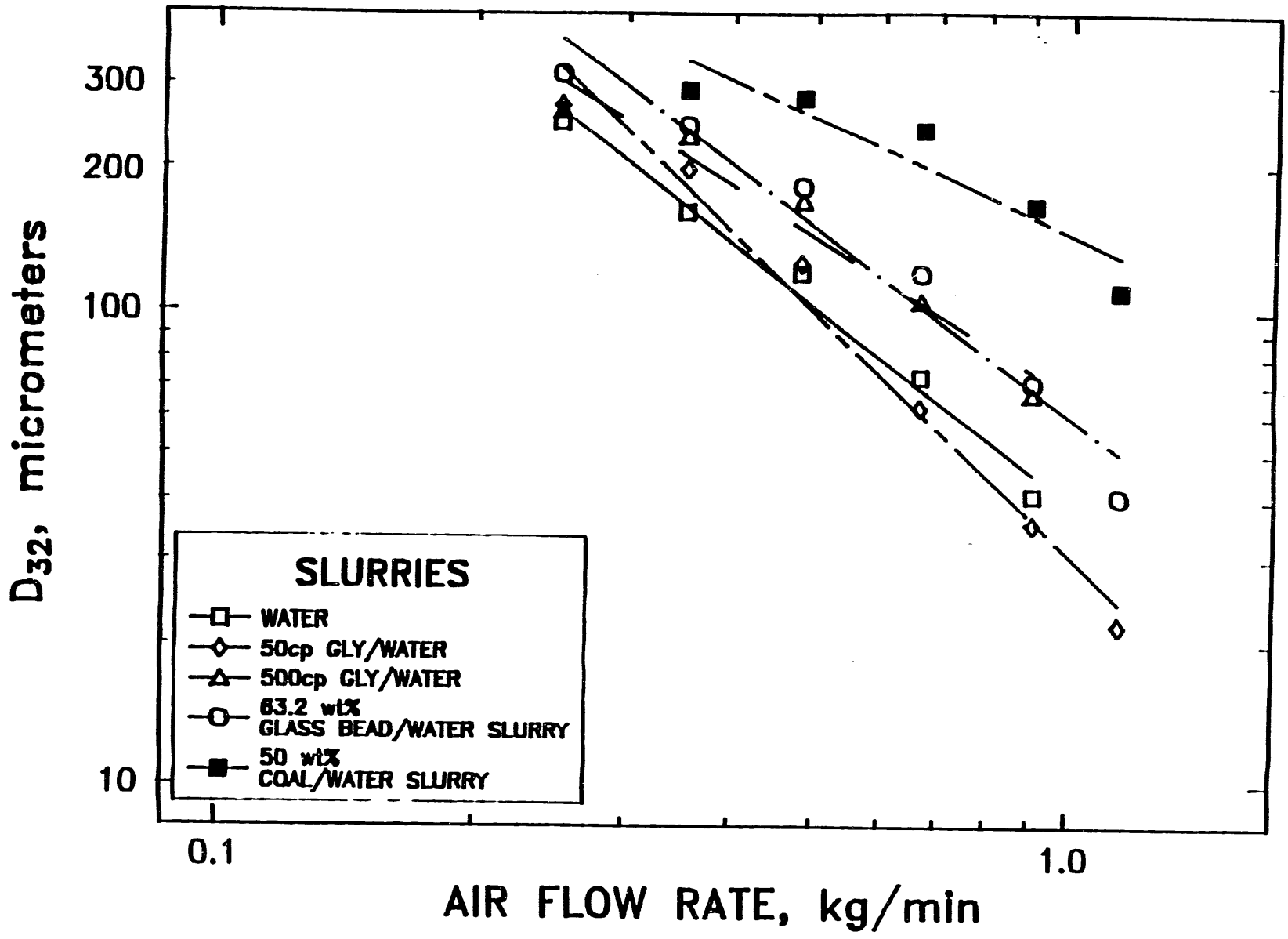

Figure 6.21. Comparison of Atomization of 50 wt.% CWM 63.2 wt.% Glass-Bead Water Mixture, and Single-Phase Fluids of Varying Viscosities in VFT Nozzle at Flow Rate of 0.885 kg/min, Fuel Gap 1.27 mm, Air Gap 1.78 mm

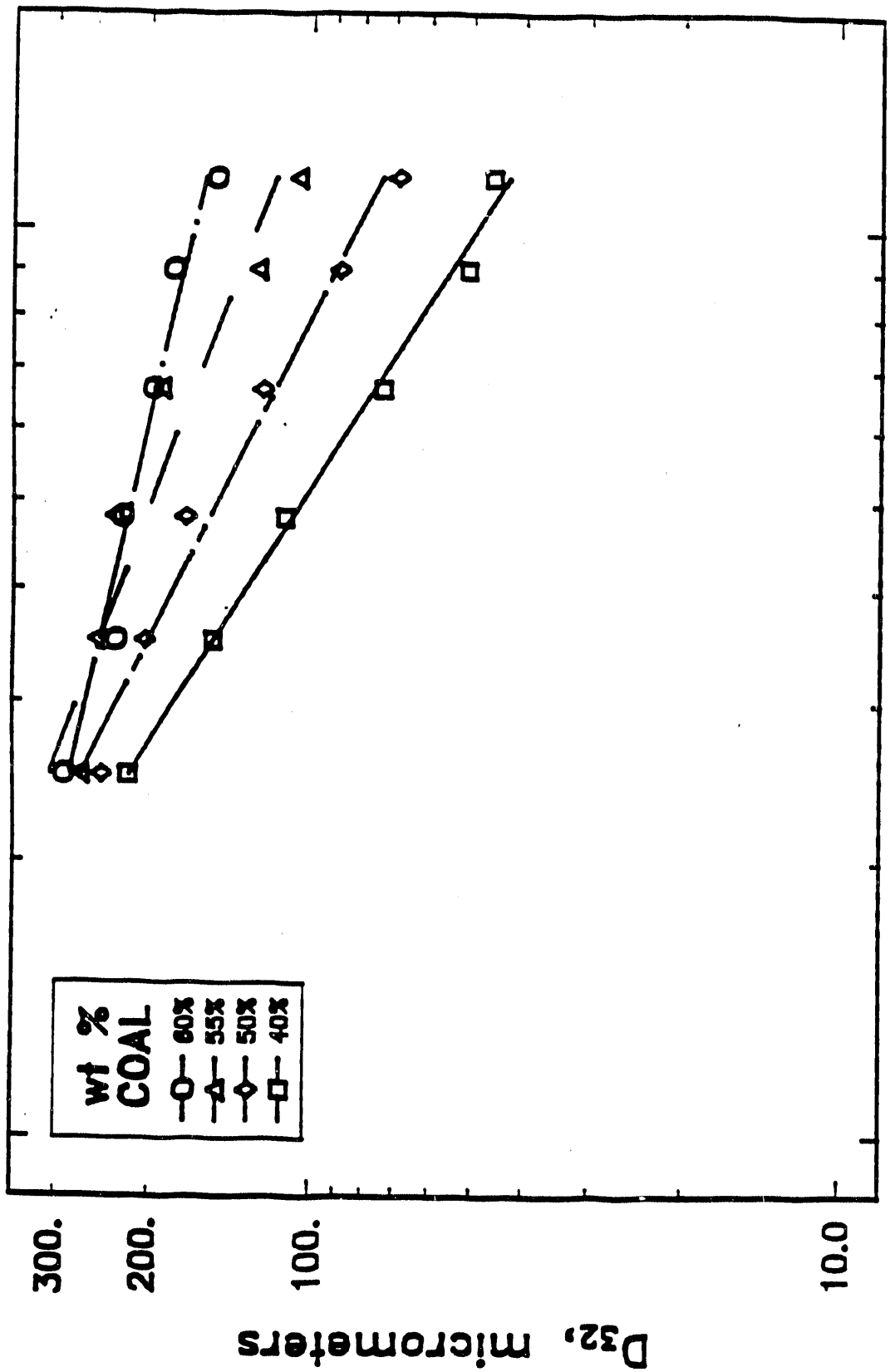

Figure 6.22. Effect of Coal Loading on Atomization of CWM in VFT Nozzle at Flow Rate of 0.293 kg/min, Fuel Gap 1.27 mm, Air Gap 1.78 mm

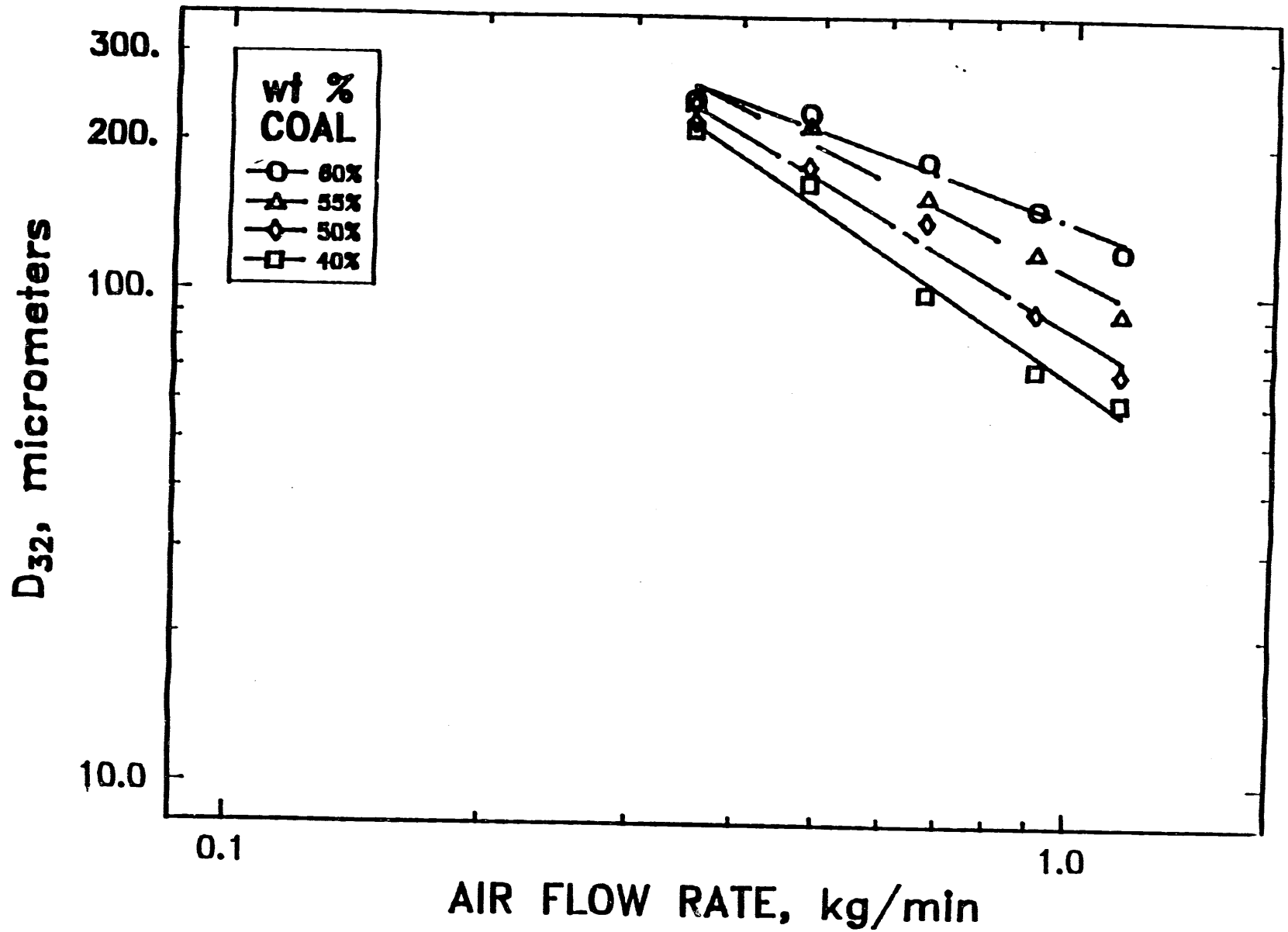

Figure 6.23. Effect of Coal Loading on Atomization of CWM in VFT Nozzle at Flow Rate of 0.885 kg/min, Fuel Gap 1.27 mm, Air Gap 1.78 mm

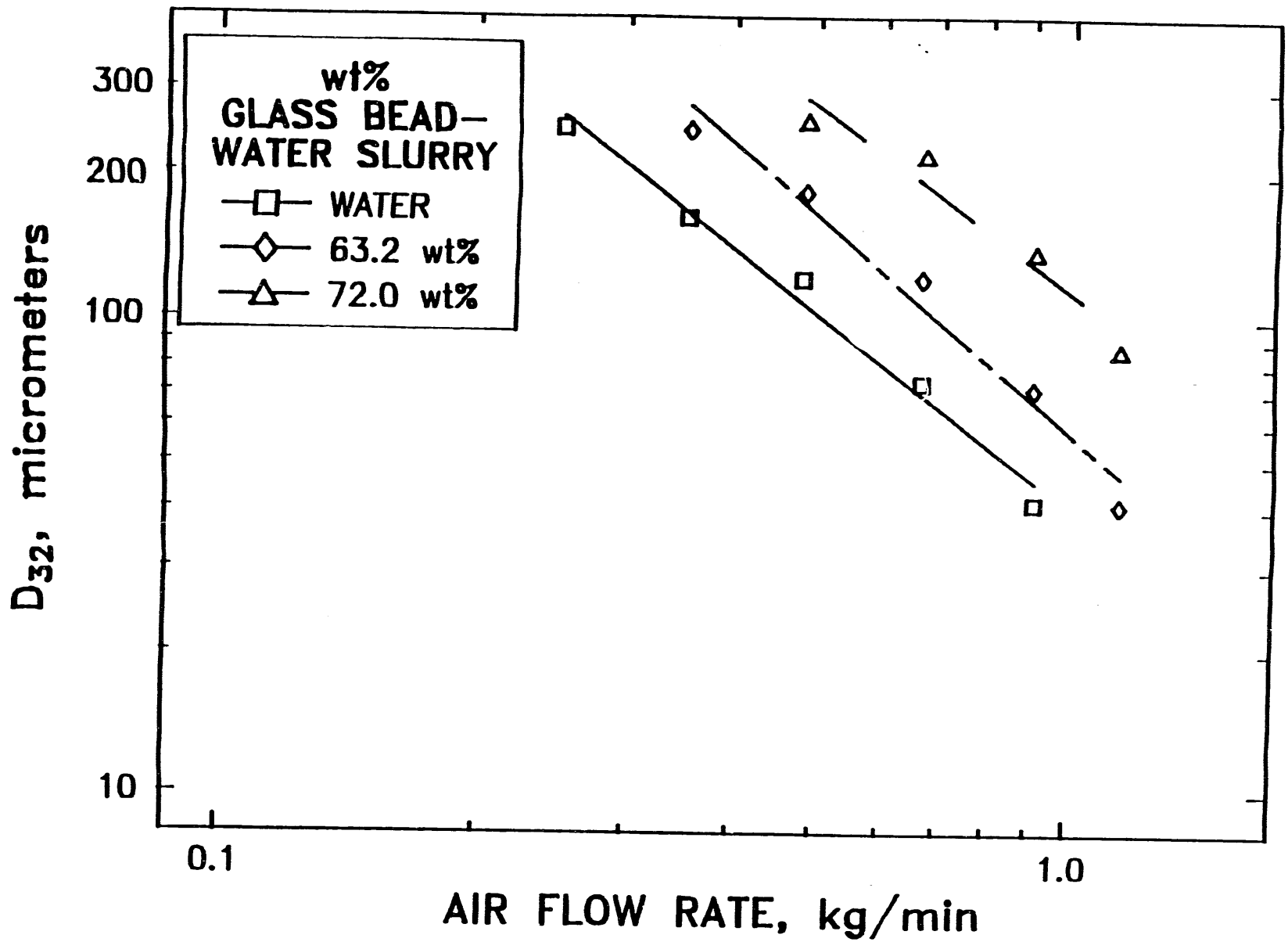

Figure 6.24. Comparison of Atomization of Water and Glass-Bead Water Mixtures in VFT Nozzle at Flow Rate of 0.885 kg/min, Fuel Gap 1.27 mm, Air Gap 1.78 mm

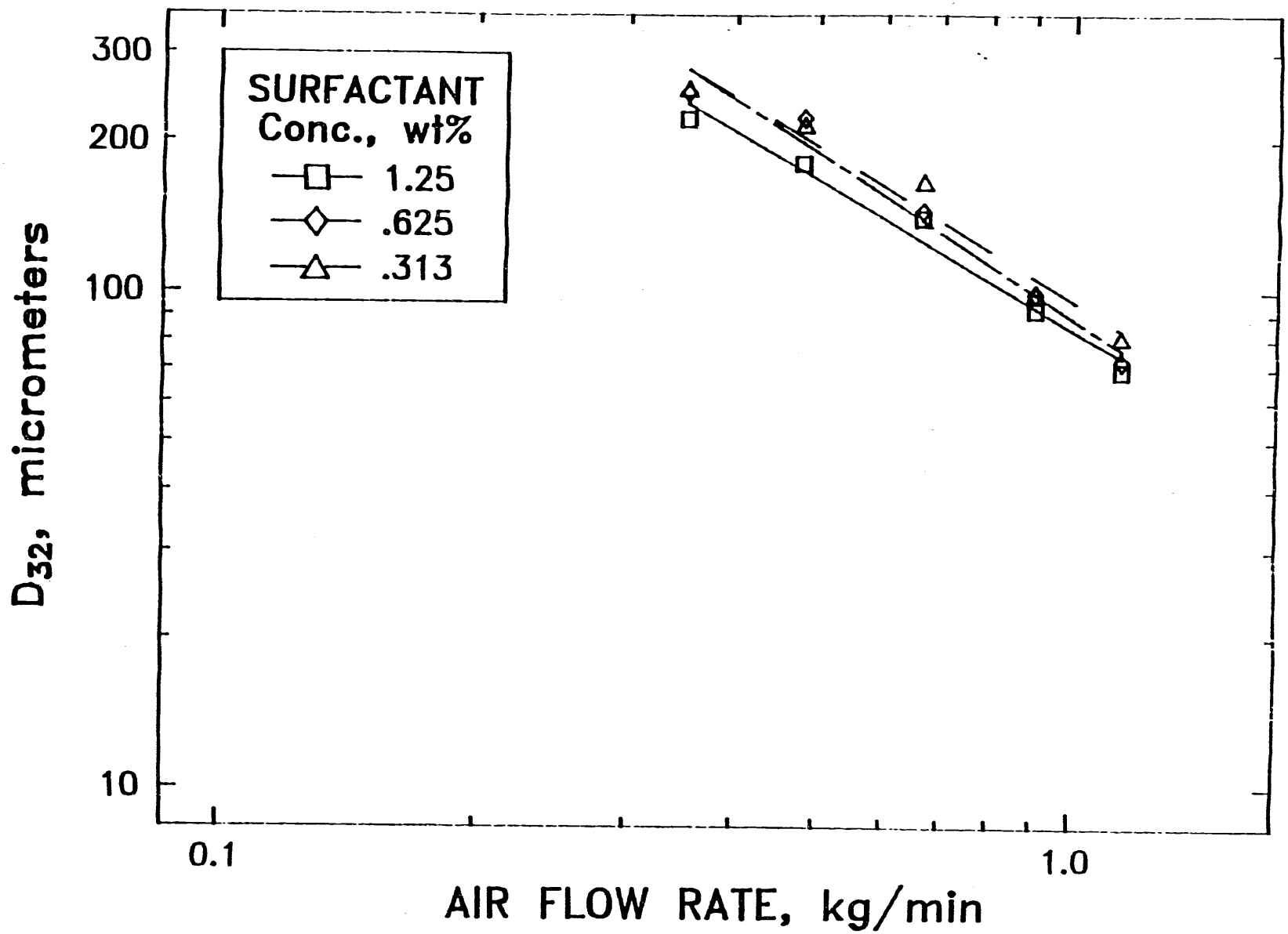

Figure 6.25. Effect of Surfactant Concentration on Atomization of 50 wt.% CWM (CF14-W) in VFT Nozzle at Flow Rate of 0.885 kg/min, Fuel Gap 1.27 mm, Air Gap 1.78 mm

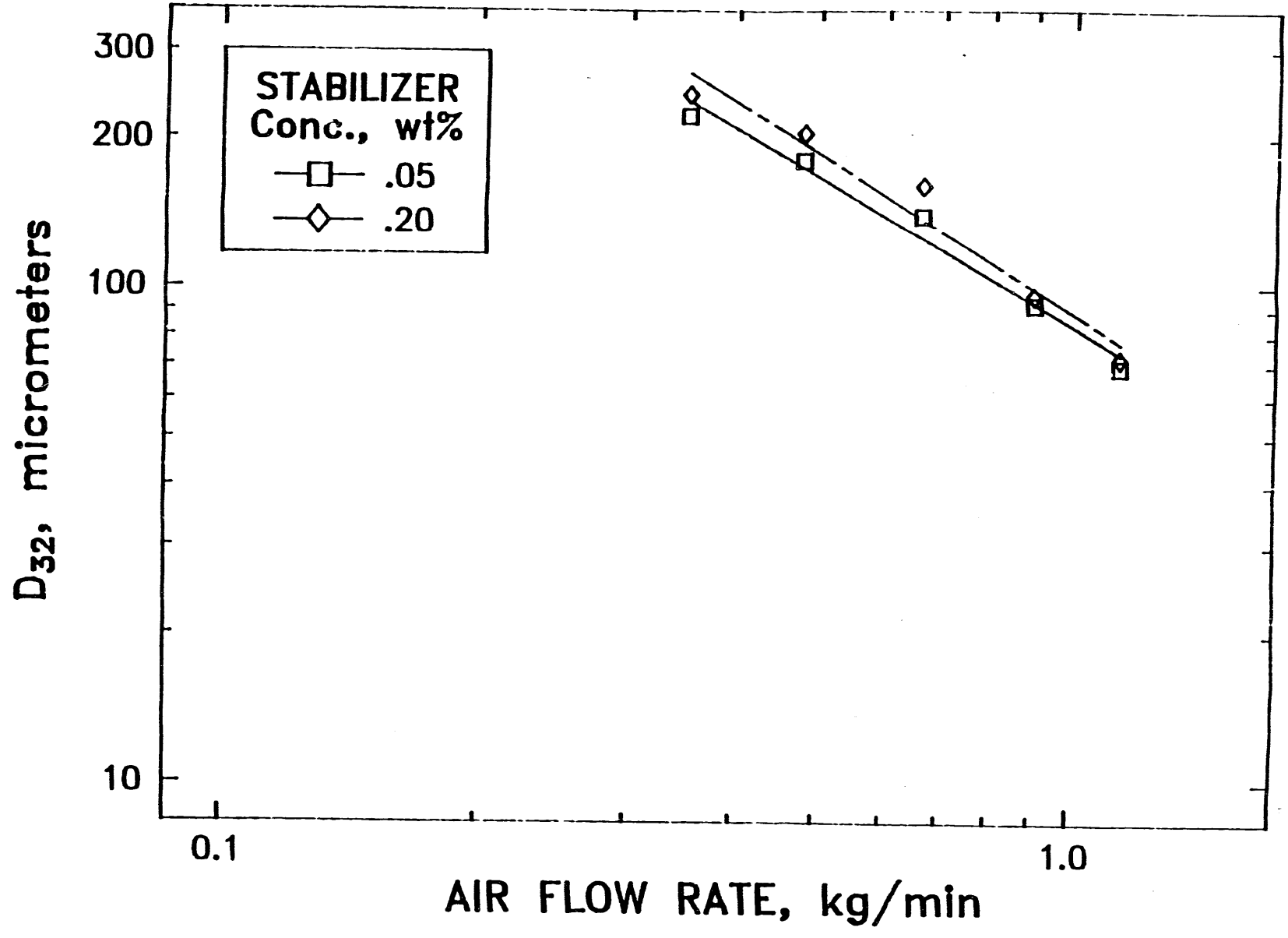

Figure 6.26. Effect of Stabilizer Concentration on Atomization of 50 wt.% CWM (CF14-W) in VFT Nozzle at Flow Rate of 0.885 kg/min, Fuel Gap 1.27 mm, Air Gap 1.78 mm

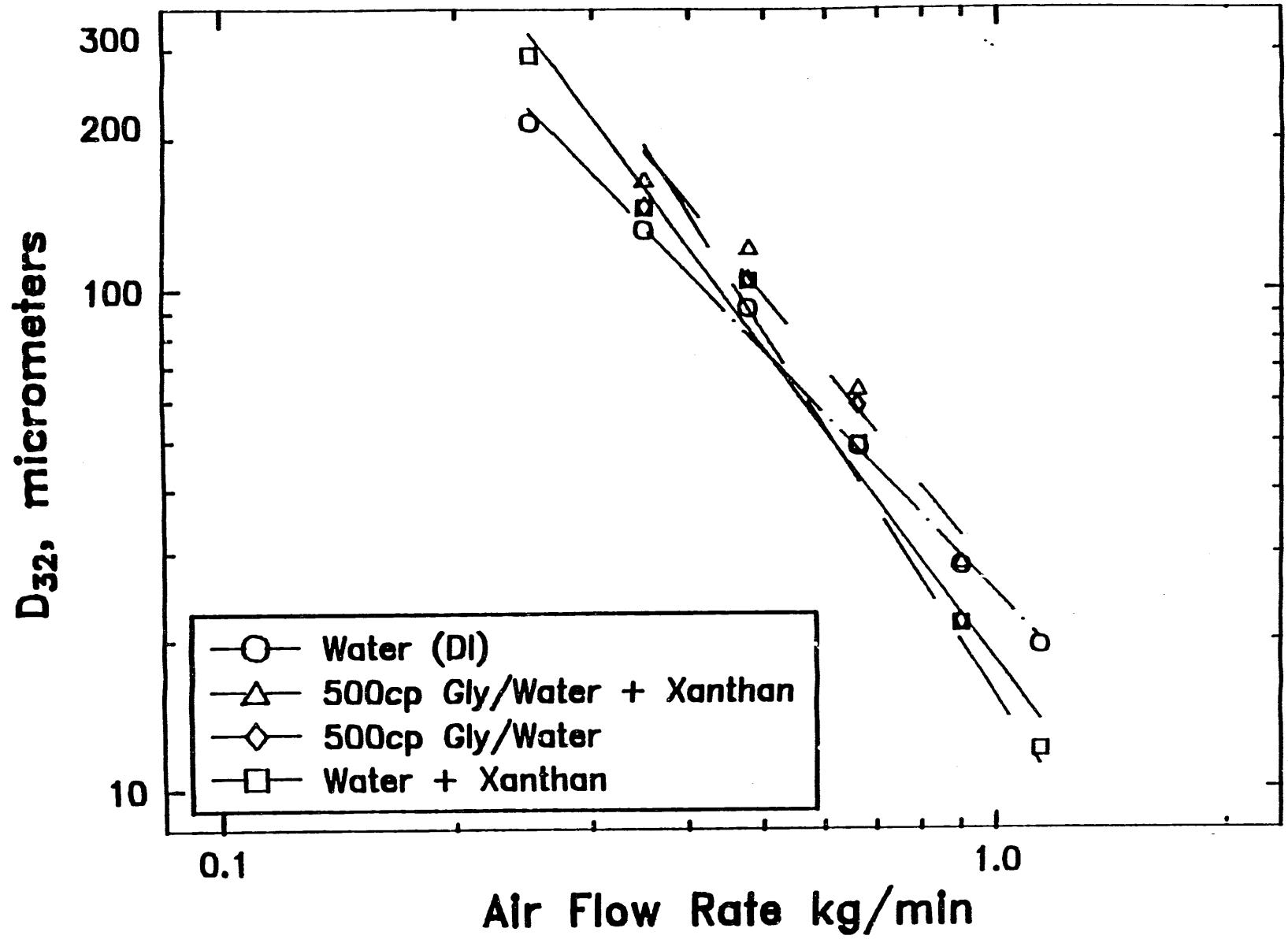

Figure 6.27. Effect of 0.45 wt.% Xanthan Stabilizer on Atomization of Single-Phase Fluids in VFT Nozzle at Flow Rate of 0.293 kg/min, Fuel Gap 0.381 mm, Air Gap 1.78 mm

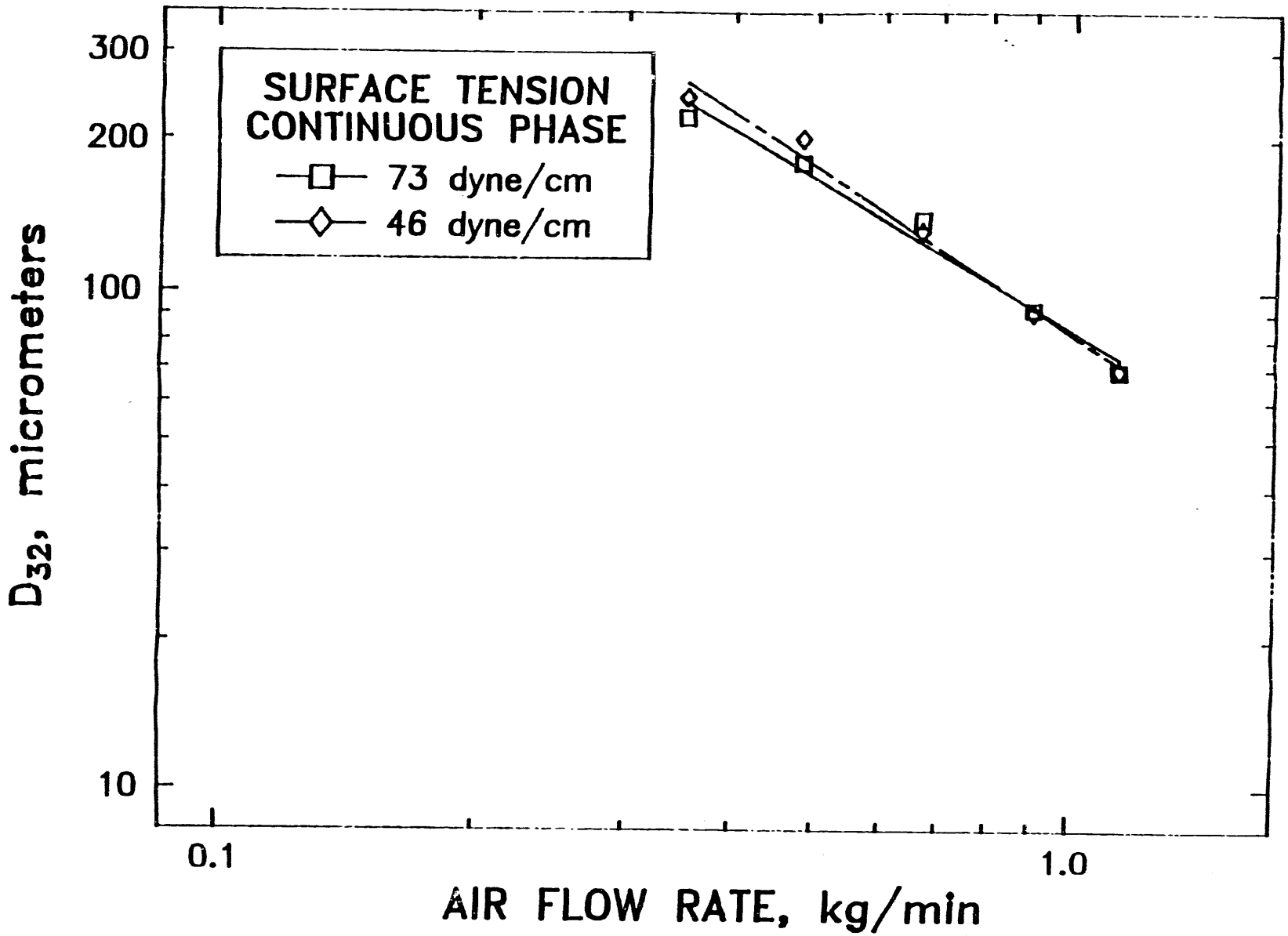

Figure 6.28. Effect of Surface Tension of Continuous Phase on Atomization of 50 wt.% CWM in VFT Nozzle at Flow Rate of 0.885 kg/min, Fuel Gap 1.27 mm, Air Gap 1.78 mm

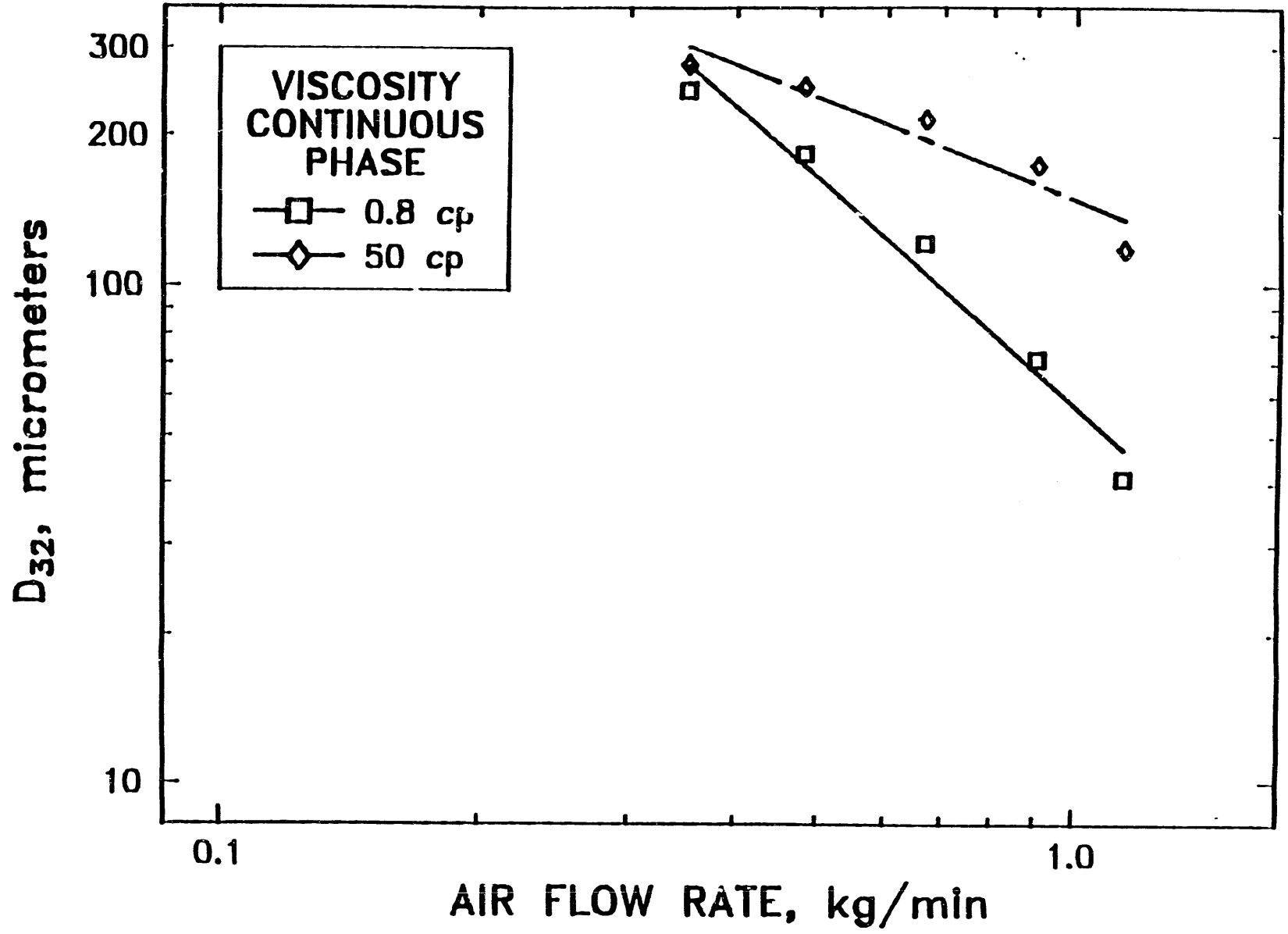

Figure 6.29. Effect of Viscosity of Continuous Phase on Atomization of Glass-Bead Water Mixtures in VFT Nozzle at Flow Rate of 0.885 kg/min, Fuel Gap 1.27 mm, Air Gap 1.78 mm

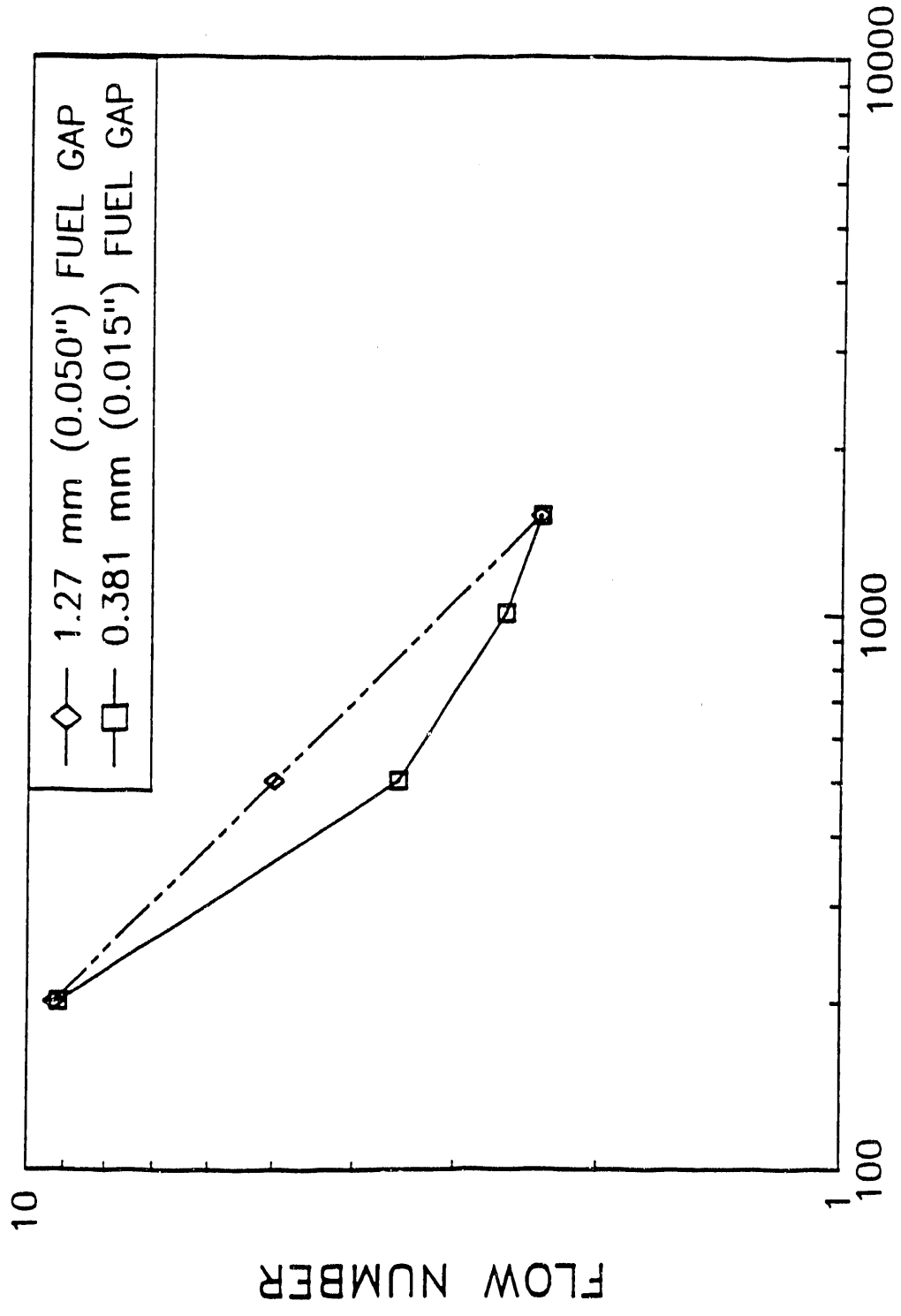

Figure 6.30. Effect of Viscosity on Flow Number of VFT Nozzle

7.0 COMMERCIAL, AIR-ASSIST, GAS TURBINE NOZZLE

Coal-water slurry atomization measurements were performed with a Parker Hannifin air-atomizing coal slurry nozzle P/N EDL 6850638. The atomizer, which is shown in Figure 7.1, can be thought of as an axially symmetric version of the planar VFT nozzle. That is, atomizing air flows on each side of the CWM in both nozzle designs. Referring to Figure 7.1, atomizing air flows through the center hole, coal slurry through the first annulus around the center hole, and atomizing air through the second annulus. Figure 7.1 also shows an air shroud around the end of the nozzle to prevent carbon buildup, but the atomizer tested does not have an air shroud. The diameter of the inner air tube is 4.01 mm (.158"), the fuel gap width is 1.37 mm (.054"), and the outer air gap width is 1.08 mm (0.42"). Nominal air flow rate is 200 lbm/hr (.0252 kg/s) and nominal fuel flow is 750 lbm/hr (.0945 kg/s). Atomization tests were performed at the nominal air flow rate and at fuel flows of one-half of nominal, 375 lbm/hr (.0473 kg/s), and nominal values. An air pressure of 90 psid (621 kPa differential) is required to establish the nominal air flow.

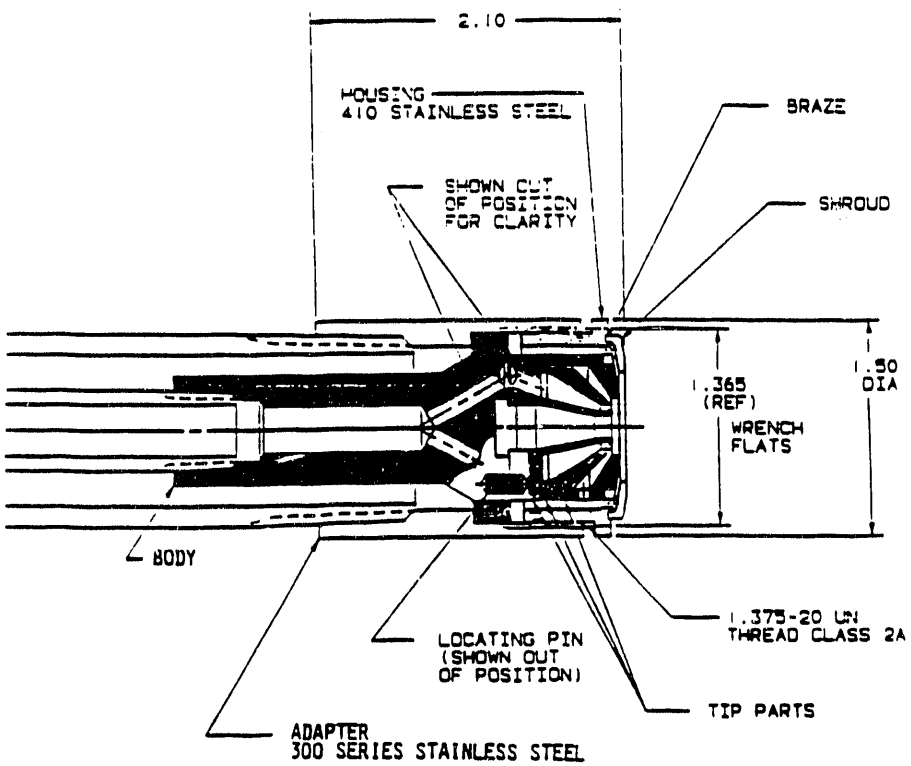

Figure 7.1. Parker Hannifin Air-Atomizing Coal Slurry P/N EDL 6850638

7.1. EXPERIMENTAL APPARATUS FOR GAS TURBINE NOZZLE TESTS

Atomization tests of the gas turbine nozzle were performed in the atmospheric pressure, low-turbulence test chamber that includes a computer-controlled nozzle positioner. Measurements of slurry drop size and number density were made through several chords of the cone-shaped spray from the centerline to the edge of the spray, as shown in Figure 7.2, using a Malvern Model 2200 laser-diffraction drop sizer at an axial distance of 110 mm from the nozzle tip to the centerline of the laser beam. Using procedures developed under this program and included in Appendix A, these line-of-sight integral measurements were deconvoluted into drop size and number densities for each ring. These values were then summed up with appropriate weighing factors to arrive at a cross-section-average Sauter mean diameter (D_{32}) for the spray.

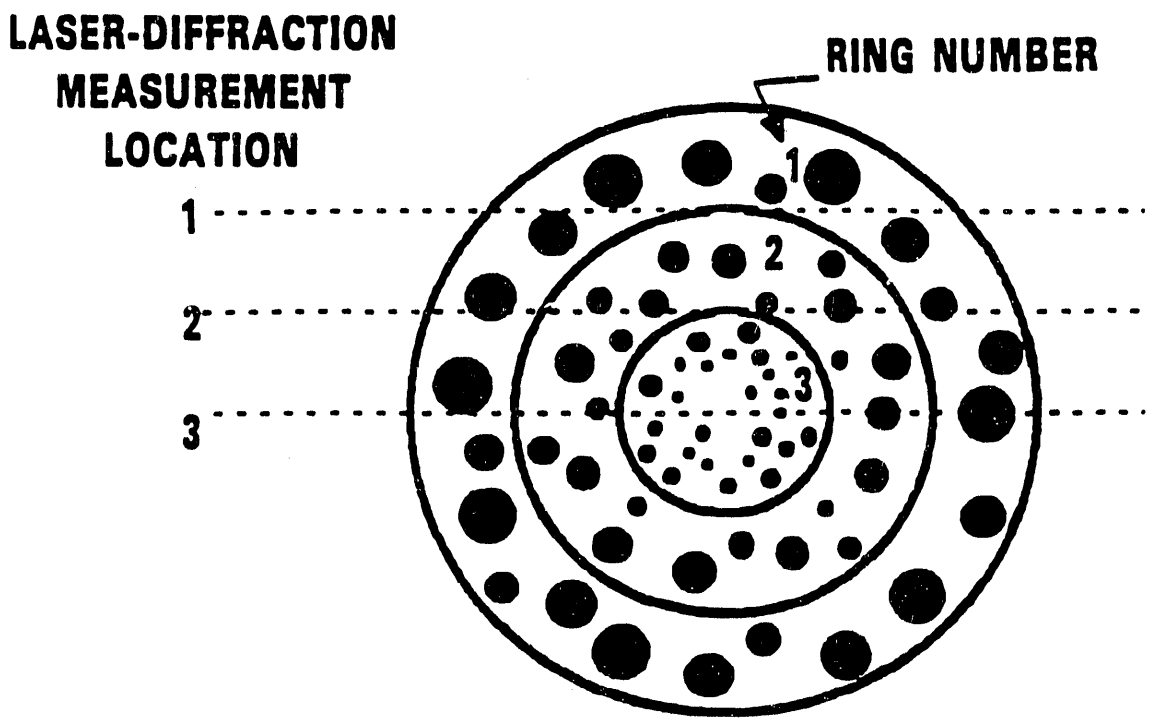

Figure 7.2. Cross-Section of the Spray Showing the Line-of-Sight Measurement Locations With the Laser-Diffraction Drop Sizer

Because of the relatively high fuel flow rates, severe problems were encountered in making measurements with the laser-diffraction instrument, because the laser beam photons were typically scattered from several drops before traversing the spray and being measured at the receiver. Since

the theory for the laser diffraction instrument requires that photons are scattered from only a single drop, the multiple-scattering phenomena produces an error in the measurements. This problem was attached in two ways. First, specially designed tubes were inserted into the spray so that the laser beam intersected only a portion of the spray. After several design iterations and tests, the best design was one which blocked one-half of the spray on the receiver-size of the instrument. With one-half of the spray blocked, the multiple-scattering problem was significantly reduced, but corrections were still necessary and were performed using the procedure developed by Felton et al. (1985).

7.2. EXPERIMENTAL RESULTS FOR COMMERCIAL, AIR-ASSIST, GAS TURBINE NOZZLE

Measurements of spray characteristics were attempted for water, glycerol-water mixtures, and CWM. Because of problems with multiple-scattering and collection of liquid on the spray blocking tube, the atomization of the glycerol-water mixtures could not be accurately determined. Results for the water and some of the CWM are given below.

The Parker-Hannifin air-assist gas turbine nozzle produced a spray with considerable variation of average drop size with radius, with the smallest drops toward the center of the spray, qualitatively similar to Figure 7.2. Spatially resolved values of drop size, drop number density, and drop volume fraction (drop volume/air volume) were obtained by deconvoluting the line-of-sight integral values measured by the laser-diffraction instrument as illustrated in Figure 7.2, with results for a typical case (40 wt.% CWM) shown in Figures 7.3 - 7.5 for drop size, number density, and volume fraction, respectively. When these drop size data were weighted for area and number density, the resulting cross-section average SMD's were as shown in Figure 7.6. It may be seen that the air-assist, gas turbine nozzle appears to atomize the CWM with less effect of coal loading or viscosity than the VFT nozzle. The data shown in Figure 7.6 are replotted as a function of high shear rate (20,000 sec^{-1}) viscosity in Figure 7.7, and again the relative insensitivity of atomization to the coal viscosity is demonstrated.

Why is the Parker Hannifin coaxial gas turbine atomizer less sensitive to coal loading and slurry viscosity that the VFT nozzle? There are various possible explanations, but one significant difference between the operating conditions is the higher air velocities used in the coaxial atomizer. The coaxial atomizer uses sonic air velocities, ~330 m/s, while the VFT atomizer used maximum air velocities of about 143 m/s. Attempts were made to operate the gas turbine nozzle at lower air velocities to better understand its performance, but the spray cone angle discontinuously jumped to a very high angle as the air flow was decreased from nominal values. Measurements could not be performed on this broad cone angle spray.

7.3. CORRELATION OF RESULTS FOR COMMERCIAL, AIR-ASSIST, GAS TURBINE NOZZLE

Correlations of the commercial, air-assist, gas-turbine nozzle were limited to the two operating conditions of full design fuel flow rate (340 kg/hr) and one-half that flow rate, with four different fluids - water, 40 wt.% CWS, 50 wt.% CWS, and 60 wt.% CWS. The air pressure was 620 kPa (90 psig), producing sonic air velocities at the atomizer tip. The nozzle did not perform properly at air pressures lower than this design condition. The atomization data could be correlated with the coal wt.% (WF) and the fuel mass flow rate in kg/hr ($\dot{m}_l$) as,

$$D_{32} = 1.32(WF)^{0.30}(\dot{m}_l)^{0.40} \tag{7.1}$$

or with the shear viscosity measured at 20000 sec^{-1}.

$$D_{32} = 3.38(\mu_l)^{0.049}(\dot{m}_l)^{0.40} \tag{7.2}$$

where the absolute viscosity is in cP. It was not possible to check this second correlation for single-phase fluids of similar viscosity due to experimental difficulties associated with the very dense sprays produced. Thus, this dependence on viscosity may be specific to this type of CWS. However, it is of significance to note that the degradation of atomization performance with CWS relative to water shown in Figure 7.6 was much less for this sonic velocity air-assist nozzle than for the lower air velocity VFT nozzle reported in Section 6.0. The sonic air velocities may be critical to effective atomization of the slurries.

The typical variation of fuel-air ratio through the spray is demonstrated in Figure 7.5 where the ratio is expressed in terms of a liquid volume fraction rather than a weight fraction. The conversion from volume fraction to weight fraction involves multiplying the values in Figure 7.5 by the ratio of densities, which is about 1200 kg/m for the CWS (varying with the coal wt. fraction) and about 1.19 kg/m for air. This is roughly a factor of 1000, so the volume fractions of 1.0 E-4 in Figure 7.5 are equivalent to about 0.1 by total slurry weight, or a fuel/air ratio of about 0.05. Stoichiometric fuel-air ratio for a coal with a 1:1 C:H ratio would be 0.074, so the measured fuel/air ratio is in the combustible range. The data in Figure 7.5 are for on-half the design fuel flow rate, so the design condition produces a higher fuel/air ratio. At the 11 cm axial location of the measurements, the fuel/air ratio was reduced to 1/2 of its maximum value at a radial location of about 7 cm from the centerline for both the high and low fuel flow rate conditions. This cone angle did not vary significantly with fuel properties.

The fuel flow rate as a function of pressure drop across the nozzle is not so significant for an air-assist nozzle since the atomizing energy is supplied by high air velocities rather than high fuel velocities as in a pressure atomizer. Fuel pressure is only required for delivering the fuel to the nozzle, rather than for atomizing the fuel, and fuel pressures are typically only slightly above the combustion chamber pressure. For this particular atomizer, fuel pressures were typically only 70 kPa (10 psi) above atmospheric pressure to deliver fuel flows of 340 kg/hr (750 lbm/hr), resulting in a flow number of 3.60×10^{-4} kg/s $\sqrt{Pa}$ (237 lbm/hr $\sqrt{psid}$). These pressures were not measured for the various CWS, but rather a fixed fuel flow rate was maintained.

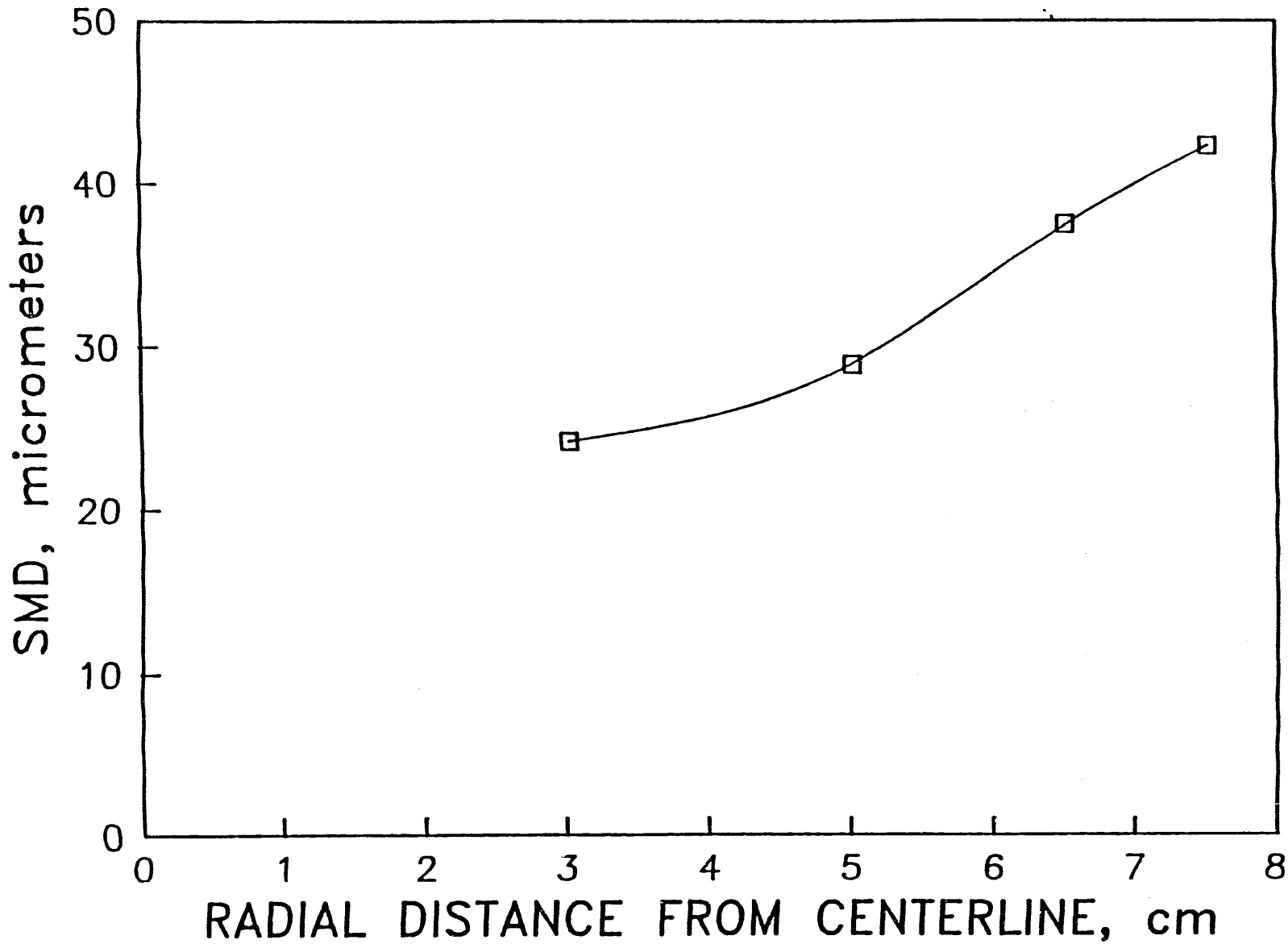

Figure 7.3. Variation of SMD with Radial Distance, 40 wt.% CWM, 375 lbm/hr (.0473 kg/s) Fuel Flow

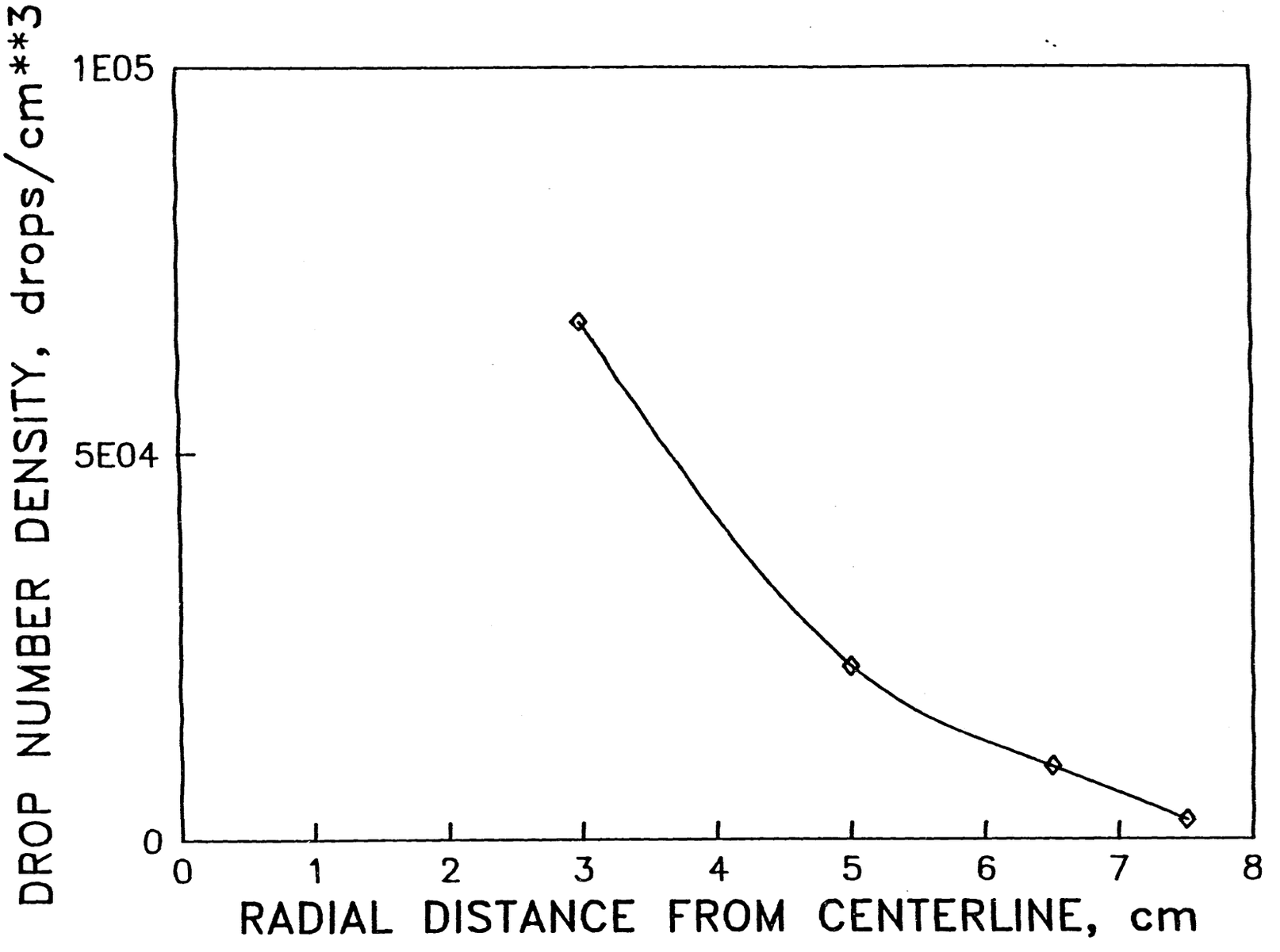

Figure 7.4. Variation of Drop Number Density with Radial Distance, 40 wt.% CWM, 375 lbm/hr (.0473 kg/s) Fuel Flow

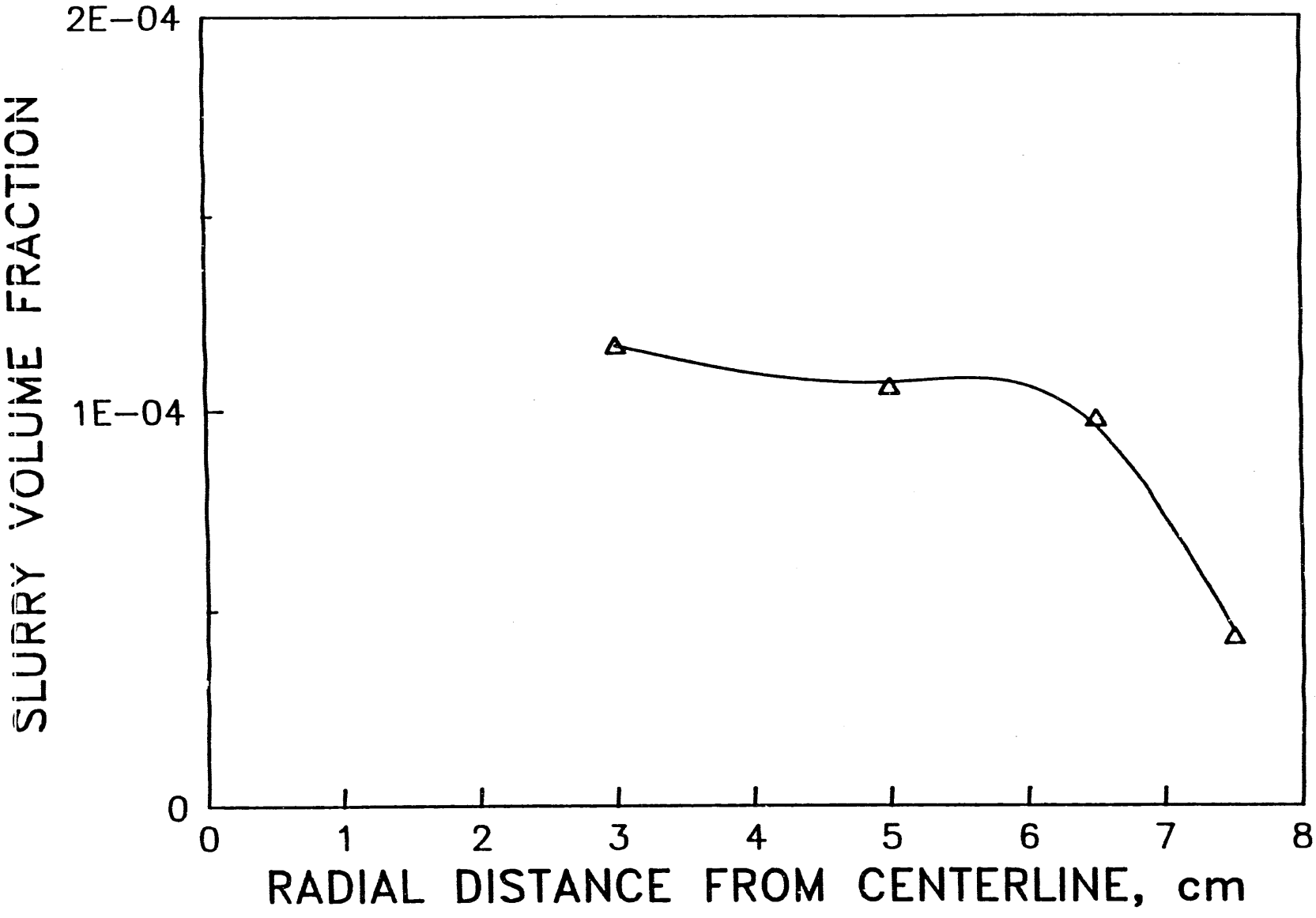

Figure 7.5. Variation of Slurry Volume Fraction with Radial Distance, 40 wt.% CWM, 375 lbm/hr (.0473 kg/s) Fuel Flow

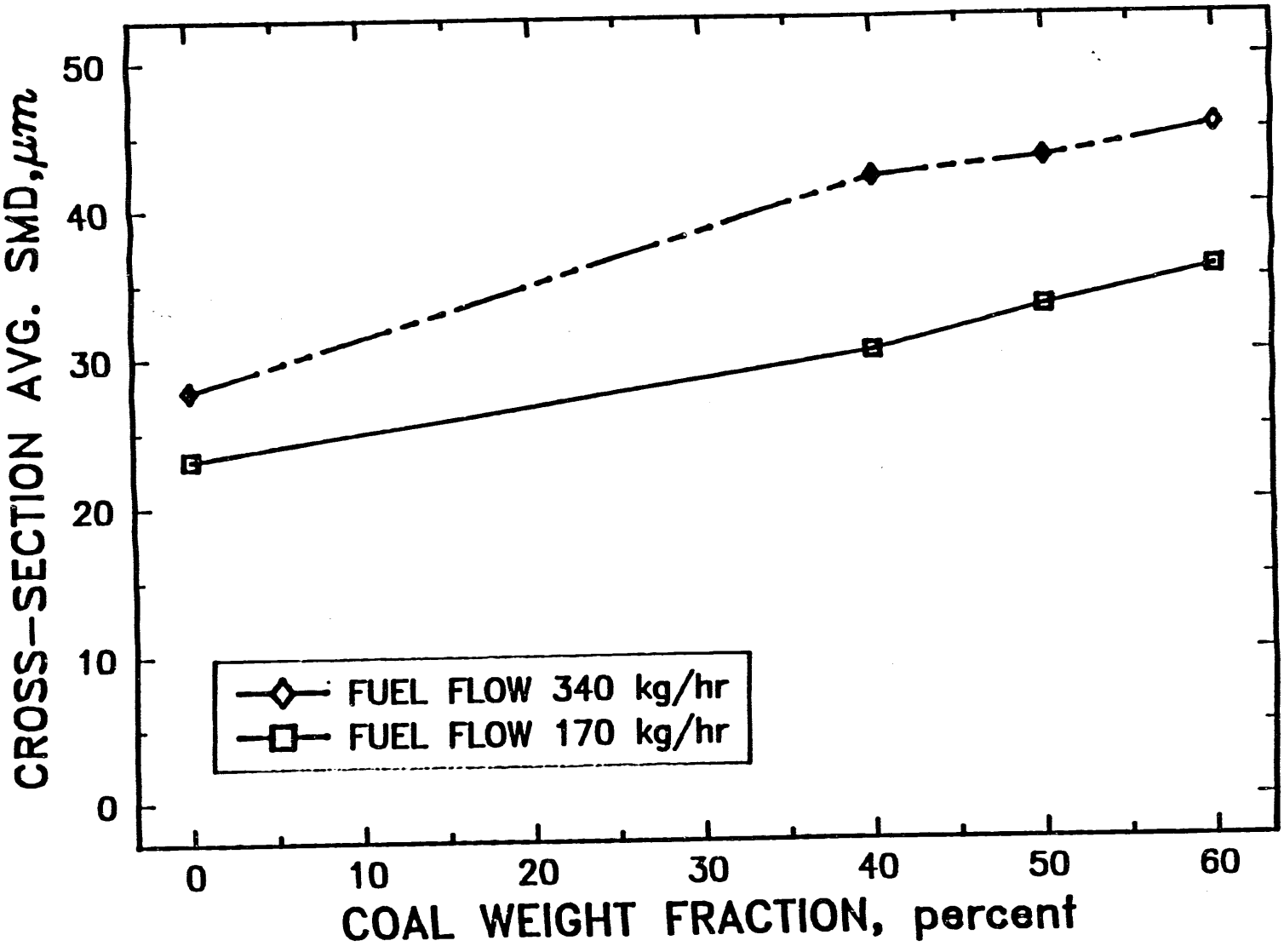

Figure 7.6. Effect of Coal Concentration on Atomization of Coal-Water Mixtures in Parker Hannifin Atomizer P/N EDL 6860701, Air Flow 90.7 kg/hr (200 lbm/hr)

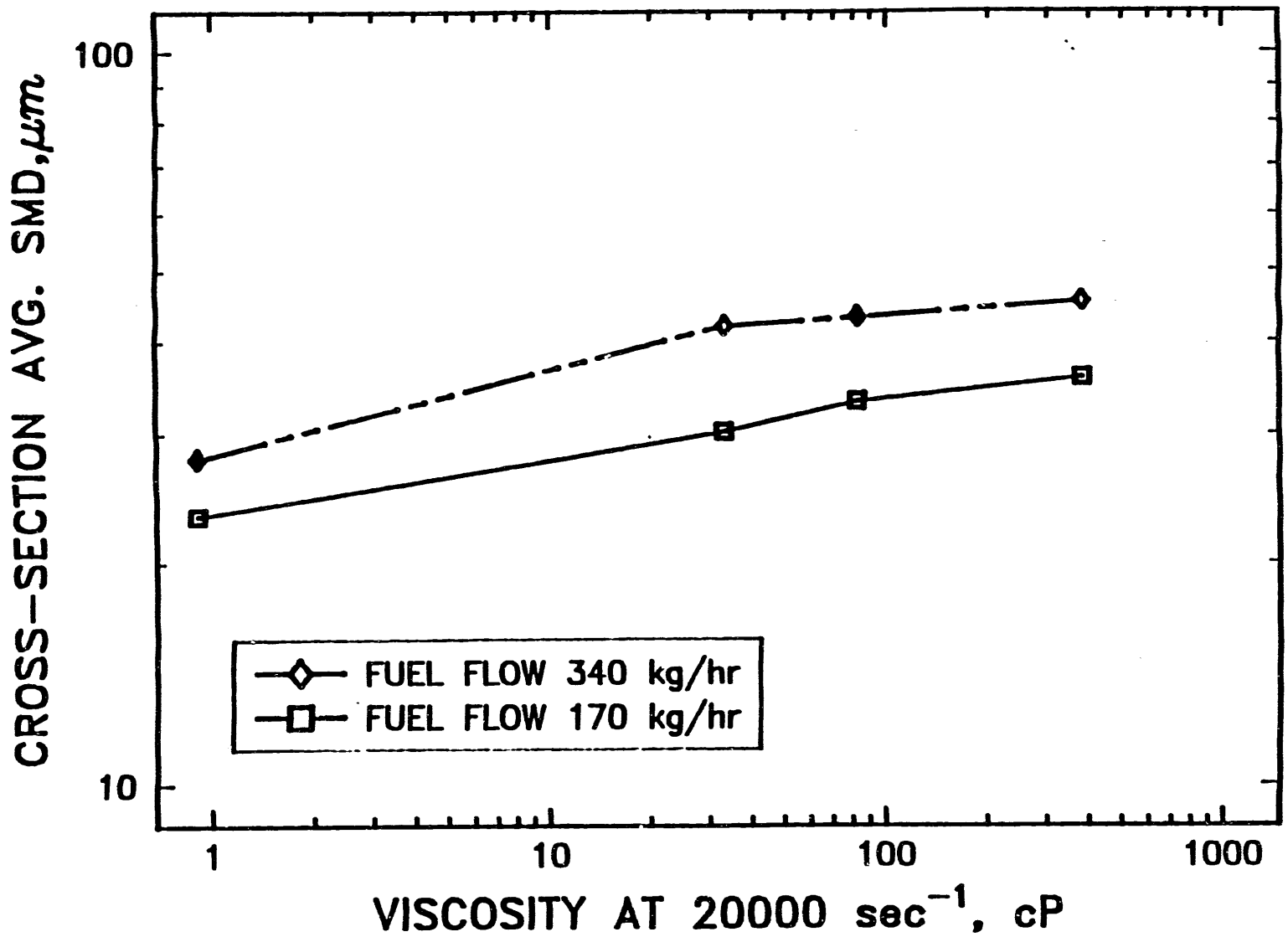

Figure 7.7. Correlation of SMD with High Shear Rate (20,000 s^{-1}) Viscosity for Parker Hannifin Atomizer P/N EDL 6860701, Air Flow 90.7 kg/hr (200 lbm/hr)

8.0 DIESEL HOLE-TYPE NOZZLES

The improvement of diesel engine performance for engines operating on single-phase or multi-phase fuels by changes in injector design is made difficult because the operation of current injection systems is not well understood. For example, it is not clear if the primary atomization mechanism is the interaction of the fuel jet with the air stream or the interaction with the piston bowl. The breakup of the intact core of the fuel jet is of significant interest, but is still difficult to measure or predict. It is clear that diesel injection systems operating with coal water mixtures (CWM) have severe problems with wear, particularly for the nozzle tips. Therefore, extensive engine tests are required to evaluate injector performance and the product development cycle becomes very time consuming and expensive.

Diesel injectors are more difficult to evaluate in terms of spray characteristics than other types of fuel nozzles such as those used in furnaces and gas turbines because: (a) they operate intermittently with injection durations of a few milliseconds; (b) injection pressures are high, ranging from 10 MPa (1450 psid) to 140 MPa (20300 psid), and vary throughout the injection cycle; (c) the fuel jet from a diesel hole-type injector is extremely dense and difficult to analyze with optical techniques because of the extreme optical opacity; and (d) air pressures at the time of injection are about 4.0 MPa (40 atm.) which can give quite different results that measurements at atmospheric air densities.

Sprays from all types of injectors tend to be nonuniform spatially, with variations in drop size and number density with distance from the atomizer and across the spray cross-section. The effect of these variations on measured characteristics has been extensively studied and documented in previous parts of this program (see Appendix A). Techniques have been developed to average spray characteristics across the spray cross-section, and those techniques have been used for much of the data reported here.

By the guidelines established for this program, tests were to evaluate the use of instrumentation in a laboratory environment to determine the performance of diesel hole-type atomizers. This laboratory environment limitation precluded the use of high-pressure chambers to evaluate sprays at realistic air densities, although those facilities are available at this laboratory. Thus, the question to be answered was, within the limits of atmospheric air densities, how could the spray characteristics of diesel hole-type injectors be characterized.

8.1. APPROACH AND EXPERIMENTAL APPARATUS

The approach selected for these tests was to avoid the ambiquities associated with the variable pressures and delivery rates in standard diesel injection systems by operating the injectors continuously at known, fixed pressures. This allowed accurate measurements of the pressures and flow rates, and considerably simplified the measurement of the spray characteristics.

A laser-diffraction particle sizing instrument was used to measure the spray characteristics as a function of axial and radial location, injection pressure, and nozzle geometry. Because a laser-diffraction instrument gives a line-of-sight integral measurement of the spray characteristics as shown in Figure 7.2, a deconvolution computer program was used to convert these measured values at several chords through the spray into the spatially resolved values for each ring in Figure 7.2 (see Appendix A for details of procedure).

Six standard commercial diesel injectors tips were obtained from AMBAC (American Bosch ADB M/77-8718-1 8-84), and machined (electron discharge machining) to provide a single hole parallel to the axis of each nozzle. The original tips were all approximately the same wall thickness, 1.19 ±0.01 mm (.0468 ±.0005 in.), but the end of three of the tips were machined to reduce the hole length to 0.83 ±0.02 mm and the other three tips were surface cut by 0.02 mm to produce the same surface finish as the three shorter tips. The "long" and "short" nozzles were then paired up, and the same nominal size hole was drilled by EDM in each pair. All machining of the blank tips was performed at Southwest Research Institute, and the length was machined first, followed by the EDM holes. The nominal hole sizes were 0.127 mm (0.005 in.), 0.178 mm (0.007 in.), and 0.254 mm (0.010 in.). The actual hole sizes were not exactly matched within each pair and were larger than the nominal hole sizes. The length of the shorter nozzles was chosen to produce a constant length/diameter (L/D) ratio between the two sets of nozzles, e.g., the 1.17 mm length/0.178 mm diameter injector has the same 6.6 L/D as the 0.84 mm length/0.127 mm diameter nozzle. Two of the long injectors had unacceptable spray patterns in terms of symmetry, leaving the four injectors described in Table 8.1.

The effective diameter shown in Table 8.1 was calculated based on the measured flow rate at a known pressure by,

Table 8.1. Description of Diesel Injector Tips

Nozzle No.	Effective Diam. (mm)	Length (mm)	L/D
8	0.215	1.18	5.4
10	0.142	0.83	5.8
11	0.239	0.83	3.5
12	0.254	0.83	3.3

$$Q = CA[(2\delta p/\rho)]^{1/2} \tag{8.1}$$

where Q is the volume flow rate, C is the discharge coefficient assumed to be 0.9 for these nozzles, A is the hole area, δp is the differential pressure, and ρ is the liquid density. It may be seen from Table 8.1 that the effective hole diameters were larger than the nominal diameters, but the L/D ratios are reasonable for diesel injectors.

A hydraulic system gear pump was used to supply fuel to the nozzles at a constant pressure. The needle lift spring in the injector holder was modified so that there was negligible pressure drop across the needle and seat and all of the pressure drop was across the hole. A bypass valve at the pump was used to adjust the fuel pressure drop across the hole over the range from 3.4 to 34.4 MPa (500 to 5000 psid). The fuels used for these tests included a reference diesel fuel Cat 1-H, and blends of Cat 1-H and mineral oil to achieve viscosities (at room temperature) of 3, 13, 25, 50, and 100 cSt.

The drop size distributions were measured with a Malvern Model 2600 which operates on the principle of laser-diffraction. Collimated, coherent, monochromatic light from a HeNe laser was directed through the spray and the light was diffracted at an angle inversely proportional to the drop diameter. Scattered light was collected on a set of 32 detectors arranged as annular rings centered about the undiffracted laser beam. The light was collected with a 100-mm focal length lens, and precautions were taken to avoid vignetting of the signal by placing the spray within 125 mm of the receiver lens (Dodge, 1984). Laser beam diameters of the standard 9 mm and a reduced diameter of 3 mm were used, as discussed in the results section. Corrections for multiple scattering used the procedures developed by Felton (1985).

The line-of-sight integral spray characteristics measured with the laser-diffraction instrument were converted into spatially resolved data for each annular ring as shown in Figure 7.2 using the procedure developed by Hammond (1981). This procedure is related to the Abel Inversion problem and is also referred to as deconvolution. Essentially the procedure involves measurements first through the outermost ring where the spray characteristics are measured directly, and then through the next chord where the characteristics of both outer rings are measured but the properties of the second ring in from the edge are computed by subtracting out the contributions of the outer ring, and so forth into the center of the spray. This procedure computes both the drop-size distribution, liquid volume fraction, and number density for each ring. Corrections for multiple scattering (Felton, 1985) are performed before the data are deconvoluted. The cross-section average SMD and other spray characteristics may then be computed by summing the data for each ring with appropriate weighting factors for the ring area and the drop number density.

An alternative and simpler technique for obtaining a cross-section average was developed during this project and consists of continuously scanning the laser beam through the spray while recording the light-scattering data (Appendix A). Although this technique is simpler than the deconvolution and summation method described above, it does not allow a correction for multiple-scattering of photons in dense sprays. This continuous-scan technique was used in addition to the deconvolution/summation technique for most of the measurements reported and offers the chance to compare the two approaches.

8.2. RESULTS AND DISCUSSION OF SPRAY CHARACTERIZATION

Some of the results exhibited trends expected for diesel hole-type atomizers, but other results were surprising. The effect of pressure drop on average drop size is shown in Figure 8.1 for the line-of-sight integral measurement through the centerline of the spray. As discussed earlier, the line-of-sight integral value does not properly represent the overall spray, but is useful to show trends. The average drop size was represented by the SMD is related to the pressure drop by,

$$SMD = 94.6\Delta p^{-0.77} \tag{8.2}$$

The jet velocity is known to be proportional to the square root of the pressure differential, and increasing jet velocity leads to smaller average drop sizes. This dependence of average drop size on pressure drop is typical of many atomizer designs, except that the exponent is more typically on the order of -0.5 rather than -0.77.

The variation of liquid mass fraction with radial distance is shown in Figures 8.2 and 8.3 for nozzles 8 and 11 at pressures of 10.3 MPa (1500 psid) and 20.7 MPa (3000 psid). These trends shown high liquid fractions in the central core region as expected, and the broader spray for the nozzle with a smaller L/D. However, these results were measured with the standard 9 mm beam diameter that would tend to "smear out" gradients in liquid mass fraction that were probably larger than shown.

Tip geometry can have an effect on spray shape as shown in Figures 8.2 and 8.3, where the shorter nozzle (smaller L/D) produced a broader spray. These tests were too limited to draw general conclusions, but Figure 8.4 shows some increase in average drop size with nozzle hole diameter. This was the expected trend, but the dependence on hole size was expected to be stronger.

The results presented in Figure 8.4 were determined by taking measurements through several chords of the spray from the centerline to the edge (e.g., Figure 7.2), deconvoluting those measurements to determine the spatially resolved SMD's and volume fractions, and then summing those results to get a cross-section average SMD at a given condition. However, the line-of-sight SMD values were relatively constant across the spray with a minimum toward the center of the spray, as shown in Figure 8.5. This trend is somewhat contrary to what would be expected for a spray that is originating as continuous liquid jet that is sheared by air friction into large drops and then progressively smaller drops. From this description of the spray break-up process, the largest drops would be expected to be at the center of the spray with smaller drops at increasing radial distances. To investigate the radial variations of the spray characteristics, the laser beam diameter was reduced from 9 mm to 3 mm, and the measurements were repeated. Note in Figure 8.5 that the reduced laser beam diameter did detect and measure the larger drops in the center of the spray that were "missed" with the larger beam. Because the radial extent of the spray was only about 7 mm from centerline to edge, a beam diameter smaller than 9 mm was required to resolve radial variations in spray characteristics. In general, diesel hole-type nozzles produce sprays that are too narrow in width to sample accurately with a standard 9 mm laser beam diameter.

Using the reduced laser beam diameter, the effect of viscosity on atomization was evaluated using nozzle #12 from Table 8.1. Sprays were characterized at an axial location of 50 mm downstream of the nozzle tip, at a differential pressure of 20.7 MPa (3000 psid). As shown in Figure 8.6, viscosity variations of 3 to 100 cSt had little effect on the drop sizes produced by the hole-type atomizer. This trend of insensitivity to viscosity is similar to the variable-film-thickness atomizer results reported in Section 6. In both of these nozzle designs, the increase in liquid viscosity

does not lead to an increase in film thickness as it would for a pressure-swirl or prefilming atomizer, since the film thickness is fixed by the hole diameter of the injector. Liquid viscosity does not have a significant effect on spray cone angle as shown in Figure 8.7.

The peak in centerline liquid mass fraction appears to decrease with increasing viscosity in Figure 8.7. This is probably due to delayed break-up of the central jet of intact liquid with increasing viscosity. The laser diffraction instrument only responds to drops within the laser beam. In addition to the normal scattering signature, there was some scattered light on the innermost rings for the sprays of the viscous liquids, and this was probably due to refraction of the laser beam through, or diffraction around, a stream of unbroken liquid making up the central jet. Tests with the same nozzle at low differential pressures produced an unbroken liquid stream that scattered light only onto the innermost detector rings, similar to the "extra" scattering signal from the viscous liquid sprays.

These results illustrate some of the difficulties of measuring diesel spray characteristics. Some of the complexities are illustrated above, but there are also some subtle effects not clear from the above discussion. These sprays consist of a very dense collection of drops, particularly near the centerline, but the drop density varies rapidly with radial distance (Figure 8.3). Corrections for errors due to multiple scattering are required, and these corrections are computed based on the intensity of the unscattered portion of the laser beam. However, in those cases where the laser beam diameter is very large relative to the radial variation of drop densities, these corrections cannot be applied accurately. Although a 3-mm beam was used in place of the standard 9-mm beam in the experiment reported above, it is somewhat larger than the ideal diameter of about 1 mm for the radial variations in these types of sprays. There are both experimental and theoretical limits on how small the laser beam can be. For the diffraction theory to work correctly, the laser beam diameter must be much larger than the largest particles measured. For the case reported here, the largest drops were on the order of 200 micrometers, so the laser beam diameter should be at least 1 to 2 mm (1000 to 2000 micrometers) in diameter. Experimentally, the Malvern laser-diffraction instrument requires a completely different beam expander and spatial filter if a beam smaller than 3-mm is used. Alternatively, it might be possible to omit the spatial filter and use the raw laser beam with a diameter of 0.83 mm.

An additional problem associated with the very dense sprays is that the centerline may be so dense that very little light penetrates the spray, and the scattering signature is lost in some cases. This problem can be evaluated if the laser beam diameter is comparable to the dense spray

region. A 9-mm laser beam is much larger than the dense region of a diesel hole-type injector spray at axial measurement locations of 100 mm or less, corresponding to the distances available before the spray strikes the piston.

A further problem with laser-diffraction measurements of drop sizes in these sprays is the possible presence of a liquid core or large ligaments in the sample region. A liquid core or large ligaments would tend to scatter light onto the inner detector rings, but the laser-diffraction instrument does not necessarily give a clear indication of the presence of the liquid core. Thus, it has been demonstrated experimentally and phenomenologically that laser-diffraction measurements of a diesel hole-type injector intended to determine radial drop size profiles require a laser beam diameter much smaller than the standard 9-mm beam used with a Malvern instrument. Also, radial variations can only be determined by deconvoluting the data, as the line-of-sight integral values may not reveal the actual trends.

As described in the Approach and Experimental Apparatus Section, both the deconvolution-summation technique and the continuous-scan technique were used to measure the cross-section average spray characteristics. All of the above results were based on the deconvolution/summation technique that allows correction for errors due to multiple scattering of photons off more than one drop before being detected. A comparison of cross-section average SMD's by the two techniques is given in Table 8.2. As can be seen in Table 8.2, the SMD's measured by the continuous-scan technique track closely with those computed by deconvolution-summation method, except that the continuous-scan values are systematically smaller by roughly 35 percent, in agreement with the fact that they were not corrected for multiple-scattering errors. The magnitude of the difference is somewhat larger than expected. The deconvolution-summation technique is judged to be more accurate than the continuous-scan technique because of the multiple-scattering correction, but the second technique shows all the correct trends. The deconvolution-summation technique also gives the radial variation of the spray properties which were needed for this project.

Table 8.2 Comparison of Cross-Section Average SMD's Measured by the Deconvolution/Summation and Continuous-Scan Methods

Nozzle No.	Axial Dist. (cm)	Cross-Section Avg. SMD (μm) $\delta p = 10.3 MPa$ Decon./ Sum.	$\delta p = 10.3 MPa$ Cont. Scan	$\delta p = 20.7 MPa$ Decon./ Sum.	$\delta p = 20.7 MPa$ Cont. Scan
8	10.0	18.7	12.3	14.0	8.7
	20.0	21.7	14.1	15.8	10.1
10	2.5	20.7	13.3	14.6	8.8
	5.0	20.0	13.5	14.6	8.7
	10.0	21.1	14.1	14.8	10.6
	20.0	24.1	18.7	17.6	13.0
11	10.0	20.8	13.8	14.4	8.4
	20.0	22.2	15.8	16.5	12.3
12	2.5	22.9	15.9	14.8	8.3
	5.0	24.0	14.9	15.7	9.5
	10.0	21.6	13.8	17.0	9.1

8.3. EFFECT OF VISCOSITY ON FLOW RATE

The fuel flow rate at a constant differential pressure of 2.07 MPa (3000 psid) decreased with increasing viscosity over the range from 3 to 100 cSt, as expected for a hole-type atomizer. Fuel flow rate would normally be correlated with the viscosity raised to a power, as shown in Figure 8.8. For these particular experiments, the fuel flow rate correlated better with a linear fit to the viscosity as shown in Figure 8.9. The reason for the better correlation with the linear model rather than the power model is not known.

8.4. SUMMARY

Laboratory techniques for measuring the spray characteristics of diesel hole-type injectors have been demonstrated. It has been shown that the standard beam diameter used on some commercial laser-diffraction instruments is too large to accurately resolve radial variations of spray characteristics for this type of injector at axial distances corresponding to those of importance in engine applications. Improved results with a smaller laser beam have been demonstrated.

Two techniques have been applied to these sprays from diesel injectors to obtain cross-section average spray characteristics using laser-diffraction instruments. The simpler of these two techniques involves the continuous scanning of the spray relative to the laser beam while a

cumulative light-scattering signal is obtained. The second technique involves measurements at various chords through the spray from one edge to the other edge of the spray, followed by a deconvolution procedure to determine density, followed by a summation procedure to arrive at cross-section average characteristics. The second procedure is more tedious, but has the advantage that corrections can be made for multiple scattering errors, and the radial variations in the spray characteristics are determined. In many types of sprays, corrections for multiple scattering are small, but in diesel hole-type injector sprays the corrections are usually significant. Thus, the continuous scan technique is a much simpler approach if only a cross-section average is required, but some errors are introduced by multiple scattering that cannot be corrected.

The sprays of four diesel hole-type injectors were characterized. It was determined that the Sauter mean diameter (SMD) decreased with liquid pressure differential raised to the 0.77 power, increased with hole diameter raised to approximately the 0.1 power, and was independent of the liquid viscosity over the range of viscosities from 3 to 100 cSt. The spray width was unaffected by changes in liquid viscosity over the same range, but did increase with decreasing length/diameter ratio of the hole.

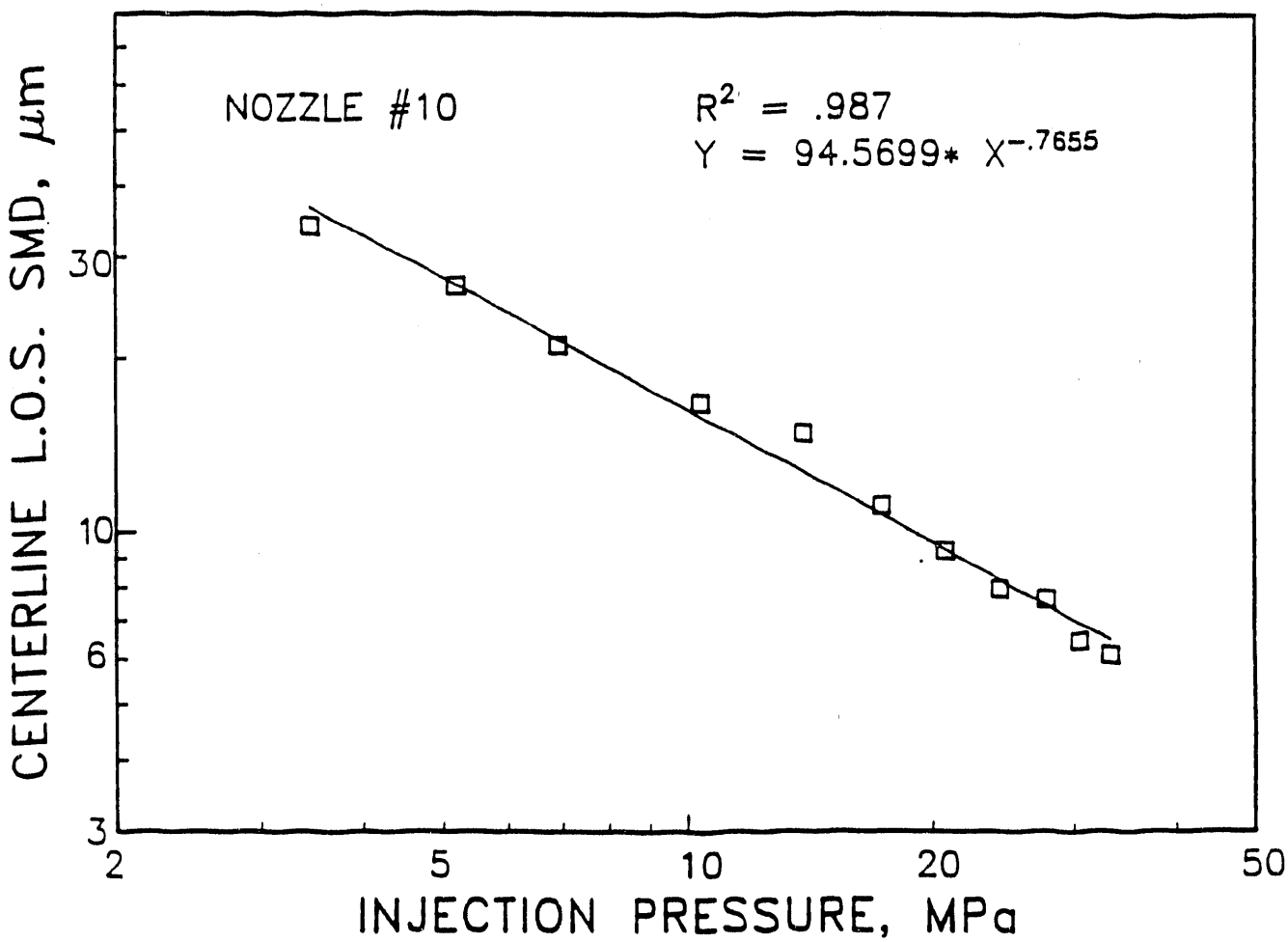

Figure 8.1. Effect of Injection Pressure on Centerline Line-of-Sight SMD, Axial Location 50 mm.

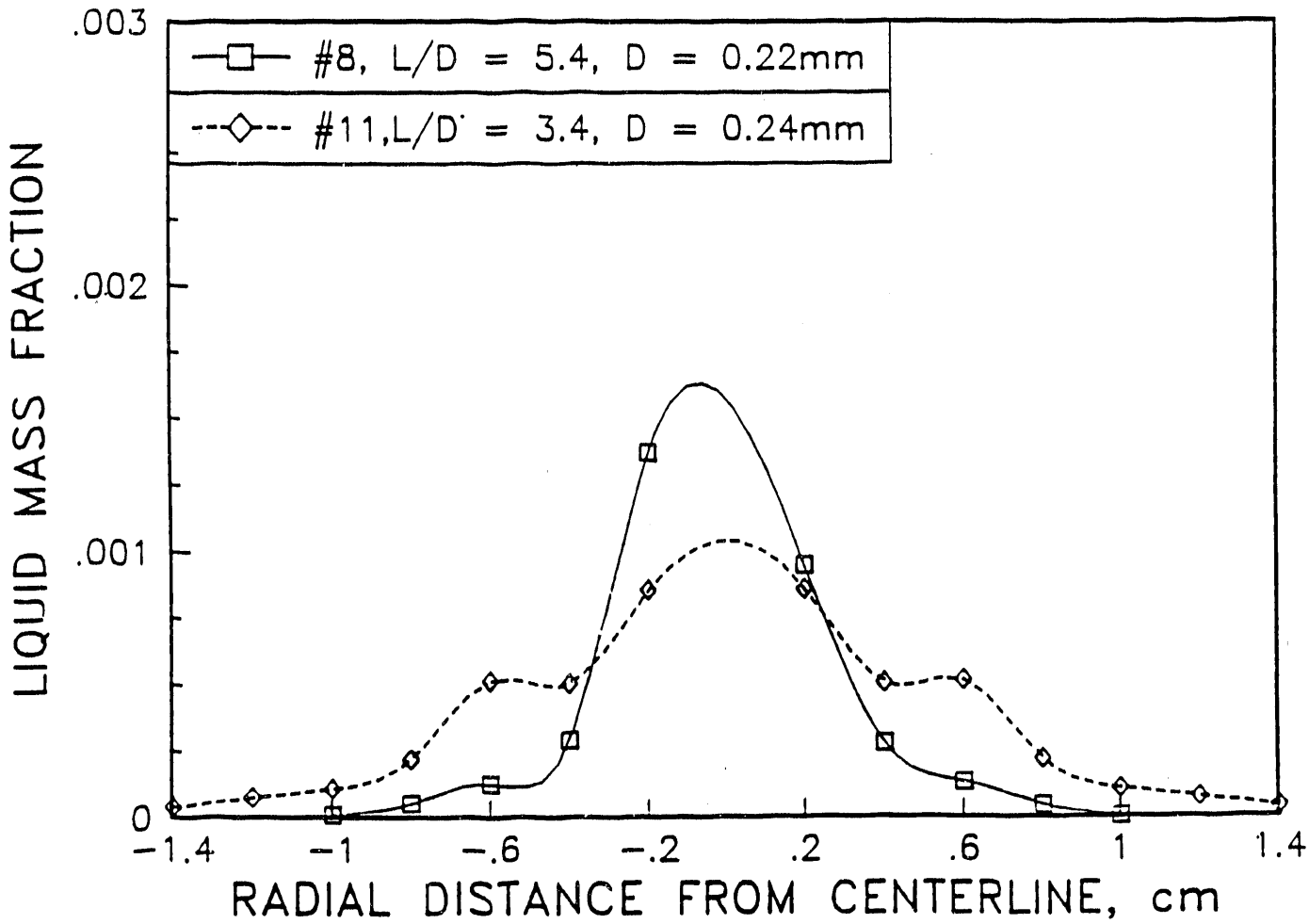

Figure 8.2. Effect of L/D on Spray Width at Axial Location of 100 mm, Injection Pressure = 10.3 MPa (1500 psi)

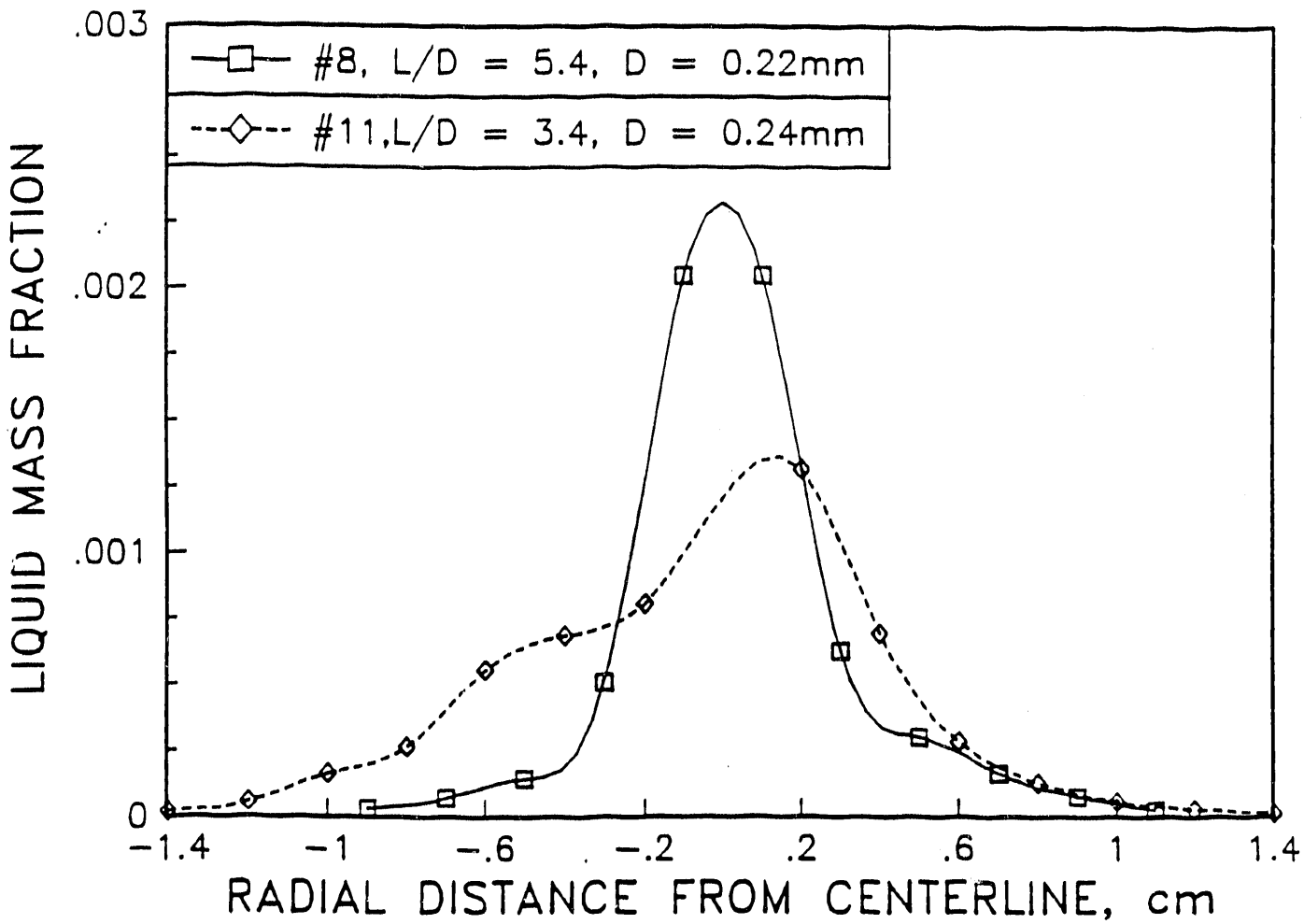

Figure 8.3. Effect of L/D on Spray Width at Axial Location of 100 mm, Injection Pressure = 20.7 MPa (3000 psi)

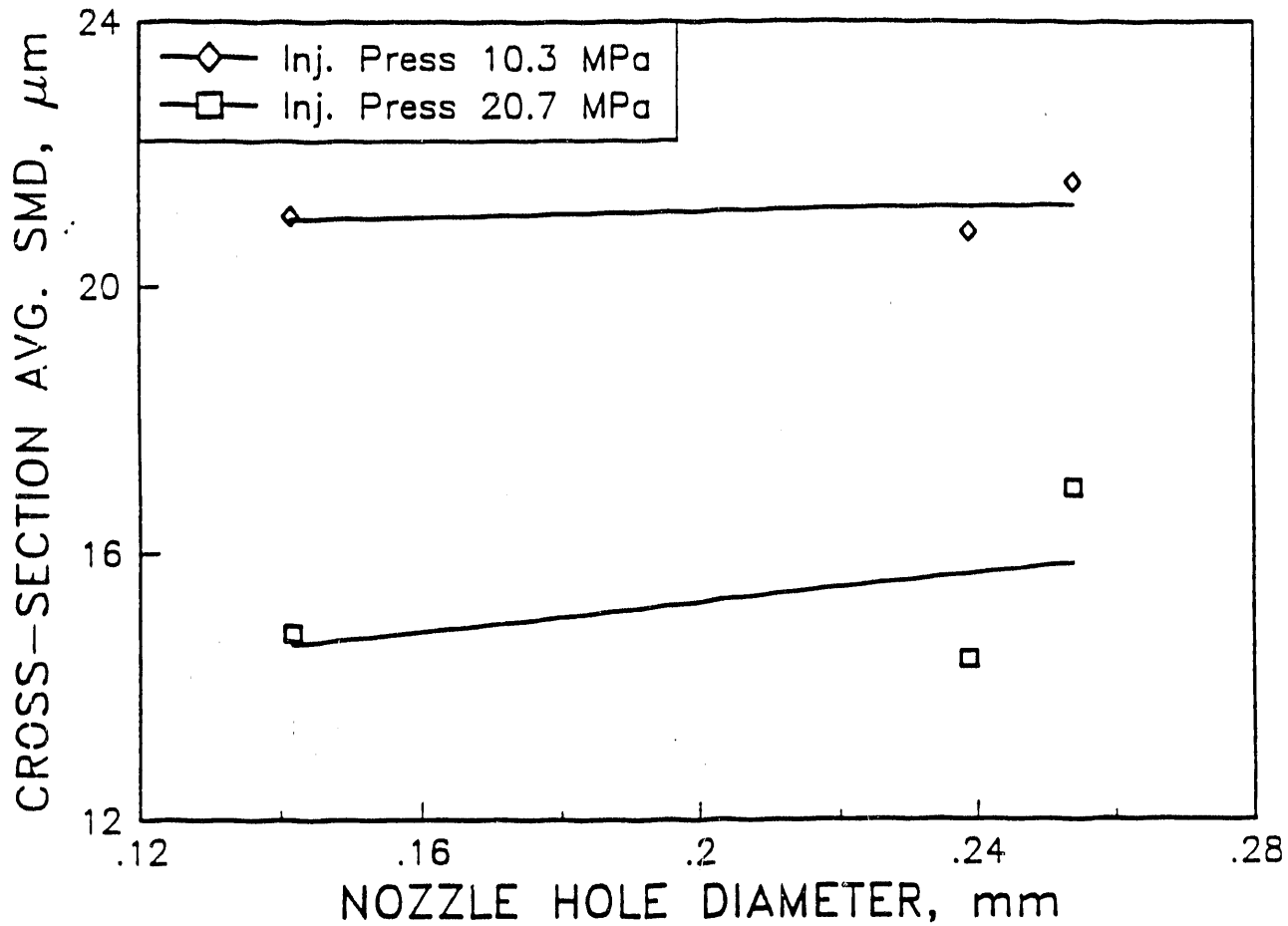

Figure 8.4. Effect of Hole Diameter on Average SMD Measured at 100 mm Axial Location for Nozzles #10, 11, and 12

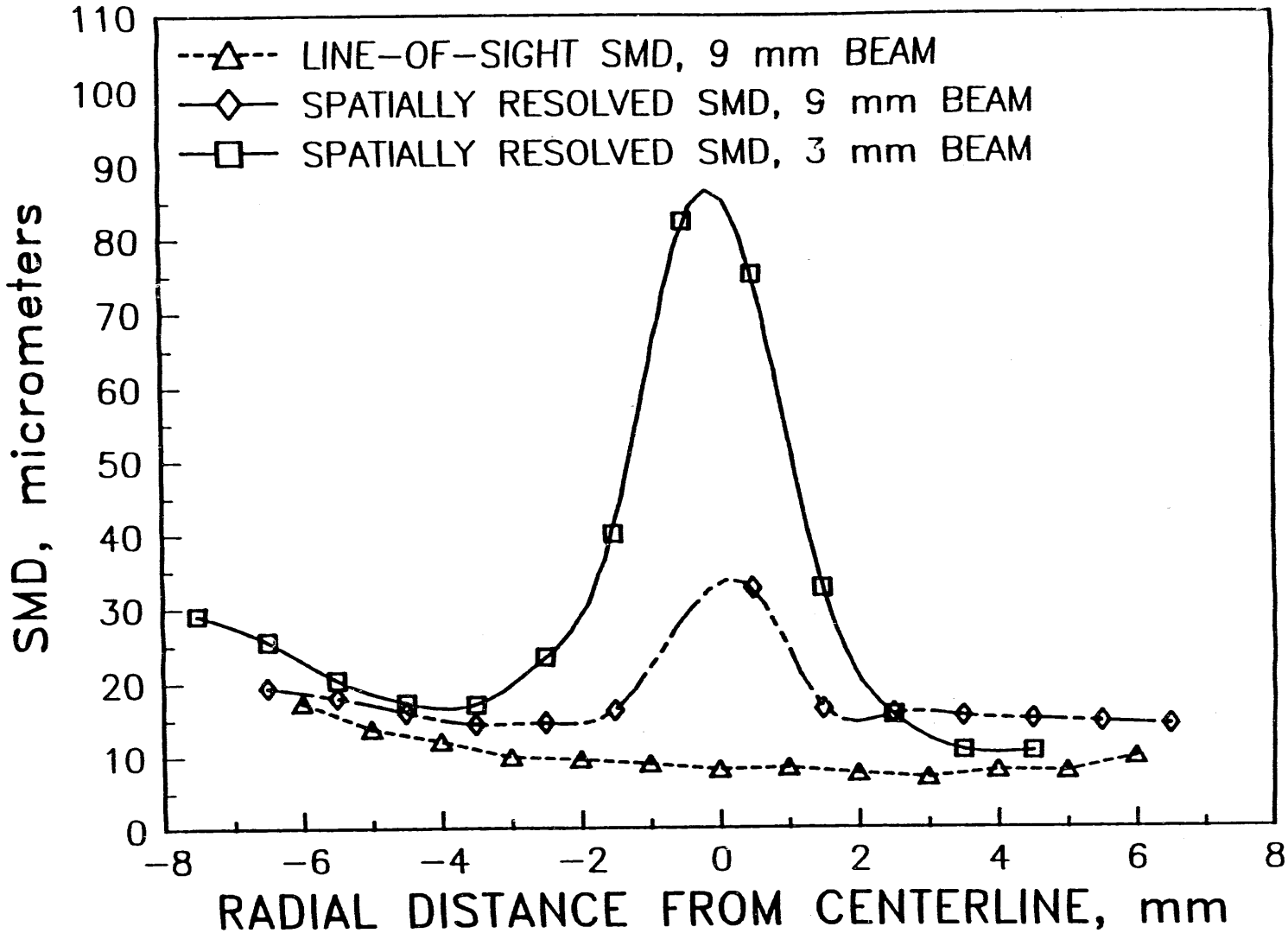

Figure 8.5. Effect of Laser Beam Diameter on SMD as a Function of Radial Location at an Axial Distance of 50 mm, Nozzle #10, Injection Pressure 20.7 MPa (3000 psi)

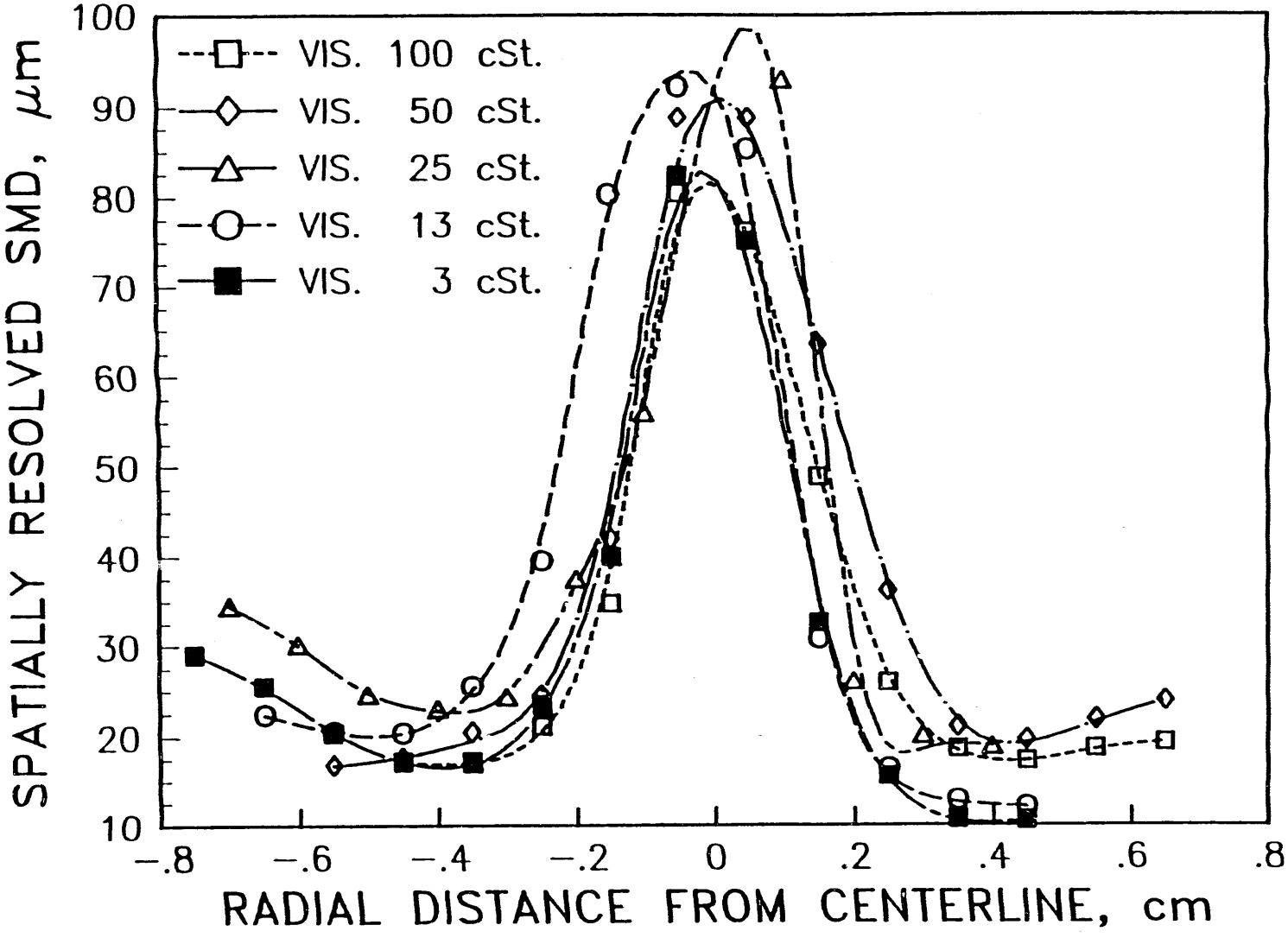

Figure 8.6. Effect of Viscosity on SMD as a Function of Radial Location at Axial Distance of 50 mm, Nozzle #12, Injection Pressure 20.7 MPa (3000 psi)

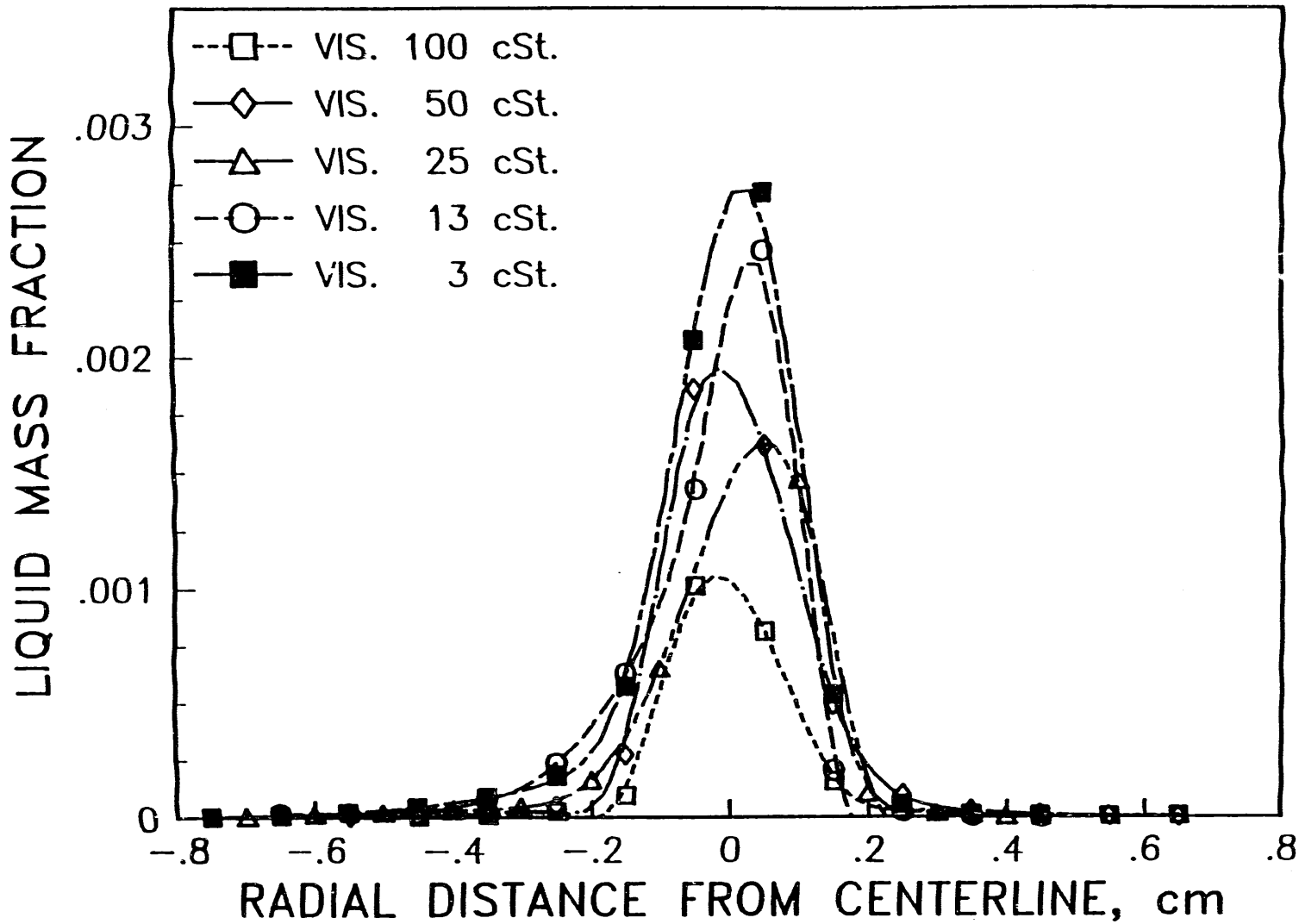

Figure 8.7. Effect of Viscosity on Spray Width and Density at an Axial Location of 50 mm, Nozzle #12, Injection Pressure 20.7 MPa (3000 psi)

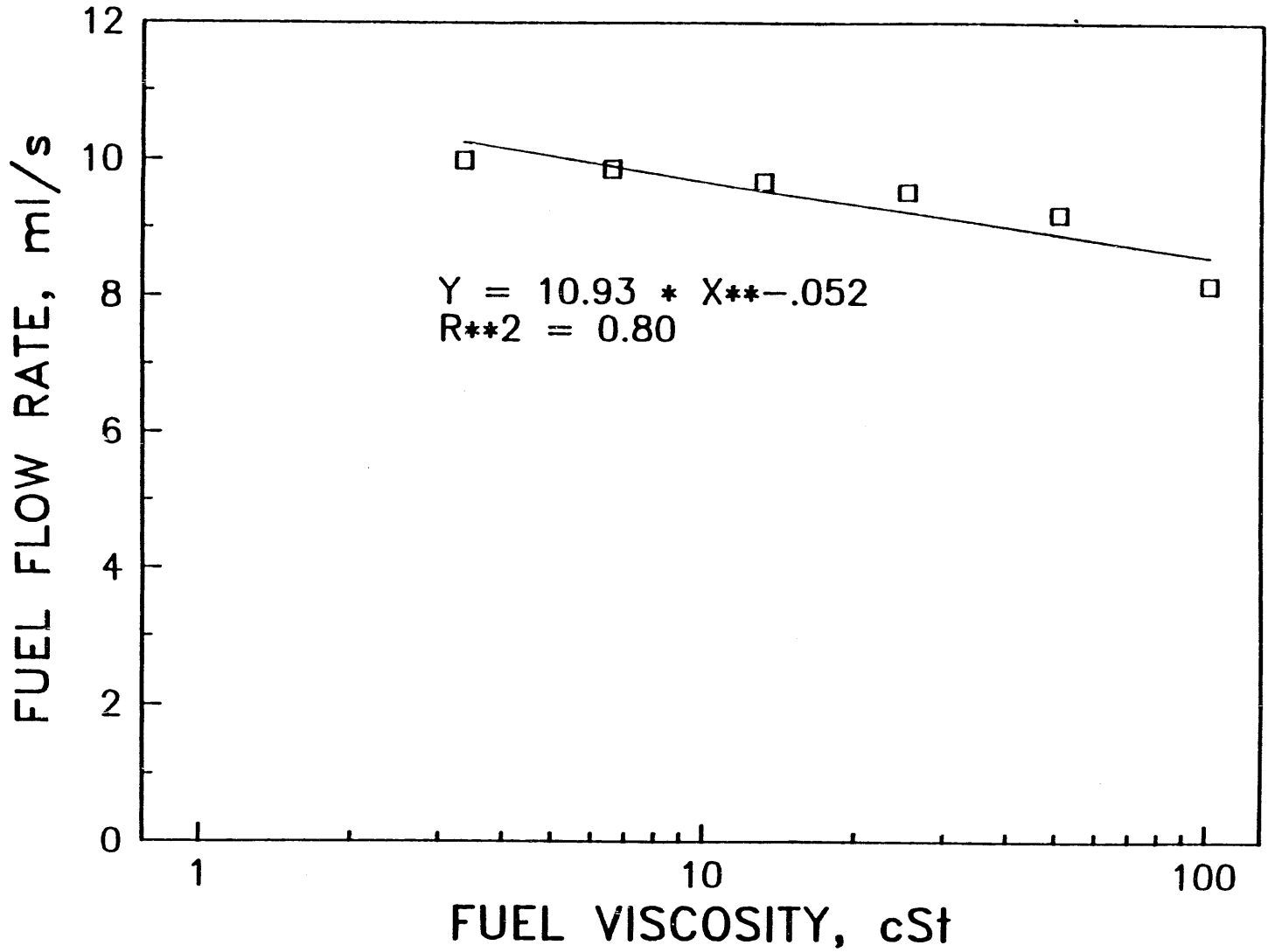

Figure 8.8. Effect of Fuel Viscosity on Fuel Flow Rate at Differential Pressure of 20.7 MPa (3000 psi), Nozzle #12, Power Law Fit

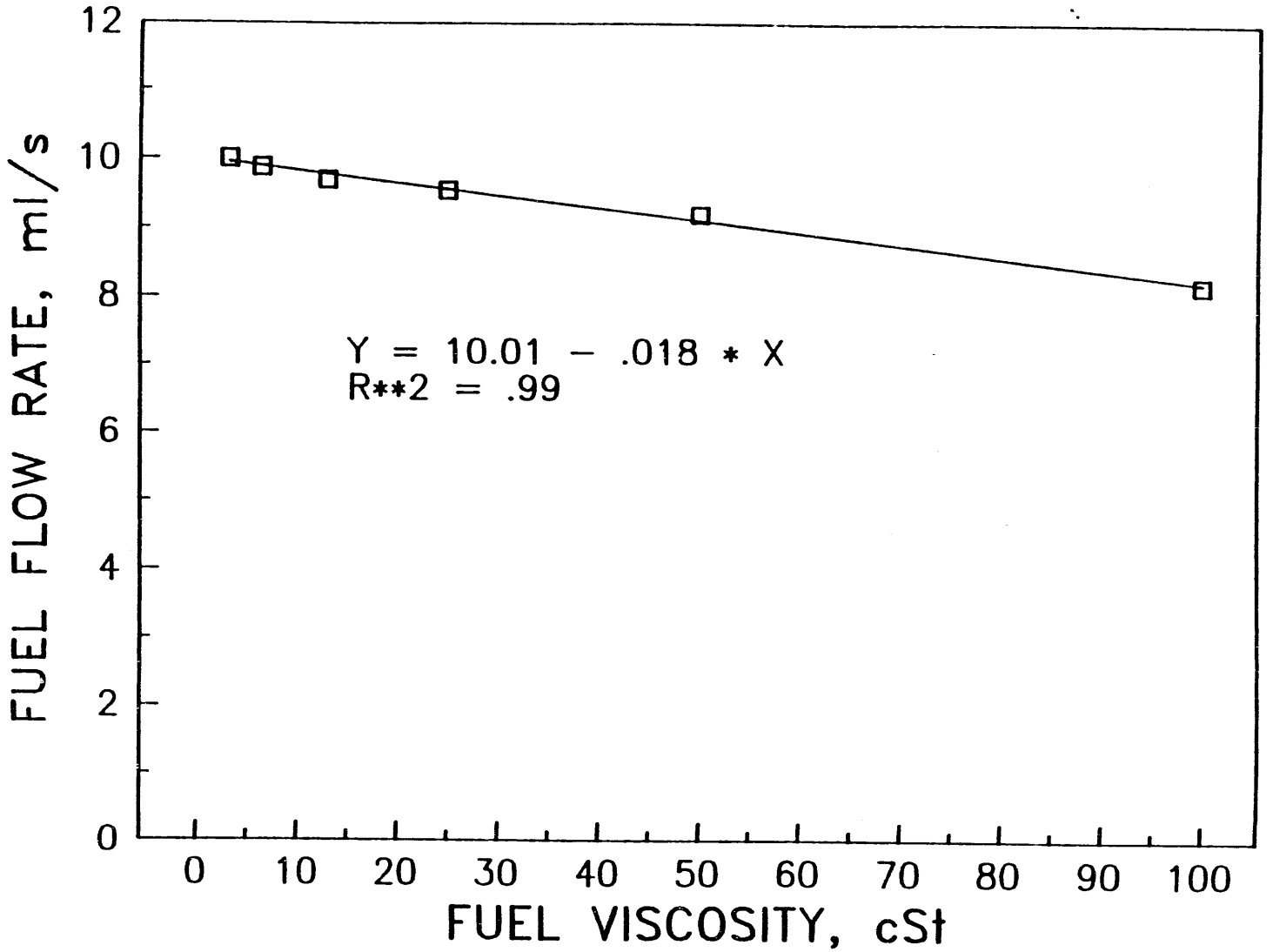

Figure 8.9. Effect of Fuel Viscosity on Fuel Flow Rate at Differential Pressures of 20.7 MPa (3000 psi), Nozzle #12, Linear Fit

9.0 GAS-SOLID NOZZLE TESTS

The hydrodynamic performance of straight-tube nozzles conveying mixtures of gas and solid particles were determined by highly-instrumented tests. The objectives of these tests were:

- measure such hydrodynamics characteristics as the nozzle mass flow rates, nozzle pressure drops, and particle fluxes and distributions in the spray; and

- develop methods to allow laboratory tests to characterize nozzles for applications.

Although the dispersal of mixtures of micronized coal and air is the most common application for gas-solid nozzles, the particles used in the present tests were monodisperse glass beads. The substitution of glass beads for micronized coal was made to simplify the test procedures. This substitution does not limit the utility of the test results, and it has the advantage that glass beads have been widely used in other laboratory tests (Crowe and Plenk, 1984, and Morris, et al, 1986).

9.1. FLOW TEST FACILITY

All the gas-solid tests were conducted in a specially-constructed facility shown schematically in Figure 9.1. and photographically in Figure 9.2. The main components of the facility are:

- **Pressure vessel.** This vessel contains the solid particle reservoir, the particle feeder, and the mixer for the air and particle flows. Pressurized air is supplied to the vessel for the air flow. Provisions are included for seeding the air with micron-sized water droplets when needed to make air velocity measurements.

- **Connecting tube between mixer and nozzle.** The upstream end of the tube is attached to the outlet of the air-particle mixer. The test nozzle is attached to the downstream end. The tube is 0.5 in (12.7 mm) inside diameter and 5.0 in (127 mm) long.

- **Laminar-flow test section.** The test section is 20 in (514 mm) square by 20 in (514 mm) long. Air at low-velocity (≈ 0.1 m/sec) is drawn through the test chamber to prevent recirculation during nozzle tests; the air enters and exits through honeycomb panels at the top and the bottom of the test section. The walls of the test section are optical-grade clear plastic to permit flow visualization and measurements.

- **Support frame and translating table for LDV.** An Aerometrics® velocimeter is used to make spray measurements. It is mounted on a translating table supported by a massive frame. The table has two degrees of freedom, vertical and horizontal (transverse). The minimum adjustment of the table in either degree of freedom is 0.001 in (.25 mm), although such fine adjustments were not employed in the tests.

- **Aerometrics® laser phase-doppler velocimeter.** The velocimeter is used to determine the velocity and number density of particles in the spray. The data acquisition and reduction system for the velocimeter is contained in a PC/AT-class computer.

- **Flow instrumentation.** The air flow is measured by a flowmeter in the supply line. The particle flow rate is measured by the speed of the feeder motor, which was calibrated in advance. Chamber pressure is determined by a direct-reading gage.

9.2. TEST PLAN

Two types of tests were conducted:

- facility validation/calibration tests, and

- gas-solid nozzle data tests.

9.2.1. Facility validation/calibration test plan

Calibration tests using gas-only flows served to (1) verify the quality of the test chamber and instrumentation and (2) acquire baseline data to serve as a comparison for the gas-solids tests. Straight-tube nozzles ten diameters long, with inside diameters of 3/16 in (4.8 mm) and 3/8 in (9.5 mm), were used to inject jets of air into the test chamber. The jets were seeded with micron-size water drops to allow the LDV to measure the velocities and turbulence quantities.

To conduct a test, the air flow to the chamber was regulated to the desired value. When the chamber pressure had stabilized, indicating steady-state flow conditions through the nozzle, the jet centerline velocity and turbulence levels were measured at 12 downstream locations (x/d = 0 to 40) and the velocity and turbulence distribution across the jet width were measured at four downstream locations. Two centerline velocities, 40 and 80 m/sec (131 and 262 ft/sec), were used in the tests.

Detailed results of the tests are given in Appendix B. In summary, the tests showed that:

- the test section contained no recirculation cells; and
- the free-jet characteristics agreed well with both theory and other experiments (Schlicting, 1979), thus validating the data acquisition system.

9.2.2. Gas-solid nozzle test plan and procedures

The original test plan for the gas-solids tests called for two nozzles of two different geometries. As the tests progressed, it became apparent that more emphasis should be given to gaining a fundamental understanding of the flow processes for a relatively simple nozzle. Therefore, the test plan was modified to optimize the analysis of test results and to make the best use of project resources. The final test plan considered only straight-tube nozzles, having diameters of 3/16 in and 3/8 in (4.8 mm and 9.5 mm), and lengths of ten diameters. The matrix of tests is shown in Table 9.1.

The gas velocities were chosen to give the same Reynolds numbers based on nozzle diameter, for both the 3/16 and 3/8 in nozzles. The Stokes numbers:

TABLE 9.1 TEST PLAN FOR GAS-SOLID NOZZLES

Tube Diam. (inch)	Gas Vel. (m/sec)	Part. Diam. (microns)	Loading (kg solid/kg gas)	Reyn. No.	Stokes No.
3/16	30	40	1	9500	7.8
3/16	30	40	2	9500	7.8
3/16	30	80	1	9500	30.7
3/16	30	80	2	9500	30.7
3/16	60	40	1	19000	15.6
3/16	60	40	2	19000	15.6
3/16	60	80	1	19000	61.4
3/16	60	80	2	19000	61.4
3/8	15	40	1	9500	1.9
3/8	15	40	2	9500	1.9
3/8	15	80	1	9500	7.7
3/8	15	80	2	9500	7.7
3/8	30	40	1	19000	3.8
3/8	30	40	2	19000	3.8
3/8	30	80	1	19000	15.4
3/8	30	80	2	19000	15.4

$$St = \frac{\rho_p d^2 V_g}{18 \mu_g l} \tag{9.1}$$

were chosen to vary the relative influence of aerodynamic drag on the particle motion over a wide range; small values of St represent a large influence. The symbols in the definition of St are:

d = particle diameter

L = nozzle length

V_g = gas velocity in nozzle

ρ_p = particle density

μ_g = gas viscosity

The solids loading ratios LR were varied by a factor two. Although these loadings were reasonably large, particle concentrations were still fairly low; for example, for a loading ratio of 1, the volume fraction of particles in the flow is 0.048%.

To conduct a gas-solids test, the compressed-air flow into the pressure chamber was regulated to the desired value using the flow meter in the line. The air flow was maintained without a particle flow until the inlet flow to the chamber and the outlet flow through the nozzle became equal, as indicated by a steady chamber pressure. The particle feeder to the nozzle was then turned on and adjusted to give the desired particle mass flow. Sufficient time was allowed for the chamber pressure to stabilize at a new, higher value. (The gas flow meter reading did not change, so the air flow remained at its pre-set value.) Spray characteristics were then measured with the velocimeter. Particle velocities (time average and rms) and concentrations were sampled along the spray centerline at twelve axial locations, ranging from 1 nozzle diameter to 40 nozzle diameters downstream, and across the spray width (8 radial positions) at four downstream locations.

Initially, it was planned to measure the air velocity in the spray as well as the particle characteristics. However, the water droplets needed to seed the air flow tended to make the glass beads agglomerate, so the air velocity measurements were abandoned.

9.3. TYPICAL TEST RESULTS FOR GAS-SOLID NOZZLES

Data plots for all the gas-solid nozzle tests have been submitted separately (Data Package, 1988). Only representative steady-flow parameters will be discussed here. But, as a brief summary of the unsteady, or turbulence, parameters, the centerline turbulent velocity was typically 8% of the steady centerline velocity, and the turbulence gradually increased with radial distance from the centerline to values of about 12% of the steady velocity at the edge of the spray.

9.3.1. Particle velocity at the nozzle exit

Gas-solid nozzles do not usually have L/D ratios large enough to allow the particles to achieve the same velocity as the gas. In the tests conducted here, the particles entered the feeder tube with essentially a zero velocity. The particles were accelerated in the feeder tube and in the nozzle by the gas flow to an exit velocity that depended on the Stokes number of the flow. Figure 9.3 shows the test results in the form of the ratio of the particle velocity to the gas velocity at the exit of the nozzle. The velocity ratio is less than unity for all the tests but approached unity for the smallest Stokes numbers, for which aerodynamic drag is the largest compared to particle inertia.

9.3.2. Gas-solid nozzle pressure drop

The pressure drop across the nozzle is shown in Figure 9.4, in the form of the ratio of the gas-solid pressure drop ΔP_{gs} to the pressure drop ΔP_g for the initial gas-only flow. Adding particles to the flow increased the pressure drop substantially. The pressure drop increased with loading ratio LR and Reynolds number Re, and decreased with Stokes number St.

9.3.3. Spray velocity characteristics

Figures 9.5 shows typical particle velocities along the centerline of the spray as a function of the ratio of downstream distance x to nozzle diameter D. For comparison, the centerline velocities of a free-gas jet for the same total air flow and nozzle diameter are also shown. Since the particle velocity at the nozzle exit was less than the gas velocity, the particles were accelerated by the gas for some distance downstream. Eventually, the particles attained the same velocity as the gas. The greater inertia of the particles then caused them to maintain a higher velocity than the air for a considerable distance. (Note that the actual gas velocity was probably somewhat less than the free jet velocity shown in the figures because of momentum interchange with the slower particles.)

9.3.4. Particle Mass Flux Distribution

The particle mass flux at a point in the spray is defined as the product of the measured particle velocity, the measured number density, and the particle density; it has dimensions of mass per unit area per unit time. Figure 9.6 shows a typical test result. The flux has been normalized by the flux at the center of the nozzle exit to make the trends more evident. The width of the spray was only three or four nozzle diameters even forty diameters downstream from the nozzle. By contrast, the width of a free gas jet forty diameters downstream is seven diameters (see Appendix B).

Since the spray flow area increases with radius from the centerline and distance downstream, a clearer picture of the distribution is obtained by correcting the flux for the larger areas farther from the nozzle exit. To make the correction, each measured flux was multiplied by the annular area represented by the radius at which the measurement was made; that is, the total flow area for each measurement was an annulus having the radius of the sampling point and a width equal to the radial distance between sampling points. Figures 9.7a and 9.8a show typical corrected distributions for two representative tests. These fluxes have been normalized by the total particle mass flow rate, thereby compensating for small discrepancies between the total flow rate measured

in the spray and the total particle flow rate. The distributions are reasonably similar to each other for $x \geq 10D$. Near the nozzle exit, however, the spray distribution, somewhat like a gas jet, has not yet developed to its final form.

The downstream peaks of the flux occurred roughly at the radial location where the radial velocity of a free-gas jet is zero; that is, at the point where the gas velocity changes from an outward direction to an inward direction. Evidently, the particles accumulated near this point.

By summing the fluxes shown in Figures 9.7a or 9.8a over the width of the spray, the fraction of the total particle flow rate that occurred within any specified width of the spray can be computed. Typical results are shown in Figures 9.7b and 9.8b. By definition, the total width of the spray at a given downstream location is the point where this fraction is unity. Since the velocimeter could not determine the boundary of the spray accurately, these plots should not be used as absolute determinations of spray width.

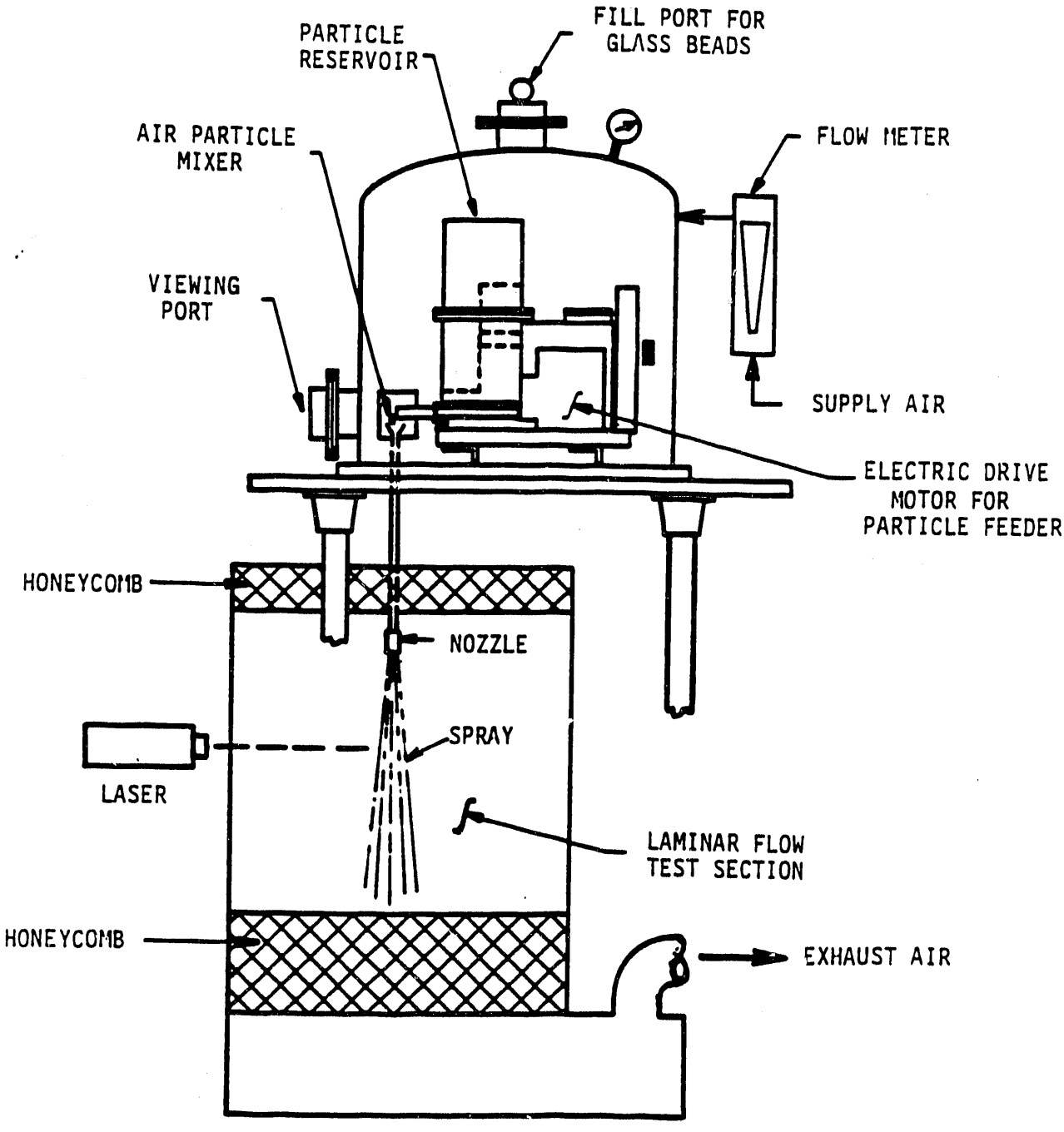

Figure 9.1. Schematic of Gas-Solid Nozzle Test Facility

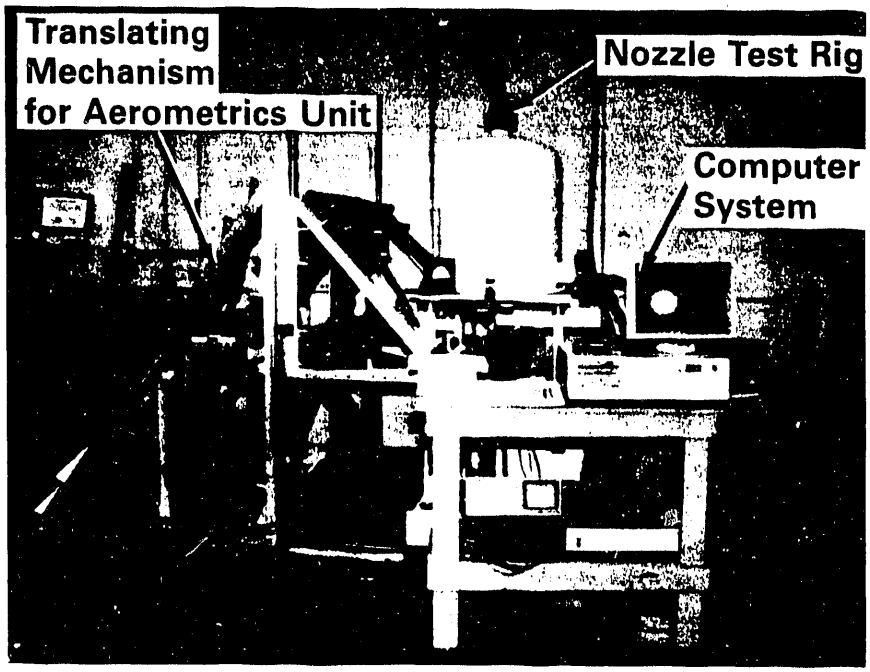

a. Overall View

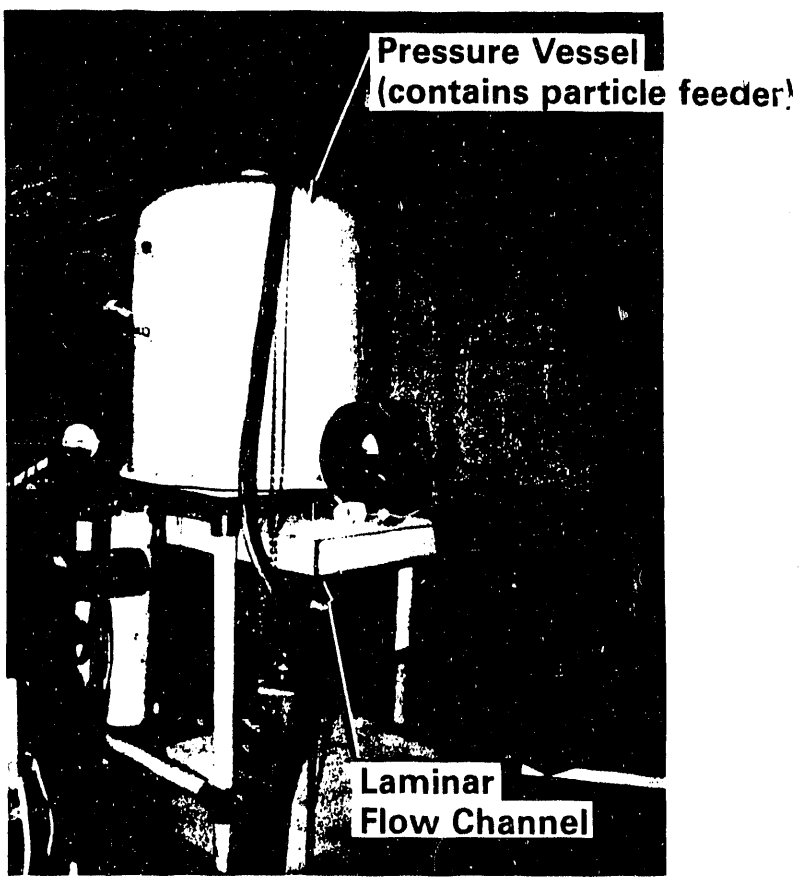

b. View of Flow Chamber

Figure 9.2. Gas-Solid Nozzle Test Facility

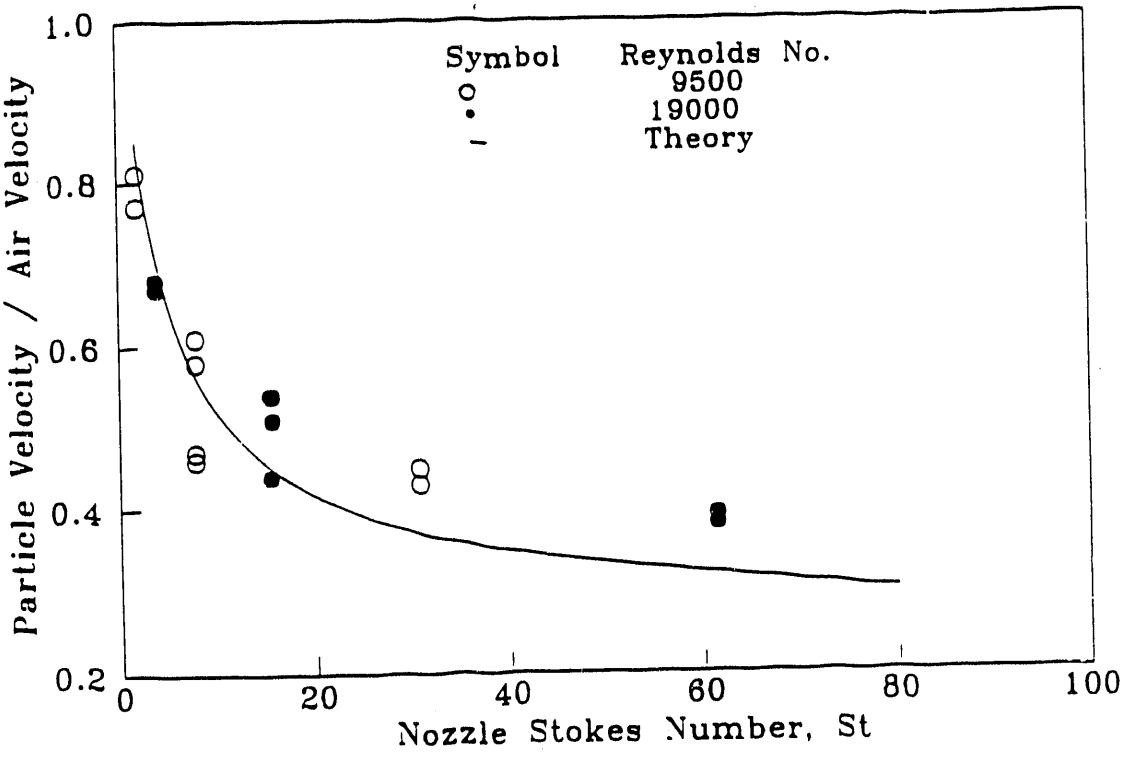

Figure 9.3. Particle Velocity at Nozzle Exit

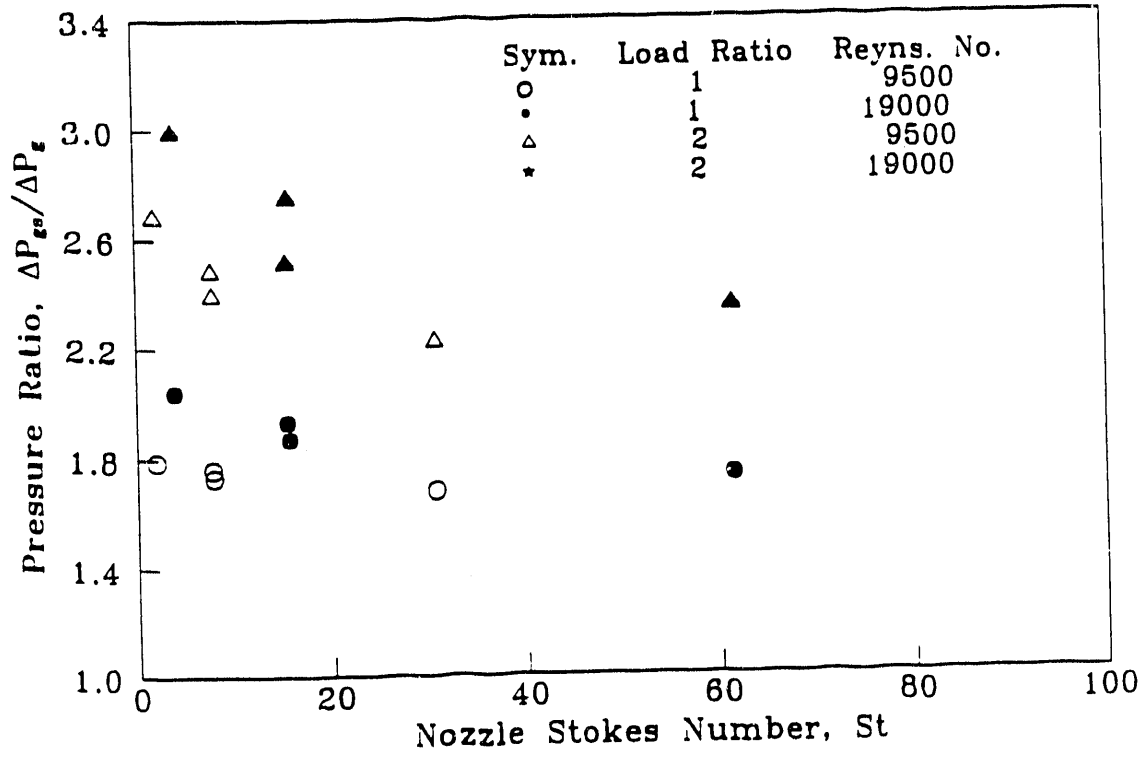

Figure 9.4. Nozzle Pressure Drop for Gas-Solid Flow Tests

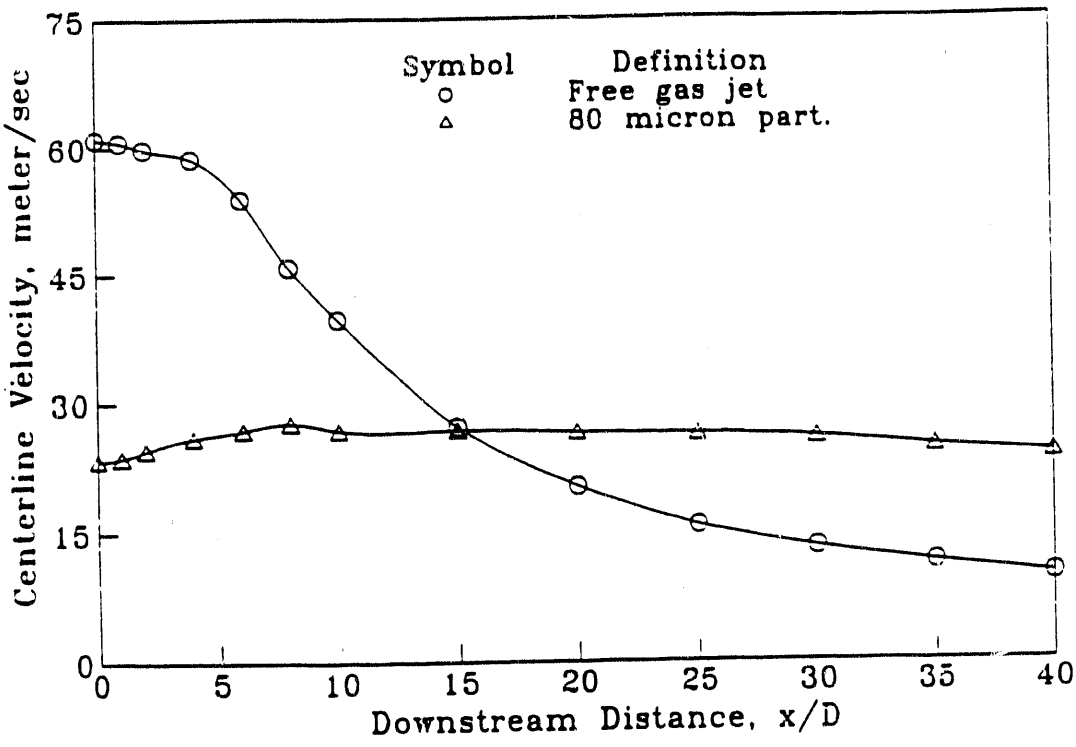

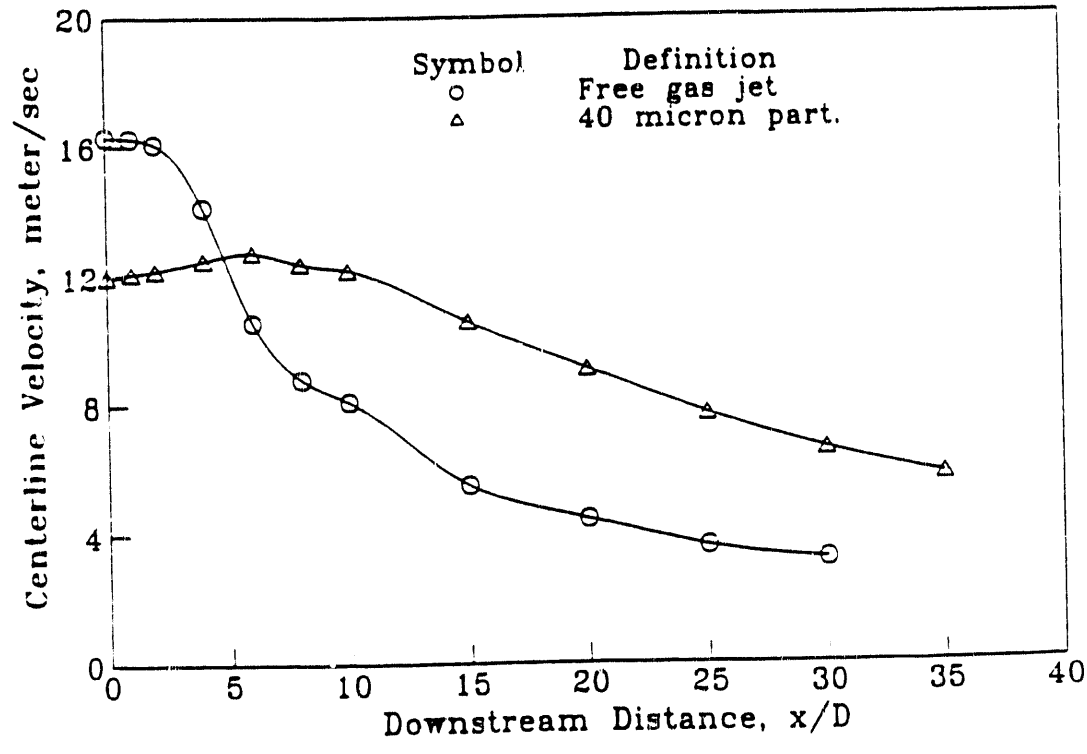

Figure 9.5. Velocity Characteristics of Gas-Solid Sprays

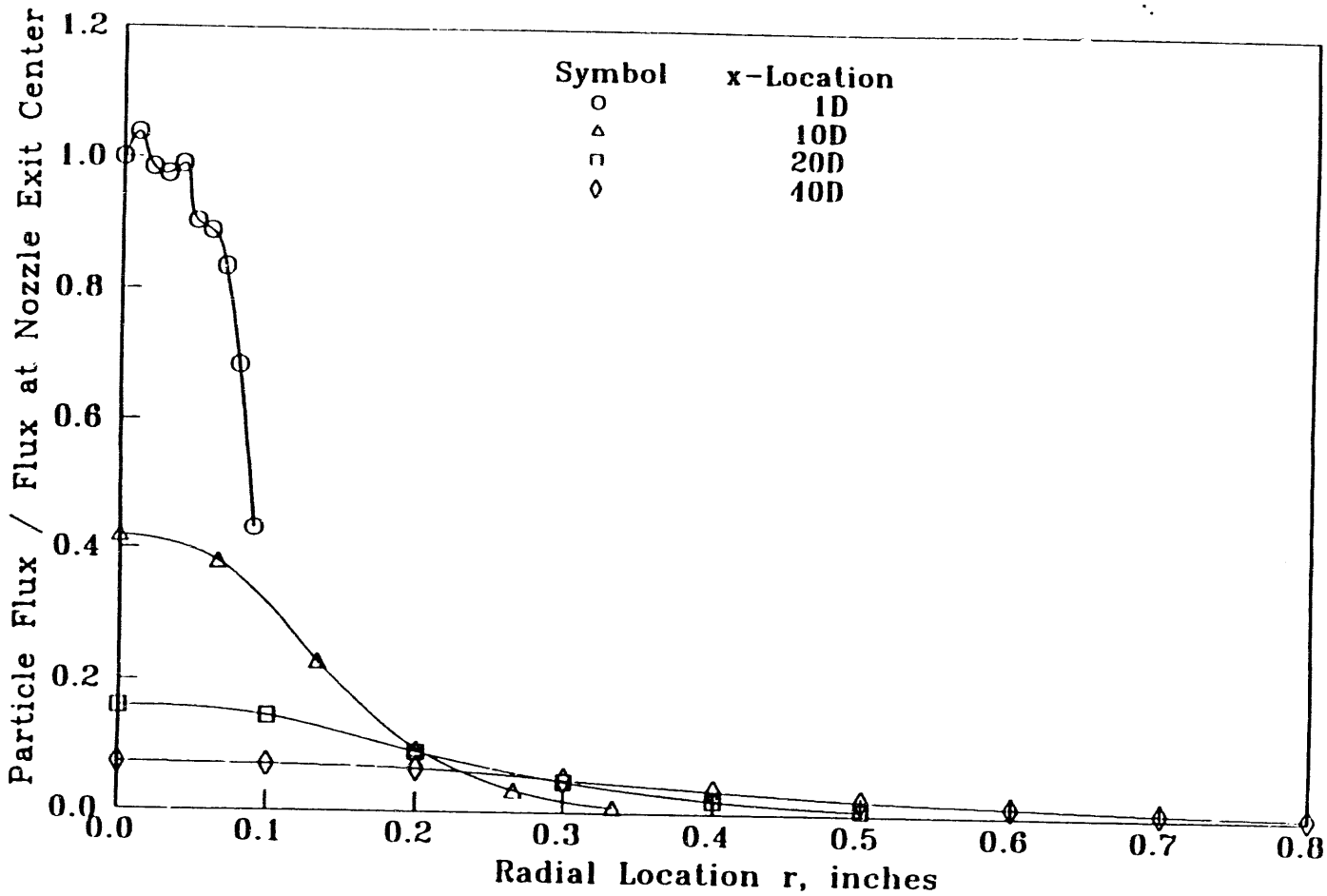

Figure 9.6. Particle Flux Distribution. D = 3/16"; Vg = 30 m/s; LR = 1; d = 80 μ

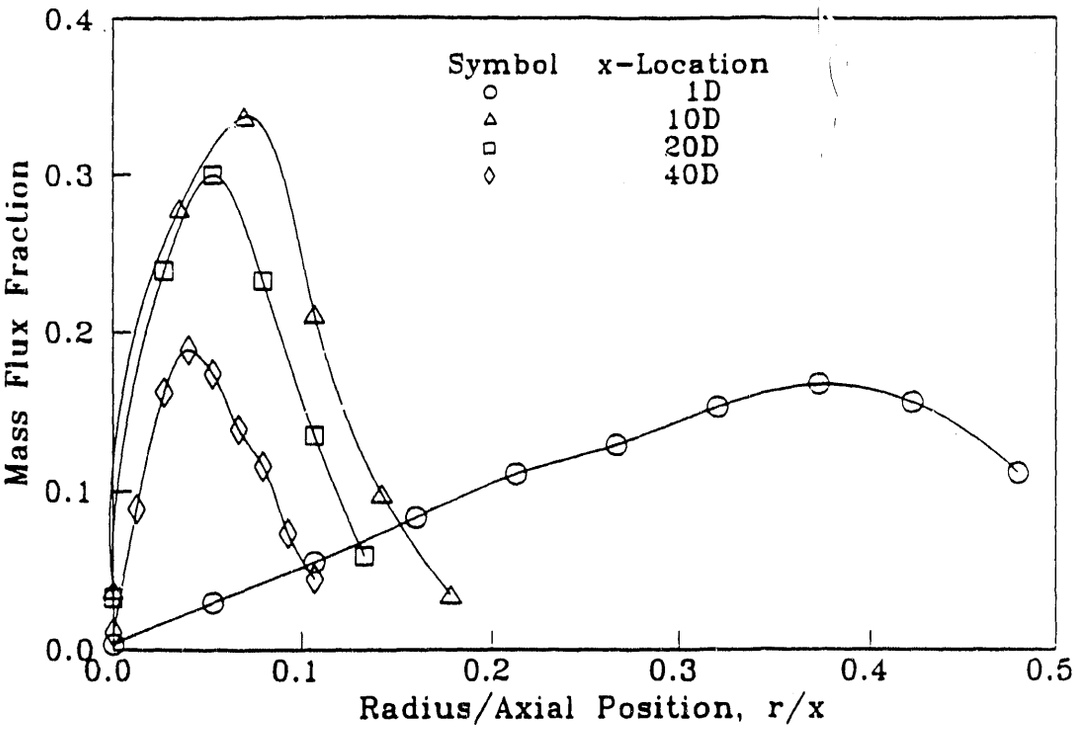

a. Mass Flux Fraction vs. r/x Position

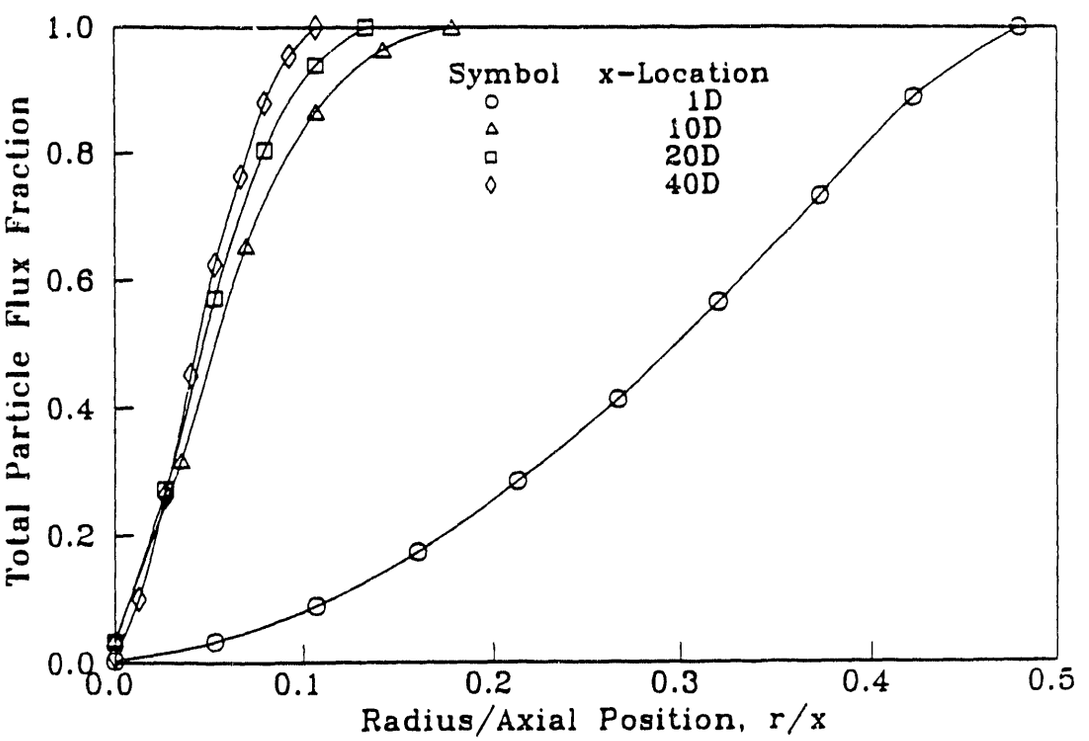

b. Total Particle Flux Fraction vs. r/x Position

Figure 9.7. Particle Flow Distribution. D = 3/16"; Vg = 30 m/s; LR = 1; d = 80 μ

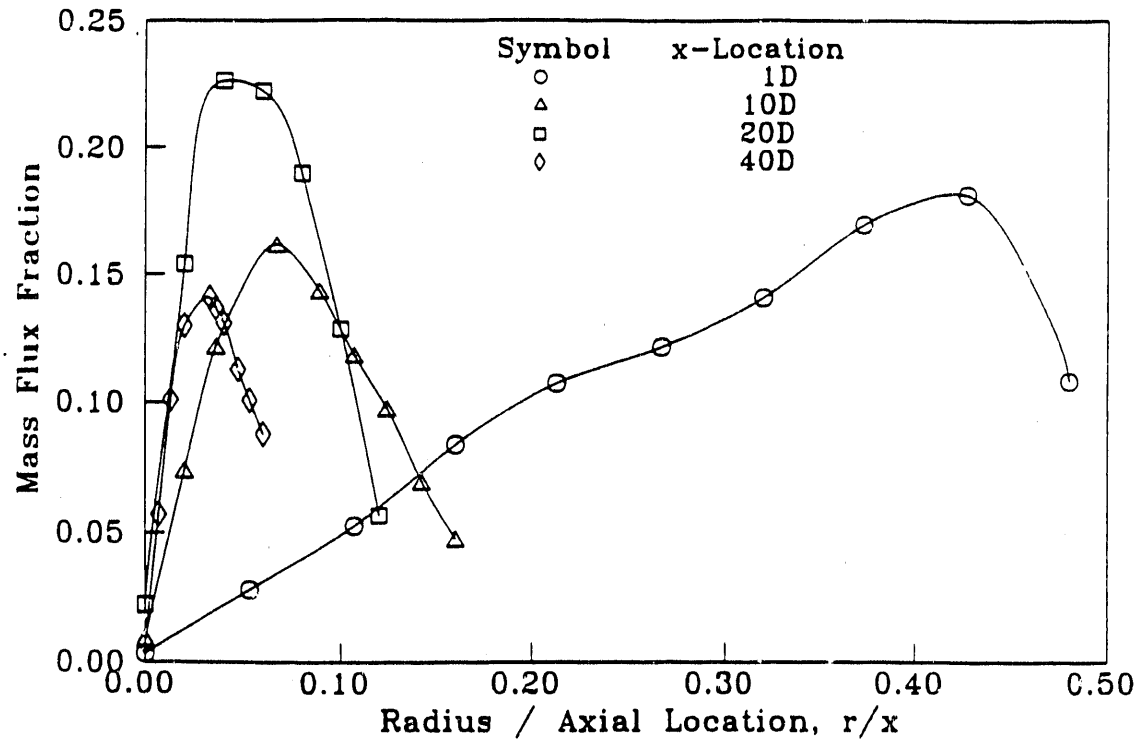

a. Mass Flux Fraction vs. r/x Position

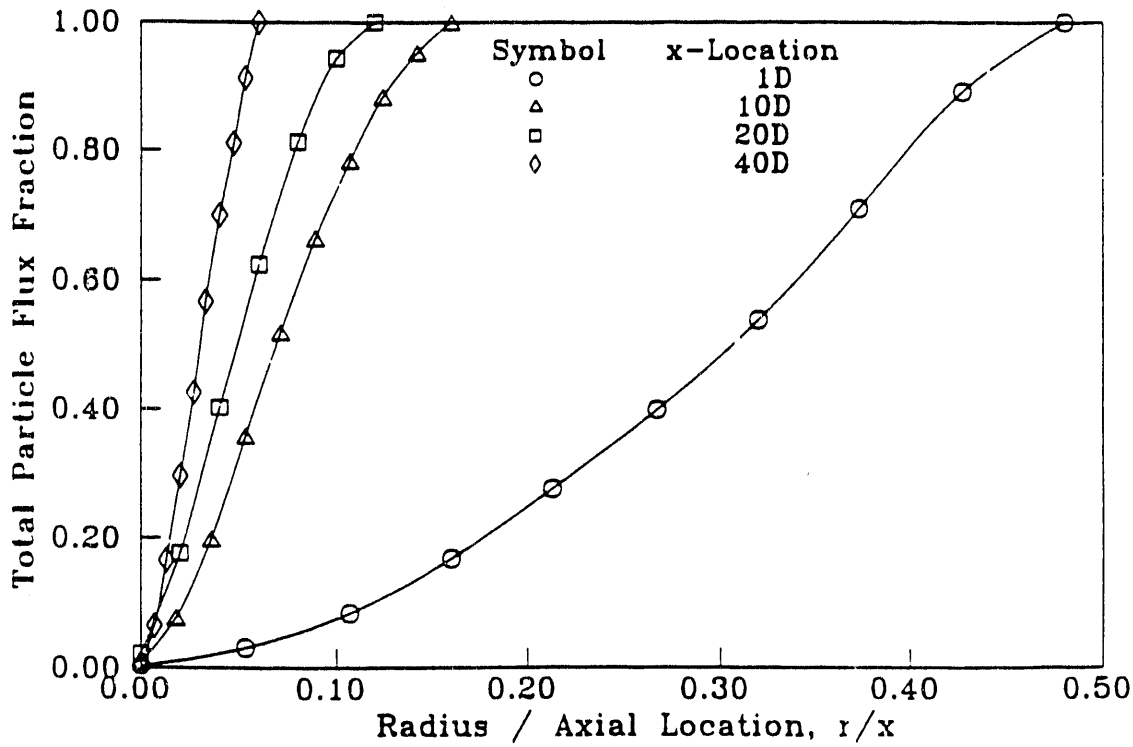

b. Total Particle Flux Fraction vs. r/x Position

Figure 9.8. Particle Flow Distribution. D = 3/8"; Vg = 30 m/s; LR = 2; d = 40 μ

10.0 COEFFICIENT OF PERFORMANCE AND CORRELATION OF NOZZLE TEST DATA

The coefficient of performance of a nozzle should provide a complete specification of the fuel injection performance. It should relate the characteristics of the nozzle to the spray, and should include at a minimum:

- the fuel flow rate as a function of pressure drop
- the drop (or solid particle) size distribution as a function of fuel properties and nozzle operating conditions
- the fuel-air ratio or spatial distribution throughout the spray

The relative importance of each of these three specifications depends upon the combustion system. For example, in the limit of an extremely long residence time combustor such as a coal burner with a grate, the fuel feed rate and possibly the coal particle size are the criteria that are important. For more compact, higher-intensity combustion systems with shorter residence times such as gas turbines, reciprocating engines, and some boilers, all three criteria above are of significance.

The first criterion, the fuel flow rate as a function of pressure drop, is well characterized for liquid and slurry injection nozzles by the flow number, which is the fuel flow rate divided by the square root of the injection pressure. This is a well established parameter for specifying nozzle performance for liquid and slurry nozzles, and there is little need for improvement. The flow number specification is of most significance for pressure atomizing nozzles that use high differential fuel pressures to generate high liquid velocities to provide the air shear required for atomization. For air-assist atomizers, the high liquid-air differential velocities are provided by accelerating the air to high velocities while the fuel is at low pressures and velocities. For these air-assist atomizers, the flow number is of less significance since the fuel pressure is only required to deliver fuel to the atomizer, rather than to provide atomization energy.

For gas-solid nozzles, the fuel flow rate as a function of pressure drop for different loading factors has been evaluated in this program, and relationships have been developed as explained in section 10.4.2.

The second criterion, the drop (or solid particle) size distribution, is important in determining the residence time required for evaporating and burning the fuel drops. The evaporation time increases with the square of the drop size, so high-intensity, short residence time combustors require small drop or particle sizes. Techniques have been developed during this program for specifying drop size distributions in a standard format, as discussed in Appendix A. Also relationships have been developed to predict drop size distributions for different nozzle types, as discussed below.

The third criterion, the fuel/air ratio or spatial distribution of fuel, is important for high-intensity, short residence time combustion systems. The distribution of fuel is important in determining combustion efficiency, gaseous and particulate emissions, combustion stability, temperature uniformity, and interaction of the fuel with the combustor walls. Procedures are described in Appendix A for determining spatial distribution of fuel within a spray. Relationships are presented below for spatial distributions of fuel measured within the nozzles evaluated for this program.

Three types of slurry nozzles were tested in this program: (1) a 2-dimensional slot, variable film thickness, air-assist nozzle with a correlation of results given in section 10.1, (2) a commercial, air-assist CWS nozzle for gas turbine and boiler applications with results correlated in section 10.2, and (3) several diesel hole-type injectors with results correlated in section 10.3. The gas-solid nozzle correlations are presented in section 10.4.

10.1. VARIABLE FILM THICKNESS NOZZLE

The variable film thickness nozzle is a two-dimensional representation of a fuel nozzle that allows the geometry to be varied over a broader range of conditions than a standard commercial atomizer. Because the geometry is different from a standard injector, the distribution of fuel in terms of fuel-air ratio is not of significance for this nozzle, but the drop size distributions can be studied easily without the complications of the cylindrical geometry characteristic of standard nozzles (e.g., the problems discussed in Appendix A). The drop size distributions for single-phase fluids are discussed in section 10.1.1, and for slurries in 10.1.2. The correlations presented in this section have been non-dimensionalized, in contrast with the results presented in section 6. The results presented in section 6 provide a more accurate fit of the measured data, but the results presented here are more easily applied to other geometries and sizes.

10.1.1. Single-Phase Fluids

Hashimoto and co-workers, (Arai, 1986) among others, have previously studied the atomization of liquids by VFT nozzles experimentally and theoretically. They found that the liquid sheet, after leaving the nozzle, waved somewhat like a flag in the wind with a frequency and amplitude that depended on the Weber number and Reynolds number of the liquid-gas flow. The mean length of the sheet before it began to break up because of the waving also depended on the Weber number and Reynolds number. The diameter of the droplets resulting from the breakup depended on the waving frequency, a characteristic velocity of the flow, and the nozzle gap width. The data presented in Section 6.0 for the tested VFT nozzle indicated in detail how the droplet SMD varied with flow rates, liquid properties, and gap width; although some of the exponential dependencies on Weber and Reynolds number did not agree numerically with Hashimoto's findings, the overall trends did coincide.

Considering the test findings and the available theories, a correlation of all the pure liquid data was formulated in terms of:

Re = Reynolds number, $\rho_g w V_g/\mu_l$,

V_r = velocity ratio, V_l/V_g , and

We = Weber number, $\rho_g w(V_g - V_l)^2/\sigma_l$,

where the symbols are defined as:

V_g = gas velocity

V_l = liquid velocity

w = nozzle gap width

μ_g = gas viscosity

ρ_g = gas density

ρ_l = liquid density

σ_l = liquid surface tension

The correlation, derived by a regression analysis, was found to be:

$$\frac{D_{32}}{w} = 5.8(Re)^{-0.025}(We)^{-0.612}(V_r)^{0.276} \qquad (10.1)$$

The correlation and all the data are shown in Figure 10.1. The correlation predicts the data well as indicated by a correlation coefficient of 0.97. The data cover a range of liquid viscosities from 0.9 to 1500 cp, liquid surface tensions from 22 to 73 dyne/cm, gas velocities from 31 to 143 m/s, liquid velocities from 0.15 to 1.5 m/s, and gap widths of 0.381 and 1.27 mm. Because of the wide range of parameters tested and the high correlation coefficient, Eq. (10.1) is thought to be an accurate predictor of drop sizes for the VFT nozzle. In the correlation, the Weber number represents the energy required to create new surface area when drops are formed from the continuous liquid sheet. The Reynolds number represents viscous dissipation. The physical implication of the velocity ratio is not quite as clear, but it can represent the shearing action of the gas stream on the liquid; however, when the gas and liquid shear viscosities were included in the velocity ratio, the correlation was degraded significantly. It is worth noting that the Weber number has the largest influence on the drop size and the Reynolds number has only a minor influence.

10.1.2. VFT Nozzle - Slurries

The drop sizes produced by the VFT nozzle for slurries were much larger than the drop sizes for liquids even when the slurries had viscosities and surface tensions comparable to the pure liquids. According to Eq. (10.1), these large drop sizes observed for slurries would have required much larger shear viscosities than the slurries actually possessed even at extremely high shear rates. In addition, for a given slurry, the drop size dependency on fuel flow rate was more pronounced than indicated by Eq. (10.1). Correlations of the form:

$$\frac{D_{32}}{w} \propto (Re)^{-a}(We)^{-b}(V_r)^{c} \qquad (10.2)$$

could be found for the slurry tests, but the exponents b and c varied with the loading ratio of coal to water. (The exponent a, conversely, was constant and about equal to the 0.025 value found for the pure liquids.). As the loading ratio increased, b decreased from 0.61, its pure liquid value, to near zero, roughly in accordance with the relation

$$b = 0.61 - 0.35(LR) \qquad (10.3)$$

This trend indicates that the energy required to create new surface as the drops are created becomes less and less important as the slurry becomes more highly loaded. The exponent c increased with the loading ratio, from roughly 0.15 to 0.25, indicating that the shearing action of the gas became relatively more important for the highly loaded slurries.

Because of these trends, further research is required to understand the atomization of slurries. It is postulated that the anomalously large drops created by slurries are a result of the energy required to separate the closely packed particles when a drop is created. (Each drop contains many particles, but nonetheless, some particles have to be separated from the other particles in the liquid sheet to create each drop.) This energy is analogous to that required to separate two plates containing liquid between them. The closer the plates are together, the more energy is required; similarly, the higher the loading ratio of the slurry is, the closer the particles are packed and the more energy is required to create drops; the result is that the drops will be larger.

10.1.3. VFT Nozzle Flow Capacities

Information on flow capacities for the VFT nozzle was previously presented in section 6.5. Flow capacities for other dimensions very different from those of this VFT nozzle are easily measured for particular designs.

10.2. COMMERCIAL, AIR-ASSIST, GAS TURBINE NOZZLE

The operating range of the commercial, air-assist, gas turbine nozzle was limited in both fuel properties and operating conditions, making the correlations more limited in range than those for the VFT nozzle. The nozzle could not be tested on the glycerol-water mixtures of varying viscosities because of the high densities in the spray. Correction procedures for multiple scattering errors in dense sprays are limited to lower densities than those encountered for the glycerol-water mixtures, highlighting the need for multiple-scattering correction procedures applicable to higher density sprays.

Sonic air velocities used in this atomizer were very effective in atomizing the CWS, but a slight reduction in air pressure from the design condition led to a break-down in cone angle of the spray, limiting the range of conditions.

The atomization quality of the atomizer was determined at two fuel flow rates for water, 40 wt.% CWS, 50 wt.% CWS, and 60 wt.% CWS. The correlation for the mean drop diameter is:

$$D_{32} = 1.32(WF)^{0.30}(\dot{m}_l)^{0.40} \tag{10.4}$$

where WF is the coal wt.%, and $\dot{m}_l$ is the mass flow in kg/hr. The atomization could also be correlated with the shear viscosity measured at 20000 sec^{-1}.

$$D_{32} = 3.38(\mu_l)^{0.040}(\dot{m}_l)^{0.40} \tag{10.5}$$

where the absolute viscosity is in cP. Since single-phase fluids of high viscosity were not tested in this atomizer, the general applicability of this relation could not be verified.

Procedures to determine the fuel volume fraction in the spray are described in Appendix A. Typical results for this atomizer were presented in Figure 7.5, but these results are limited to this nozzle design.

10.3. DIESEL HOLE-TYPE ATOMIZERS

Four diesel hole-type atomizers of different diameters and length/diameter ratios were evaluated. The drop sizes and cone angle were independent of liquid viscosity over the range from 3 to 100 cSt. The cone angles were similar to those for gas jets, and were broader for shorter L/D's.

The spray drop sizes depended on the hole size, d, and the atomizing pressure, Δp, in accordance with the correlation:

$$D_{32} = \Delta p^{-0.77} d^{0.1} \tag{10.6}$$

10.4. GAS-SOLID NOZZLES

10.4.1. Particle Velocity at Nozzle Exit

The trends of particle velocity at the nozzle exit with the flow parameters shown previously in Figure 9.3 can be understood by considering the effect of aerodynamic drag on the particles. For a dilute particle concentration, each particle can be assumed to be isolated from the rest, to a first approximation, and the equation of motion of a particle in the tube is:

$$\frac{1}{8}\pi\rho_p d^3\frac{dV_p}{dt} = F_{drag} \tag{10.7}$$

where the aerodynamic force is simply Stokes drag:

$$F_{drag} = 3\pi\mu_g(V_g - V_p)d \tag{10.8}$$

After Eq. (10.7) is inserted in Eq. (10.8), the equation of motion can be integrated to give:

$$V_g \ln\left(\frac{V_g - V_{pi}}{V_g - V_{po}}\right) + V_{pi} - V_{po} = \frac{2V_g}{St} \tag{10.9}$$

The symbols in these equations are defined as:

d	= particle diameter
L	= nozzle length
St	= Stokes Number, $\rho_p d^2 V_g / 18\mu_g L$
V_g	= gas velocity in the nozzle
V_{po}	= particle velocity at nozzle exit
V_{pi}	= particle velocity at nozzle inlet
ρ_p	= particle density
μ_g	= gas viscosity

The particle velocity at the nozzle entrance V_{pi} can be estimated by applying Eq. (10.9) to the tube connecting the pressure chamber to the nozzle, since V_{pi} is essentially zero for that tube and the exit velocity of the connecting tube is the entrance velocity for the nozzle.

Predictions from Eq. (10.9) were shown previously in Figure 9.3 as the solid line. The simplified theory tends to underestimate the particle velocity for large Stokes numbers (perhaps because of the influence of turbulence), but the overall trend of the data is predicted correctly. Equation (10.9) is sufficiently accurate as a design tool to be used to select nozzle lengths to deliver a desired particle velocity.

10.4.2. Nozzle Pressure Drop

The nozzle pressure drop for a gas-solid flow is greater than for the gas-flow alone for two reasons:

1. The density of the gas-solid flow is greater, and

2. The acceleration of the particles by the gas exerts a drag on the gas.

Considering these two effects, a physically plausible expression for the gas-solid pressure drop is:

$$\frac{\Delta P_{gs}}{\Delta P_g} = 1 + CZ \qquad (10.10)$$

where

ΔP_{gs} = gas-solid pressure drop

ΔP_g = gas-only pressure drop

C = pressure coefficient

Z = solids loading ratio, LR

This relation is similar to a form suggested in Crowe & Plank (1984). The coefficient C is supposed to be a function primarily of the Stokes and Reynolds numbers; it models the effect of particle acceleration. The parameter Z models the effect of increased mixture density. For $St \leq 1$, the acceleration effect is relatively minor, so C should approach unity; Eq. (10.10) then predicts that the gas-solid pressure drop is greater than the gas-only pressure drop in proportion to the density ratio between the two types of flows.

Equation (10.10) was used to calculate C from the pressure drops measured in the tests (Figure 9.4). The results are shown in Figure 10.2. The comparison with test data is reasonably good. The two solid lines are best-fit correlations to the data; they are:

$$C = 1.12 - 0.215 \ln(St) \qquad \text{for Re} = 19000 \qquad (10.11a)$$

and

$$C = 0.86 - 0.137 \ln(St) \qquad \text{for Re} = 9500 \qquad (10.11b)$$

The correlation coefficients for both curves are greater than 0.91. The test data do not cover a wide enough range of Reynolds numbers to propose a single correlation for all Reynolds numbers.

These kinds of correlations can be used to rate the mass flow capabilities of gas-solid nozzles.

10.4.3. Spray Velocity Characteristics

The spray characteristics shown previously in Figures 9.7 and 9.8 for various downstream locations did not overlay when plotted against r/x, as free gas-jet data do (see Appendix B). Hence, the measured distributions were not simple functions of r/x. By trial and error, it was found, however, that the radius at which the peak fluxes occurred did overlay fairly well when the axial location used in r/x was adjusted. Figures 10.3 and 10.4 show the test data re-plotted against $r/(x + 10D)$, where the additional $10D$ can be considered as a "virtual" development length for the spray. The peak of the flux distributions now overlay at about $r/(x + 10D) = 0.035$. Similarly, the total width of the spray occurred at $r/(x + 10D) = 0.1$ (with somewhat more scatter). For all the data, the best fit for the radius at which the peak flux occurred is:

$$r_{max} = 0.0354\,(x + 10D) \qquad (10.12)$$

with a standard deviation of 0.007. The correlation can equally well be expressed as a spray cone angle, θ_c:

$$\theta_c = \tan^{-1}(0.0354) \approx 2° \qquad (10.13)$$

These kinds of correlations are needed to estimate the fuel-air ratios of the sprays created by gas-solid nozzles.

10.4.4. Coefficient of Performance for Gas-Solid Nozzle

For the straight-tube gas-solid nozzles used in the tests here, a COP can be developed from the correlations developed in the previous sections.

Particle size is set by the size distribution used in the feed stream. Unless agglomeration occurs in the spray, the particle size is fixed and therefore does not enter the COP for a gas-solid nozzle.

Spatial distribution of the spray is well correlated by the radial width, r_{max}, at which the peak flux occurs:

$$r_{max} = 0.0354\,(x + 10D) \tag{10.14}$$

The correlation can equally well be expressed by a virtual cone angle, θ_c, equal to 2°. The cone angle is constant, independent of nozzle size and fluid properties.

Particle mass flow is the only variable parameter that enters the COP. It can be correlated by a non-dimensional pressure drop, somewhat similar to a valve coefficient, but depending on both Reynolds number and Stokes number. By manipulating Eq. (10.10), the total mass flow rate of particles $\dot{m}_p$ and the nozzle pressure drop ΔP_{gs} can be related functionally by:

$$\frac{\dot{m}_p Z\sqrt{1+CZ}}{\rho_g A\sqrt{\Delta P_{gs}/\rho_g}} = K_g \tag{10.15}$$

where A is the nozzle cross-section area and K_g is the nozzle pressure drop coefficient for a gas-only flow. K_g is readily calculated from the nozzle geometry. Typical correlations for C were given previously by Eqs. (10.11).

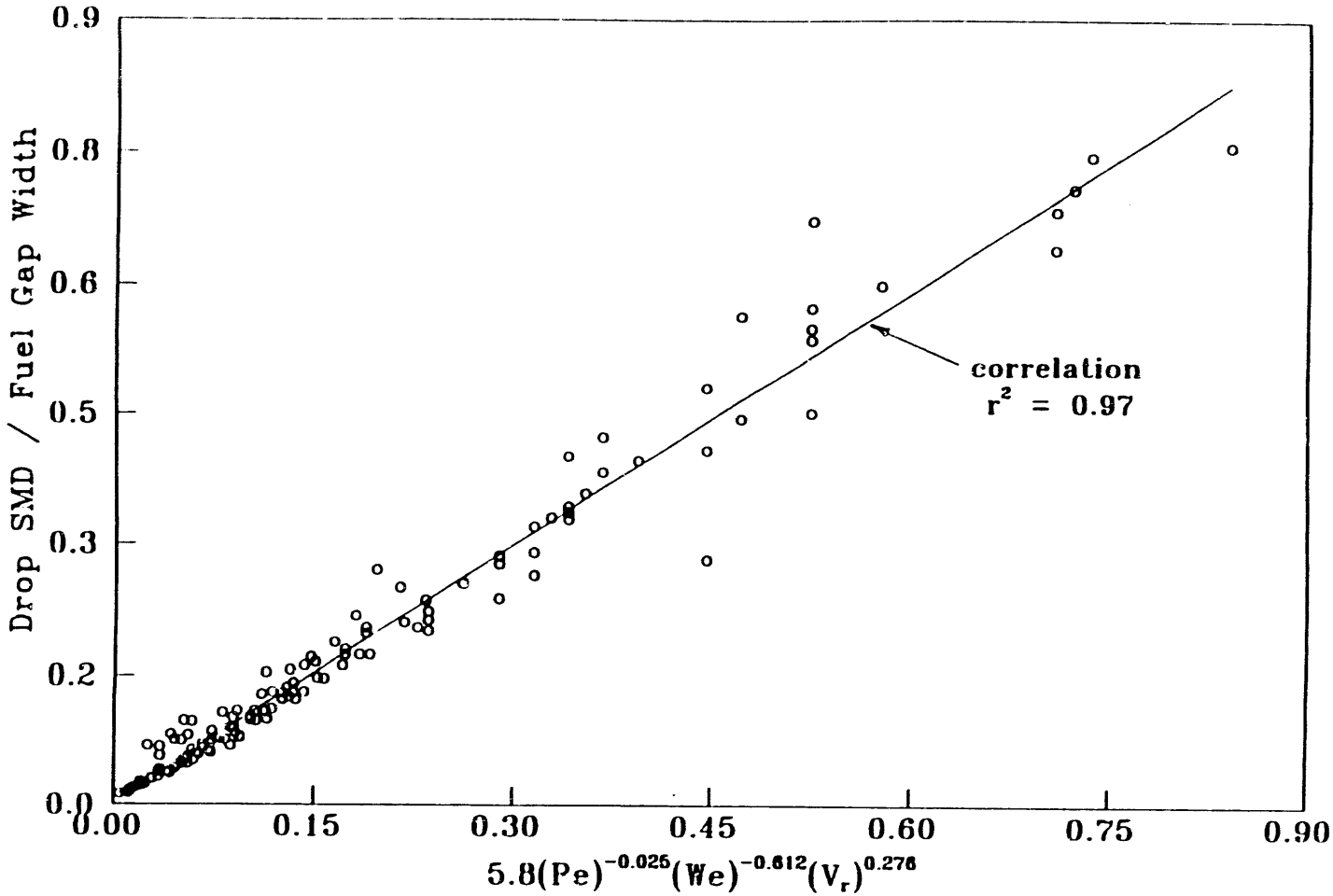

Figure 10.1. Correlation of VFT Nozzle Data for Pure Liquid Sprays

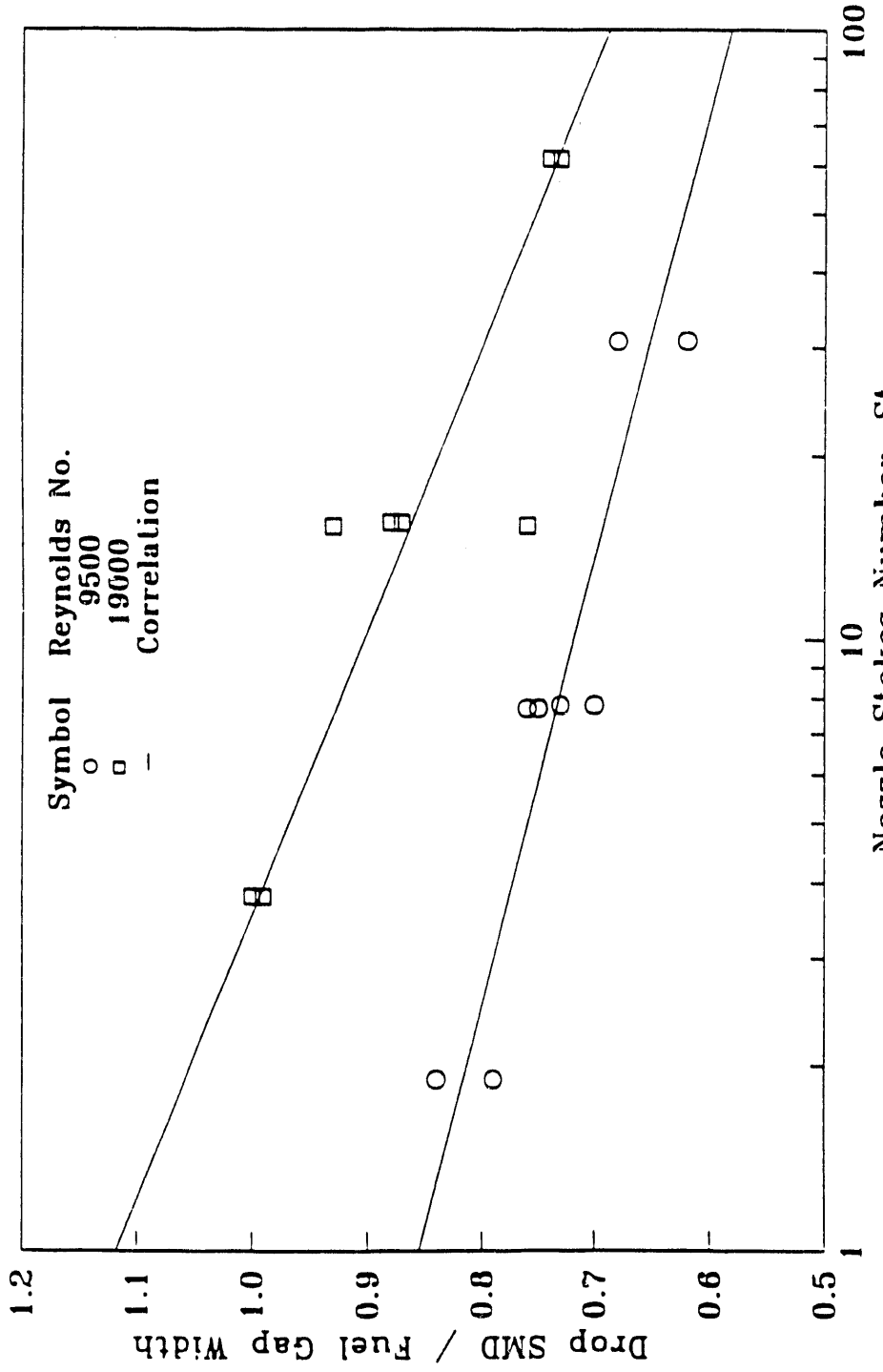

Figure 10.2. Pressure Coefficient for Gas-Solid Nozzle

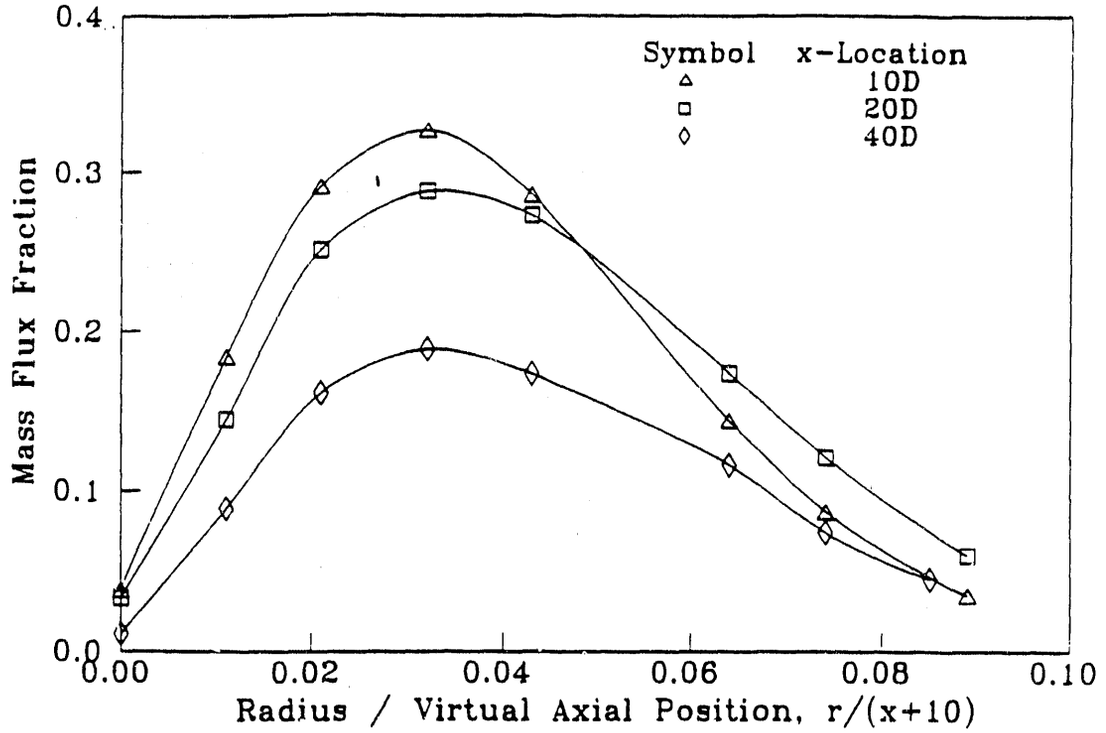

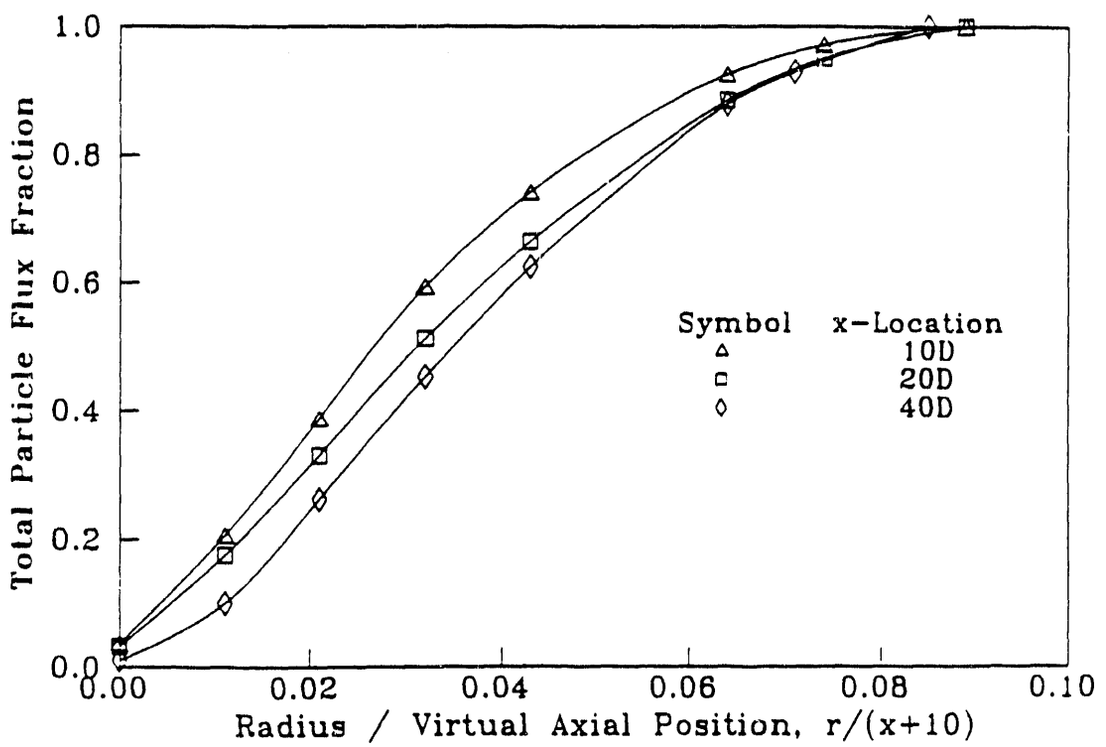

Figure 10.3. Adjusted Particle Flow Distribution. D = 3/16"; Vg = 30 m/s; LR = 1; d = 80 μ

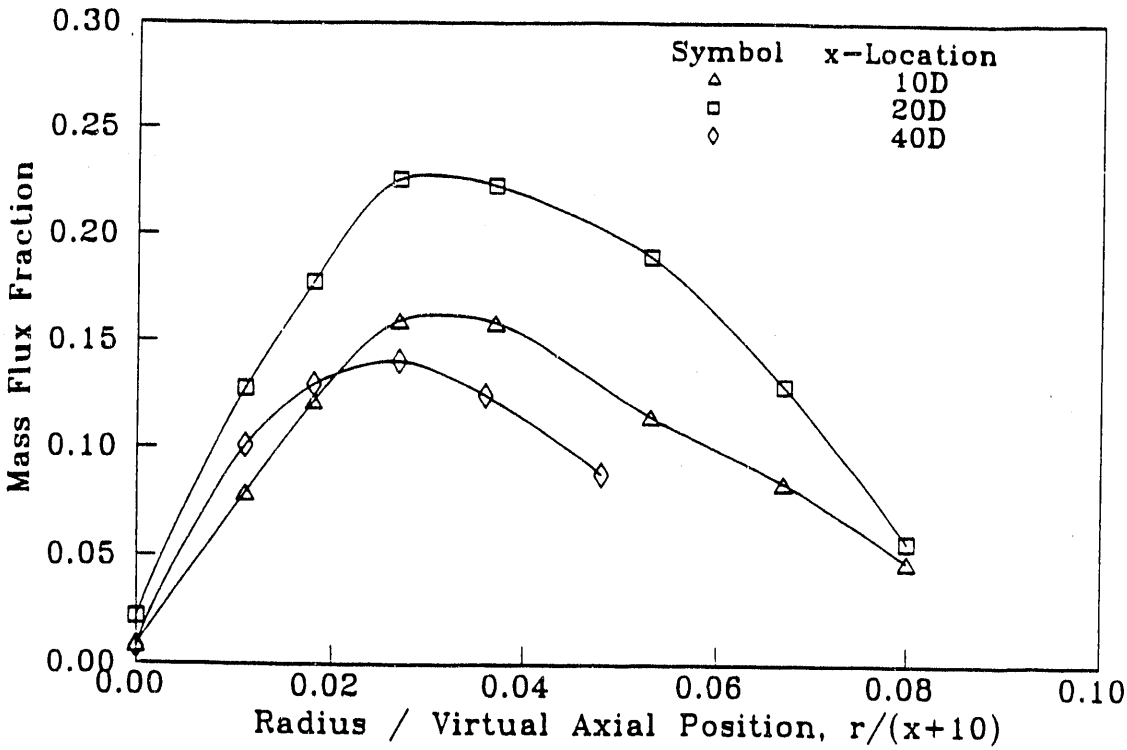

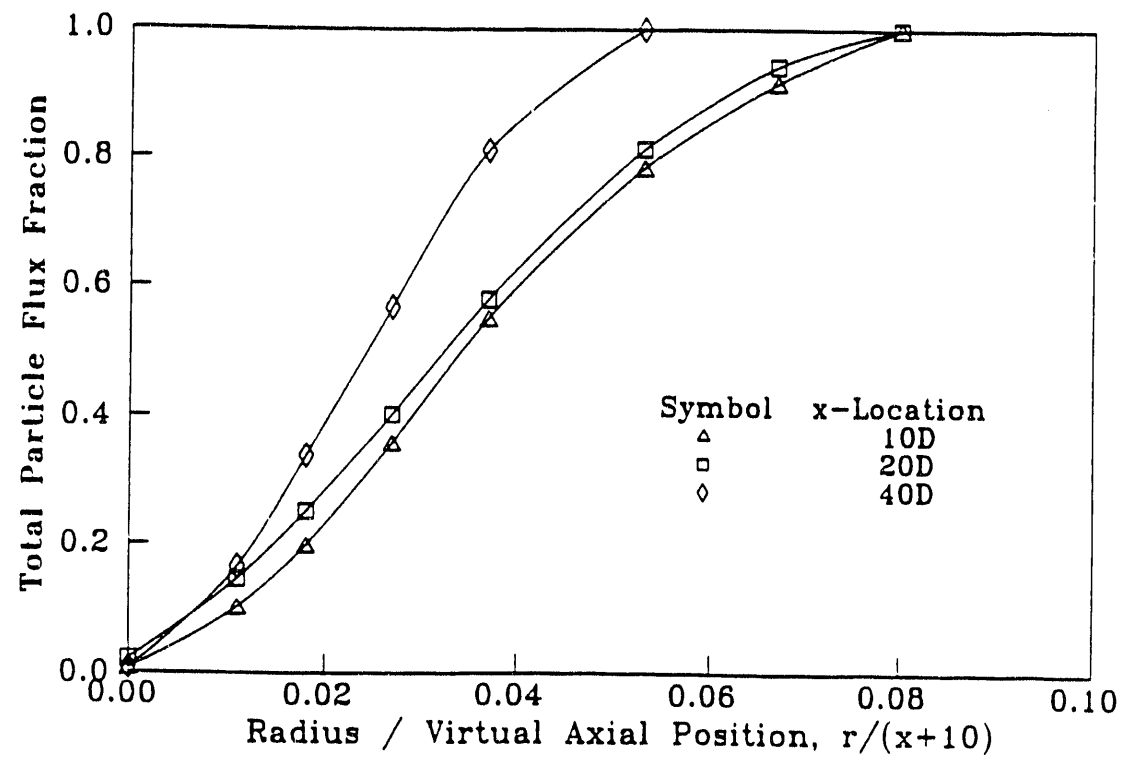

Figure 10.4. Adjusted Particle Flow Distribution. D = 3/8"; Vg = 30 m/s; LR = 2; d = 40 μ

11.0 CONCLUSIONS AND RECOMMENDATION

11.1. Summary of Project Accomplishments

1. A standardized methodology for measuring spray characteristics has been developed and published. Specifically, the methodology allows representative measures of the spray cross-section average drop sizes to be determined either from line-of-sight laser diffraction measurements, or from measurements at specific points in the spray by single-particle-counting instruments or photography.

2. Related to item (1) above, improved techniques have been developed for the characterization of sprays from diesel hole-type fuel injectors using laser-diffraction instruments. The improved techniques have detected large radial gradients in drop sizes and fuel volume flux missed with conventional approaches.

3. Studies with a 2-D variable-film-thickness, slot atomizer have shown that the average drop size for single-phase fluids can be correlated in terms of non-dimensional parameters that incorporate the effects of liquid flow rate, atomizing air velocity, surface tension , absolute viscosity, and nozzle width as shown by the correlation:

$$\frac{D_{32}}{w} = 5.8(Re)^{-0.025}(We)^{-0.612}(V_r)^{(0.276)}$$

For coal slurry atomization, the average drop size is less dependent on air velocity, and it depends strongly on coal loading. The studies show that the degraded atomization when compared with single-phase fluids cannot be explained by shear viscosity, even when the viscosity is measured at very high shear rates. This suggests that extra energy must be available in the flow for atomization because of the presence of the particles.

4. Tests of a commercial, air-assist, gas turbine nozzle showed that it was more effective for atomizing slurries than the variable-film-thickness nozzle. The gas turbine nozzle uses sonic air velocities, and the shock wave associated with sonic conditions may be especially effective in atomizing the slurries. The variable-film-thickness nozzle was not operated at sonic air velocities, although it could be.

5. Diesel hole-type fuel injectors produced sprays that were relatively insensitive to viscosity, but were dependent on operating pressure, hole diameter, and length/diameter ratio. Modifications were required to a standard laser-diffraction instrument to improve the spatial resolution sufficiently to measure radial variations of spray properties.

6. Studies conducted with gas-solid nozzle flows showed that nozzle pressure drop increases with particle loading ratio and Reynolds number, but it decreases with Stokes number, as shown by the correlation:

$$\frac{\Delta P_{gs}}{\Delta P_g} = 1 + CZ$$

The peak particle flux distribution in the spray occurred roughly at radial locations where the radial velocity of a free gas jet is zero, that is, where the gas velocity changes from an outward direction to an inward direction. Hence, it is observed that particles tend to accumulate on a conical surface formed by the locus of points where the radial velocity is zero.

11.2. Conclusions

1. A single number value such as a Coefficient of Performance that adequately and universally describes all nozzle performance characteristics is impractical. It is more practical and relevant to develop methods of predicting the important performance characteristics from laboratory-derived non-dimensional correlations using standardized measurement techniques. Based on the results of this study, performance descriptions of nozzles should include correlations for drop or particle size distribution, spatial distribution of the fuel in the spray, and a method for rating the mass flow capabilities.

2. Standardized procedures have been developed for characterizing spray drop sizes and liquid volume fractions using a variety of possible instruments. These procedures give a true cross-section average for the spray, and allow a comparison of spray performance independent of the measurement instrumentation, assuming an accurate measurement by the instrument. The American Society for Testing Materials (ASTM) is currently writing a standard for spray measurements that includes these procedures.

3. The presence of particles in slurries causes an added cohesiveness compared with single-phase fluids that makes the slurry significantly more difficult to atomize than simple fluids. The degraded atomization of slurries when compared with single-phase fluids cannot be explained by the shear viscosity alone, even when the shear viscosity is measured at high shear rates. (See item 4 under Recommendations.)

4. The presence of shock waves associated with sonic air velocities in air-assist nozzles may provide the extra energy required to effectively atomize slurries.

5. Some of the performance characteristics of diesel hole-type fuel injectors and gas-solid nozzles can be correlated with gas jet models modified for the different densities associated with the particles in the gas jet.

6. Questions remain concerning the structure of sprays from diesel hole-type fuel injectors. Recent results from various programs provide very conflicting answers. For example, the diesel sprays in this project showed large drops near the centerline not seen in some other programs. The extremely high spray densities are one deterrent to resolving these questions. Improved correction procedures are needed to reduce multiple scattering errors in laser-diffraction measurements of dense sprays.

7. For gas-solid nozzles, a set of two correlations (nozzle pressure drop and spray cone angle) was found to characterize the spray. These correlations can serve as a Coefficient of Performance for such nozzles.

11.3. Recommendations for Additional Work

11.3.1. Liquid and Slurry Nozzles

1. Because of conflicting results concerning the structure of sprays from diesel hole-type fuel injectors, a study should be conducted of the same spray utilizing several independent measurement techniques such as a laser-diffraction instrument, a phase/Doppler instrument, photography, and a patternator to evaluate drop size distributions and liquid volume fractions. The results from these independent measurements could be compared to evaluate the uncertainty in the measurement techniques. It is suggested that a continuous

spray in the pressure range of 3000 to 20,000 psid (20.7 to 138 MPa) be used to avoid uncertainties associated with intermittent sprays, and that spray into elevated pressure air should be considered.

2. Because of the extremely high optical densities associated with many practical sprays, the correction procedures for multiple-scattering errors associated with laser-diffraction measurements should be extended to higher optical densities. Improved correction procedures could be developed based on existing theoretical models for laser light scattering, and these predicted correction procedures verified with fairly straightforward experiments using standard latex spheres.

3. Questions concerning any special beneficial effects for atomization by the shock waves associated with sonic air velocities should be resolved by operating a variable-film-thickness nozzle or some other design on slurries through a range of air velocities including sonic conditions.

4. A model should be developed for the atomization of slurries based on the energy required to overcome attractive forces between particles and forces of "binding energy" due to liquids between particles. Southwest Research has a proprietary concept for experimentally investigating the energy required to atomize slurries, and that experimental technique should be used for comparison with the results predicted from the model above. Based on these results, tests could be developed for CWS capable of predicting atomization more accurately than traditional correlations based on surface energy in a single-phase drop.

11.3.2. Gas Solid Nozzles

1. The test methods and spray correlations developed in this project should be extended to a larger variety of nozzle types and solids loading ratios.

2. Analytical/computational models should be developed, starting from gas-jet theory, to predict the characteristics of gas-solid nozzle sprays.

12.0 REFERENCES

Allen, J. W., Rennie, A. G., Melbourne, M. C. (1985). "Atomization of Coal Water Mixtures." 7th International Symposium on Coal Slurry Fuels Preparation and Utilization, U.S. D.O.E., Pittsburgh, pp. 393-401.

Allen T. (1981). Particle Size Measurement, Third Edition, Chapman and Hall, P. 128.

Arai, T. and Hashimoto, H. (1986) "Disintegration of a Thin Liquid Sheet in a Cocurrent Gas Stream." **Int. J. Turbo and Jet Engines, 3**, pp. 301-306.

Arai, T., and Hashimoto, H. (1985) "Behavior of a Gas-Liquid Interface on a Liquid Film Jet (Instability of a Liquid Film Jet in a Cocurrent Gas Stream)." **Bulletin ASME, 28**, 245, pp. 2652-2659.

Ballal, D. R., and Lefebvre, A. H. (1980). "Problems and Promises in Gas Turbine Combustor Design Development," in Gas Turbine Combustor Design Problems, edited by A. H. Lefebvre, Hemisphere Publishing Corp., Washington, pp. 189-204.

Chin, J. S., and Lefebvre, A. H. "Some Comments on the Characterization of Drop-Size Distributions in Sprays" in proceedings ICLASS-85, 3rd International Conference on Liquid Atomization and Spray Systems, Institute of Energy, London.

Cronin, L., Sojka, P. E., and Lefebvre, A. H. (1985). "The Effect of Fuel Film Thickness on Coal Water Slurry Atomization," SAE Technical Paper 852086.

Cronin, L., Sojka, P. E., Smigel, R., and Jones, R. V. (1986). "The Effect of Nozzle Geometry on Coal-Water Slurry Atomization," presented at the Coal Liquid and Alternate Fuel Technology Conference (CLAFT), Halifax Nova Scotia, October 1986.

Crowe, C. T., and Plank, D. (1984). "Metering the Flow Rates of Gas-Solid Suspensions Through Venturimeters by Measuring Pressure Drop and Light Attenuation." **Gas-Solid Flows, FED, Vol. 10**, American Society of Mechanical Engineers, pp. 43-46.

"Data Package for 3/16" and 3/8" Nozzles Tested with Gas Solid Mixtures," DOE Contract DE-AC21-86MC23005, SwRI Project 04-1345, June 1988.

Dodge, L. G. (1984). "Calibration of the Malvern Particle Sizer," Applied Optics, Vol. 23, pp. 2415-1419.

Dodge. F. T., Dodge, L. G., and Johnson, J. E. (1986). "An Assessment of Nozzles for Multi-phase Flow Applications," Southwest Research Institute Report for Contract No. DE-AC21-86MC23005.

Dodge, L. G. (1987). "Comparison of Performance of Drop-Sizing Instruments," Applied Optics, 26, pp. 1328-1341.

Felton, P. G., Hamidi, A. A., and Aigal, A. K. (1985). "Measurement of Drop Size Distribution in Dense Sprays by Laser Diffraction," proceedings 3rd International Conference on Liquid Atomization and Spray Systems, The Institute of Energy, London, pp. IVA/4/1-11.

Giffen, E., and Muraszew, A. (1953). The Atomization of Liquid Fuels, John Wiley & Sons Inc., New York.

Hammond, D. C., Jr. (1981). "Deconvolution Technique for Line-of-Sight Optical Scattering Measurements in Axisymmetric Sprays," Applied Optics, Vol. 20, No. 3, pp. 493-499.

Hauserman, W. B., Patel, R. C., and Wilson, W. G. (1985). "Production and Combustion of Hot-Water-Dried Lignite Slurries," 7th International Symposium on Coal Slurry Fuels Preparation and Utilization, U. S. D.O.E., Pittsburg, pp. 268-281.

Hirleman, E. D., and Dodge, L. G. (1985). "Performance Comparison of Malvern Instruments Lasers Diffraction Drop Size Analyzers," in Proceedings, ICLASS-85, Third International Conference on Liquid Atomization and Spray Systems, Vol. 2 (Institute of Energy, London, pp. IVA/3/1.

Hudson, D. A. (1980). "Problems and Promises in Gas Turbine Combustor Design Development," in Gas Turbine Combustor Design Problems, edited by A. H. Lefebvre, Hemisphere Publishing Corp., Washington, pp. 3-12.

Hsu, B. D. (1989). "Progress on the Investigation of Coal-Water Slurry Fuel Combustion in a Medium-Speed Diesel Engine: Part 3, Accumulator Injection Performance," Jan. 22-25, ICE-Volume 7, 12th Annual Energy Sources Technical Conference and Exhibition, held in Houston, Texas.

Ishii, R., and Umeda, Y. (1986). "Nozzle and Free-Jet Flows of Gas Particle Mixture," ASME FED Vol. 35, Gas-Solid Flows - 1986, pp. 125-130.

Lefebvre, A. H. (1989). Atomization and Sprays, Hemisphere Publishing Company, New York.

Lefebvre, A. H. (1983). Gas Turbine Combustion, Hemisphere Publishing Company, New York.

Lefebvre, A. H. (1980). "Airblast Atomization," Prog. in Energy Combustion Sci., Vol. 6, pp. 233-261.

Lichty, L. C. (1951). Internal Combustion Engines, McGraw-Hill Book Co., New York, pp. 229-266.

Liu, B. L., and Schmidt, H. J. (1985). "Dense Phase Transport of Pulverized Coal," Proc. ASME Synfuels and Coal Energy Symposium, pp. 67-73.

Mannheimer, R. J. (1989). "Shear and Extensional Flow Properties of a Micronized Coal-Water Fuel," Proceedings of the Fourteenth International Conference on Coal & Slurry Technology, April 24-27, Clearwater, Florida, U.S. Department of Energy, Pittsburgh Energy Technology Center, pp. 155-166.

McVey, J. B., Russel, S., and Kennedy, J. B. (1986). "Characterization of Fuel Sprays Using a High-Resolution Patternator," AIAA Paper No. AIAA-86-1726.

Morris, G. J., Jurewicz, J. T., and Palmer, G. M. (1986). "Particle Motion in a Fluidically Oscillating Jet." **Gas-Solid Flows-1986, FED-Vol. 35**, American Society of Mechanical Engineers, pp. 53-58.

Obert, E. F. (1973). Internal Combustion Engines and Air Pollution, Intext Educational Publishers, New York, pp. 427-449.

Odgers, J., and Kretschmer, D. (1986). Gas Turbine Fuels and Their Influence on Combustion, Abacus Press, Cambridge, Massachusets.

Pohl, J. H., Sepulveda, J., and Rothfeld, L. B. (1985). "Correlation of the Spray Characteristics of Coal-Water-Fuels," 7th International Symposium on Coal Slurry Fuels Preparation and Utilization, U. S. D.O.E., Pittsburgh, pp. 357-376.

Rakitsky, W. G., McCormick, R. J. Murphy, T. J., and Baril, M. F. (1986). "Rheological Properties of Coal-Water Fuels Significant for Fine Spray Production During Combustion." Third Annual Pittsburgh Coal Conference.

Rao, K. A., et al (1989). "Cooper-Bessemer Coal-Fueled Engine System Progress Report," Jan. 22-25, ICE-Volume 7, 12th Annual Energy Sources Technical Conference and Exhibition, held in Houston, Texas.

Rosfjord, T. J. (1985). "Atomization of Coal Water Mixtures: Evaluation of Fuel Nozzles and a Cellulose Gum Simulant," ASME Paper No. 85-GT-88.

Ryan, T. W. III and Dodge, L. G. (1984). "Diesel Engine Injection and Combustion of Slurries of Coal, Charcoal, and Coke in Diesel Fuel," SAE Paper No. 840119.

Ryan, T. W. III, Calahan, T. J., Dodge, L. G., and Moses, C. A. (1982). "Injection, Atomization, and Combustion of Carbon Slurry Fuels," SAE Paper No. 821199.

Ryan, T. W., III, Callahan, T. J., Mecredy, H. E., Baker, Q. A., and Jett, B. T. (1987). "Coal Slurry Combustion-Bomb and Small Engine Test Results," to be presented at the Energy-Sources Technology Conference.

Schlicting, H. (1979). **Boundary Layer Theory**, 7th Edition, McGraw-Hill Book Co.

Smith, C. F., Sojka, P. E., and Lefebvre, A. H. (1985). "Plain-Jet Airblast Atomization of Coal-Water Slurry Fuels," SAE Paper No. 852085.

Sturgess, G. J. (1980). "Problems and Promises in Gas Turbine Combustor Design Development," in Gas Turbine Combustor Design Problems, edited by A. H. Lefebvre, Hemisphere Publishing Corp., Washington, pp. 133-150.

Swithenbank, J., Beer, J. M., Taylor, D. S., Abbot, D., and McCreath, G.C. (1977). "A Laser Diagnostic Technique for the Measurement of Droplet and Particle Size Distribution," in Experimental Diagnostics in Gas Phase Combustion Systems, ed. B. T. Zinn, Progress in Astronautics and Aeronautics, Vol. 53, pp. 421-447.

Wilson, J. C. (1984). "The Drag Force Experienced by Spherical Particles in Rectilinear Motion of Reynolds Number as Large as 70." ASME FED Vol. 10, Gas-Solid Fuels, pp. 53-56.

APPENDIX A, "Representation of Average Drop Sizes in Sprays" by Lee G. Dodge of Southwest Research Institute, has been removed from this report because of copyright laws. The article was published in *J. Propulsion*, Vol. 4, No. 6, 1987.

APPENDIX B: Results of Gas Jet Tests

Figure B.1a shows a typical centerline velocity traverse for a gas-jet test. The bulk gas velocity in the nozzle was 30 m/s. To facilitate comparisons with turbulent, free-jet theory, the measured centerline velocity $V_c(x)$ distribution is divided by the centerline velocity V_{co} at the nozzle exit, and plotted as a function of downstream distance x divided by nozzle diameter D. The data for both nozzles overlay very well, as predicted by free-jet theory (Schlichting, 1979). The potential core of the jets extends downstream to about $x/D = 8$. Beyond this constant velocity core, the centerline velocity distribution agrees with the theoretical prediction:

$$\frac{V_c}{V_{co}} = 5.6\left(\frac{D}{x}\right)$$

which is shown by the solid line.

Figure B.1b shows typical velocity profiles across the jet width at three downstream locations, all well beyond the potential core region. The velocity distribution $V(r)$ has been normalized by the centerline velocity $V_c(x)$ at each axial location. Again, the data points overlay. The theoretical prediction (Schlichting, 1979):

$$\frac{V(r)}{V_c} = \left[1+57.56\left(\frac{r}{x}\right)^2\right]^{-2}$$

is shown by the solid line. The data are in excellent agreement with theory.

Figures B.2a and B.2b show the measured turbulence quantities for the gas jets. Again, the data agree well with other measurements of turbulence jets.

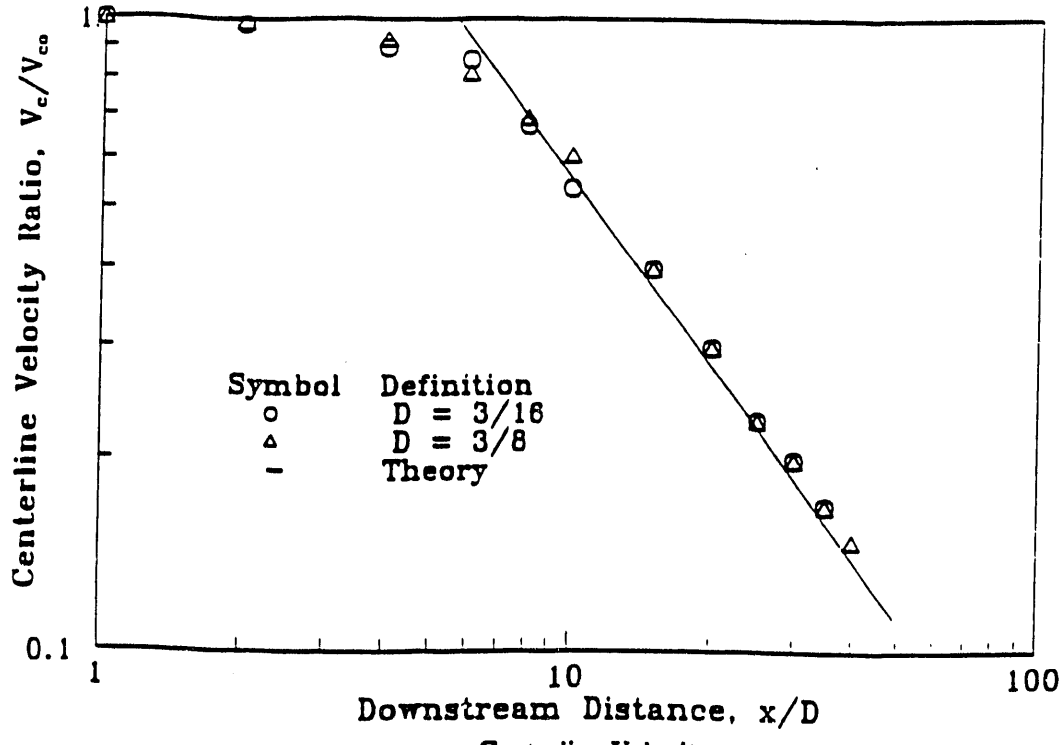

a. Centerline Velocity

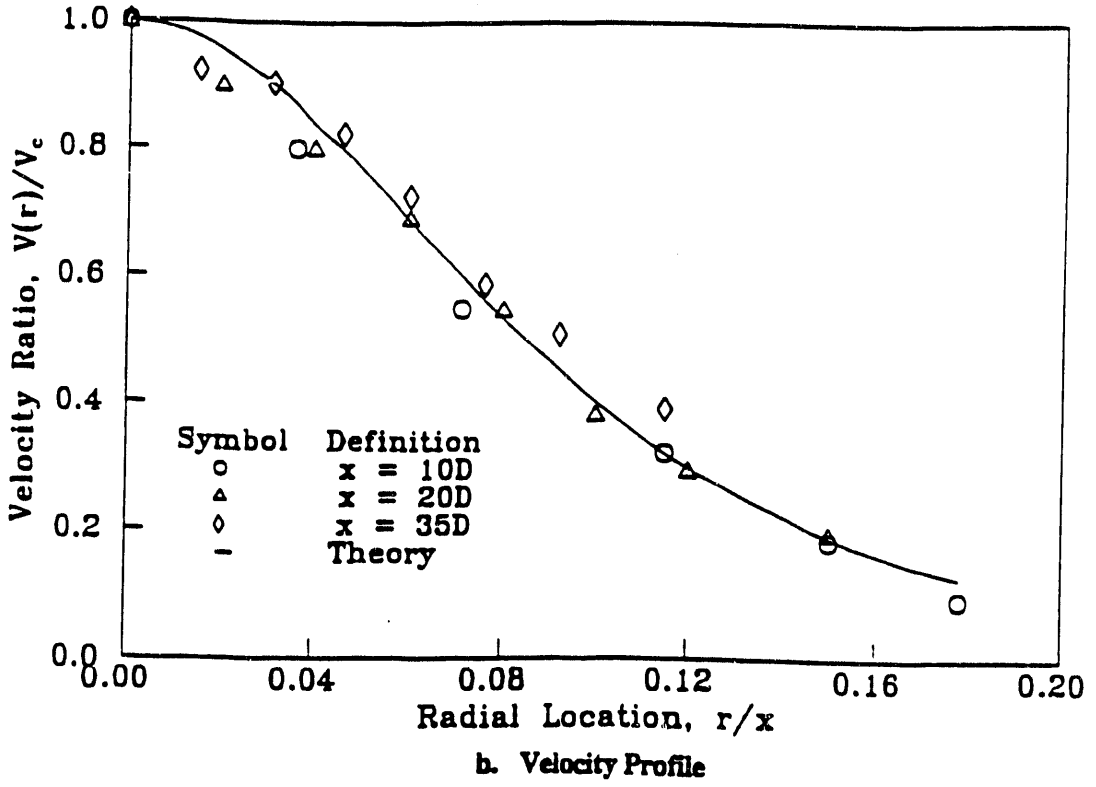

b. Velocity Profile

Figure B.1. Gas Jet Velocity Characteristics

END

DATE FILMED

09/05/91